DTIC FILE COPY

(1)

National Defence / Défense nationale

AD-A216 724

# AN ERROR SENSITIVITY MODEL FOR DOPPLER POSITIONING USING TRANSIT SATELLITES

DTIC
ELECTE
JAN 11 1990
S D
D

by

J. Christopher McMillan

**DEFENCE RESEARCH ESTABLISHMENT OTTAWA**
REPORT NO. 1015

Canada

August 1989
Ottawa

90 01 09 193

National Défense
Defence nationale

# AN ERROR SENSITIVITY MODEL FOR DOPPLER POSITIONING USING TRANSIT SATELLITES

by

J. Christopher McMillan
*Navigation and Integrated Systems Section*
*Electronics Division*

Accesion For
NTIS CRA&I
DTIC TAB
Unannounced
Justification
By
Distribution /
Availability Codes
Dist | Avail and / or Special
A-1

**DEFENCE RESEARCH ESTABLISHMENT OTTAWA**
**REPORT NO. 1015**

**PCN**
**041LJ**

**August 1989**
**Ottawa**

## ABSTRACT

Until very recently the Transit satellite positioning system was the only accurate navigation system available on a (practically) global basis. Therefore Transit is a commonly used navigation aid and was included in the DREO developed Marine Integrated Navigation System (MINS-B II) and Primary Land Arctic Navigation System (PLANS). MINS and PLANS are both Kalman filter based multi-sensor optimally integrated navigation systems and as such require detailed stochastic and deterministic error models for all of their sensors. This paper provides a detailed geometric derivation of the deterministic error model relating the position error of a Transit satellite Doppler position fix (or similarly a SARSAT fix) to the error in the velocity and height that is fed into the Transit receiver (or assumed for the SARSAT transponder). This error model is presented in the form of explicit functions of variables which are normally provided by a Transit receiver with each position fix, namely the satellite maximum elevation angle, the satellite direction of travel and the receiver latitude. Sample plots of these sensitivity functions are presented, along with experimental results for verification. This model is used in MINS and PLANS to form the Kalman filter measurement error sensitivity matrices.



## RÉSUMÉ

Jusqu'à très récemment, le système de positionnement par satellite Transit était le seul système de navigation précis disponible pratiquement partout. Par conséquent, Transit est un aide à la navigation utilisé communément et a été inclus dans le Système de Navigation Intégré pour la Marine (SNIM-B II) et pour le Système de Navigation Primaire pour la Terre Arctique (SNPTA) développés par le CRDO. SNIM et SNPTA sont tous deux des systèmes de navigation intégrés da façon optimum utilisant de multiples détecteurs basés sur le filtre Kalman, et commes tels, requièrent des modèles stochastiques et déterministiques détaillés par les erreurs pour tous les détecteurs. Cet article fournie une dérivation géométrique détaillée d'un modèle pour l'erreur déterministique reliant l'erreur sur la position d'un satellite Transit par un fix Doppler (ou de façon similaire un fix SARSAT) à l'erreur sur la vitesse et la hauteur qui est communiqué au receveur Transit (ou assumée pour le transpondeur SARSAT). Ce modèle pour l'erreur est présenté sous la forme de fonctions explicites de variables qui sont normalement fournis par le receveur Transit avec chaque fix sur la position, e.g. l'angle d'élévation maximum du satellite, la direction de la trajectoire du satellite et la latitude de receveur. Des graphiques échantillons de ces fonctions de sensibilité sont présentés, avec des résultats expérimentaux pour vérification. Ce modèle est utilisé pour SNIM et SNPTA pour former des mesures du filtre Kalman pour des matrices de sensibilité des erreurs.

## EXECUTIVE SUMMARY

Transit is a satellite based navigation system, which was originally developed for the U.S. Navy Polaris submarine fleet by the Applied Physics Lab of John Hopkins University. The system has been operational since 1964, and was released for public use in 1967.

The Transit Satellite positioning system basically consists of 5 or 6 satellites in circular polar orbits, with an orbital height of about 1,075 km, and a 107 minute period. These satellites transmit continuously at two very stable frequencies (150 MHz and 400 MHz). An earthbound receiver can obtain a position fix whenever a satellite passes overhead by measuring the Doppler frequency shifts due to the relative motion as the satellite rises towards the receiver, passes over and sets away from the receiver. The transmitted signal is modulated with a data message which contains ephemerides and timing marks. From this message the receiver can accurately calculate the absolute position and velocity of the satellite throughout the pass. From this known satellite position and velocity profile, and the Doppler derived relative velocity profile, the receiver can calculate its own position.

In order to calculate its position however, the receiver must be able to remove the effect of its own velocity from the Doppler measurement. Thus the receiver must either be stationary during the satellite pass, as is the case with survey instruments, or the receiver motion (velocity) relative to the earth must be known during the pass. Generally then, the receiver must be continuously fed the receiver velocity. Any error in this velocity input will lead to an error in the position fix that the receiver produces. The exact relationship between this velocity input error and position output error is the primary concern of this paper. This relationship is needed primarily for use in Kalman filter based integrated navigation systems, where velocity and position errors are estimated. DREO has developed two such multi-sensor systems: MINS (Marine Integrated Navigation System) and PLANS (Primary Land Arctic Navigation System), which use Transit as one of their sensors.

There is another important source of error that can be modelled in a similar manner, namely the position error that is caused by the error in the height above sea level that is provided to the receiver. Although it is possible to use the Doppler measurements to solve for the three dimensional position of the receiver (four dimensional if time is included), the accuracy is very poor in the direction that is orthogonal to the satellite velocity vector and to the receiver-satellite range

vector. The "error ellipsoid" is therefore very prolate, being elongated in this one direction and narrow in the others. This would generally cause an uncertainty in all three spatial dimensions. Fortunately it is possible to solve this problem by providing the receiver with height above a reference ellipsoid ("sea level"). This height surface will intersect the error ellipsoid in a small, nearly circular error ellipse, (except in the case when the major axis of the ellipsoid is near the horizontal plane in which case the satellite maximum elevation angle is close to 90 degrees and the receiver will be unable to solve for position). Therefore most Transit receivers require the user to supply a height input (a constant for marine applications) and consequently any error in this height will produce a position error.

This report provides a complete derivation of the explicit linear relationship between the velocity and height error input and the position error output of a Transit receiver. The derivation is geometric in nature, and provides some useful insights along the way. A strictly analytical approach was not used because it seemed too intractable, and without intermediate verifiable steps. Therefore the geometric approach was taken, which although more intuitively complicated, had the great benefit of having intermediate results which had clear physical significance and could be verified to some extent. Thus through a combination of elementary spherical geometry, planar geometry and differential techniques, the required exact linear relations were found in the form of a 2x3 matrix, whose components are explicit functions of 4 parameters which are normally provided by the Transit receiver with its position fix (the maximum satellite elevation angle, the receiver latitude, the satellite north-south directions of travel and east-west direction from the receiver).

An algorithm is given to efficiently calculate this error relationship. Numerical results are presented to illustrate the functional dependence of the sensitivity matrix elements. One significant new result shown is the substantial change in these functions at high latitudes. The qualitative error models shown in the literature are therefore seen to be invalid, even qualitatively, at high latitudes. Substantial experimental results are presented which verify the high fidelity of the model for all satellite directions of travel, at all satellite elevation angles, at mid-latitudes.

One of the intermediate results found in this way was a lower bound which can be placed on the maximum elevation angle of a satellite pass, as a function of receiver latitude. This provides a consistency check on the elevation angle provided as part of the Transit fix data set. Upper and lower bounds were also found for the range to the satellite subpoint, which can be used to justify linearization.

TABLE OF CONTENTS



CONTINUED...

TABLE OF CONTENTS (CONTINUED)

## LIST OF FIGURES

page

## LIST OF TABLES

## 1.0 INTRODUCTION

Transit is a satellite based navigation system, which was originally developed for the U.S. Navy Polaris submarine fleet by the Applied Physics Lab of John Hopkins University. The system has been operational since 1964, and was released for public use in 1967. Reference [1] gives a more complete description.

The Transit Satellite positioning system basically consists of 5 or 6 satellites in circular polar orbits, with an orbital height of about 1,075 km, and a 107 minute period. These satellites transmit continuously at two very stable frequencies (150 MHz and 400 MHz). An earthbound receiver can obtain a position fix whenever a satellite passes overhead by measuring the Doppler frequency shifts due to the relative motion as the satellite rises towards the receiver, passes over and sets away from the receiver. The transmitted signal is modulated with a data message which contains ephemerides and timing marks. From this message the receiver can accurately calculate the absolute position and velocity of the satellite throughout the pass. From this known satellite position and velocity profile, and the Doppler derived relative velocity profile, the receiver can calculate its own position. Section 4.0 below gives more details.

In order to calculate its position however, the receiver must be able to remove the effect of its own velocity from the Doppler measurement. Thus the receiver must either be stationary during the satellite pass, as is the case with survey instruments, or the receiver motion (velocity) relative to the earth must be known during the pass. Generally then, the receiver must be continuously fed the receiver velocity. Any error in this velocity input will lead to an error in the position fix that the receiver produces. The exact relationship between this velocity input error and position output error is the primary concern of this paper, and is derived in Sections 6.1 to 6.4 below.

There is another important source of error that can be modelled in a similar manner, namely the position error that is caused by the error in the height above sea level that is provided to the receiver. Although it is possible to use the Doppler measurements to solve for the three dimensional position of the receiver (four dimensional if time is included), the accuracy is very poor in the direction that is orthogonal to the satellite velocity vector and to the receiver-satellite range vector. The "error ellipsoid" is therefore very prolate, being elongated in this one direction and narrow in the others. This would generally cause an uncertainty in all three spatial dimensions. Fortunately it is possible to solve this problem by providing the receiver with height above a reference ellipsoid ("sea level"). This height surface will intersect the error

ellipsoid in a small, nearly circular error ellipse, (except in the case when the major axis of the ellipsoid is near the horizontal plane in which case the satellite maximum elevation angle is close to 90 degrees and the receiver will be unable to solve for position). Therefore most Transit receivers require the user to supply a height input (a constant for marine applications) and consequently any error in this height will produce a position error.

This report describes the linearized relationship between the velocity and height error input and the position error output. This relationship is expressed in the form of a sensitivity matrix H, where:

$$\begin{pmatrix} \text{north position error} \\ \text{east position error} \end{pmatrix} = \begin{pmatrix} h11 & h12 & h13 \\ h21 & h22 & h23 \end{pmatrix} \begin{pmatrix} \text{height error} \\ \text{north velocity error} \\ \text{east velocity error} \end{pmatrix} \quad (1)$$

or

$$\begin{pmatrix} \Delta N \\ \Delta E \end{pmatrix} = \begin{pmatrix} h11 & h12 & h13 \\ h21 & h22 & h23 \end{pmatrix} \begin{pmatrix} \Delta h \\ \Delta vn \\ \Delta ve \end{pmatrix} \quad (2)$$

where difference "$\Delta$" is defined to be the true value minus the estimate. For example:

$$\Delta N \equiv N - \hat{N}$$

As shall be shown, the components of this sensitivity matrix H are complicated functions of the satellite maximum elevation angle, the satellite direction of travel (north to south or vice versa), the receiver latitude, and whether the satellite subpoint is east or west of the receiver at maximum elevation. These parameters are defined in the next section.

The relationship defined by equation (2) is not only useful in predicting accuracies, but forms an important part of the measurement matrix for a Kalman filter. The measurement equation of a Kalman filter has the form:

$$Z = H(X) + V \qquad (3)$$

which relates the state vector X, of quantities that the filter is trying to estimate, to the measurement vector Z of quantities fed into the filter, and the measurement noise vector V. In a linear filter the vector-valued function H(X) is simply the product of a "measurement matrix" H with the state vector X, and the measurement equation becomes:

$$Z = H X + V \qquad (4)$$

At DREO we have developed two Kalman filter based optimally integrated navigation systems which utilize Transit measurements: a Marine Integrated Navigation System (MINS), described in reference [2], and a Primary Land Arctic Navigation System (PLANS), described in reference [3]. It was for these two systems that this detailed error model was developed. In 1983 the author first developed an implicit error model, for use in MINS. The numerical results were presented at reference [4] and are essentially the same as the results shown in Section 9.0 below. The explicit error model derived in this report was developed in 1989, for the PLANS ADM. This explicit model leads to a much more efficient algorithm, and greater confidence in the results.

This error model is particularly important for the PLANS application, where the relationship given by equation (2) is in effect partially inverted to solve for an otherwise unbounded velocity error. This velocity error arises in high latitude operations between the geographic and geomagnetic poles where an accurate heading cannot be reliably obtained, either magnetically or with a gyrocompass.

A geometric approach is taken in deriving the H matrix of equation (3), and some preliminary geometric quantities must be defined first.

## 2.0 DEFINITIONS

Table 1 lists the relevant variables and parameters while Figure 1 illustrates the primary quantities of interest. Note that vectors are underlined. The magnitude of a vector is represented by the vector symbol without the underline.

Table 1: Summary of Relevant Variables.

| | |
|---|---|
| **PRIMARY VARIABLES: (whose relationships are sought)** | |
| $\underline{\Delta v}$ | receiver velocity error (true - estimate) |
| $\Delta\alpha$ | heading of receiver velocity error (not heading error) |
| $\Delta h$ | Receiver height error |
| $\underline{\Delta r}$ | receiver position error ($\Delta N, \Delta E$) |
| $\Delta N$ | North position error of receiver (due to $\Delta v$, $\Delta\alpha$ & $\Delta h$) |
| $\Delta E$ | East position error of receiver (due to $\Delta v$, $\Delta\alpha$ & $\Delta h$) |
| **SECONDARY: (available directly from the receiver if needed)** | |
| $\underline{r}$ | Receiver position vector (latitude $\lambda$, longitude L) |
| $v$ | Receiver speed |
| $\alpha$ | Receiver heading |
| $h$ | Receiver height |
| $\sigma$ | Satellite maximum elevation angle |
| NS | satellite north-to-south direction of travel (at PCA) ( = 1 if towards the south, -1 if towards the north ) |
| EW | satellite east-to-west direction from receiver (at PCA) ( = 1 if towards the east, -1 if towards the west ) |
| **INTERMEDIATE: (derived from secondary variables if needed)** | |
| $\underline{s}$ | Satellite position vector |
| $\underline{p}$ | Satellite subpoint position vector ($\lambda p$, Lp) |
| $\rho$ | slant range from receiver to satellite |
| $\Theta$ | subpoint/ receiver separation angle (at earth centre) |
| $\psi$ | bearing (from north) to subpoint from receiver |
| $\phi$ | bearing (from north) to receiver from subpoint |
| $\beta$ | heading (from north) of subpoint track at subpoint |
| $\gamma$ | angle between slant range and satellite velocity |
| $\eta$ | angle between slant range and receiver velocity error |
| $\nu$ | angle from receiver velocity error to subpoint at r |
| $\underline{V}$ | satellite velocity vector |

Note: all these quantities are defined in an earth fixed frame.

**Figure 1. Primary Variables of a Transit Satellite Pass (in earth fixed coordinates).**

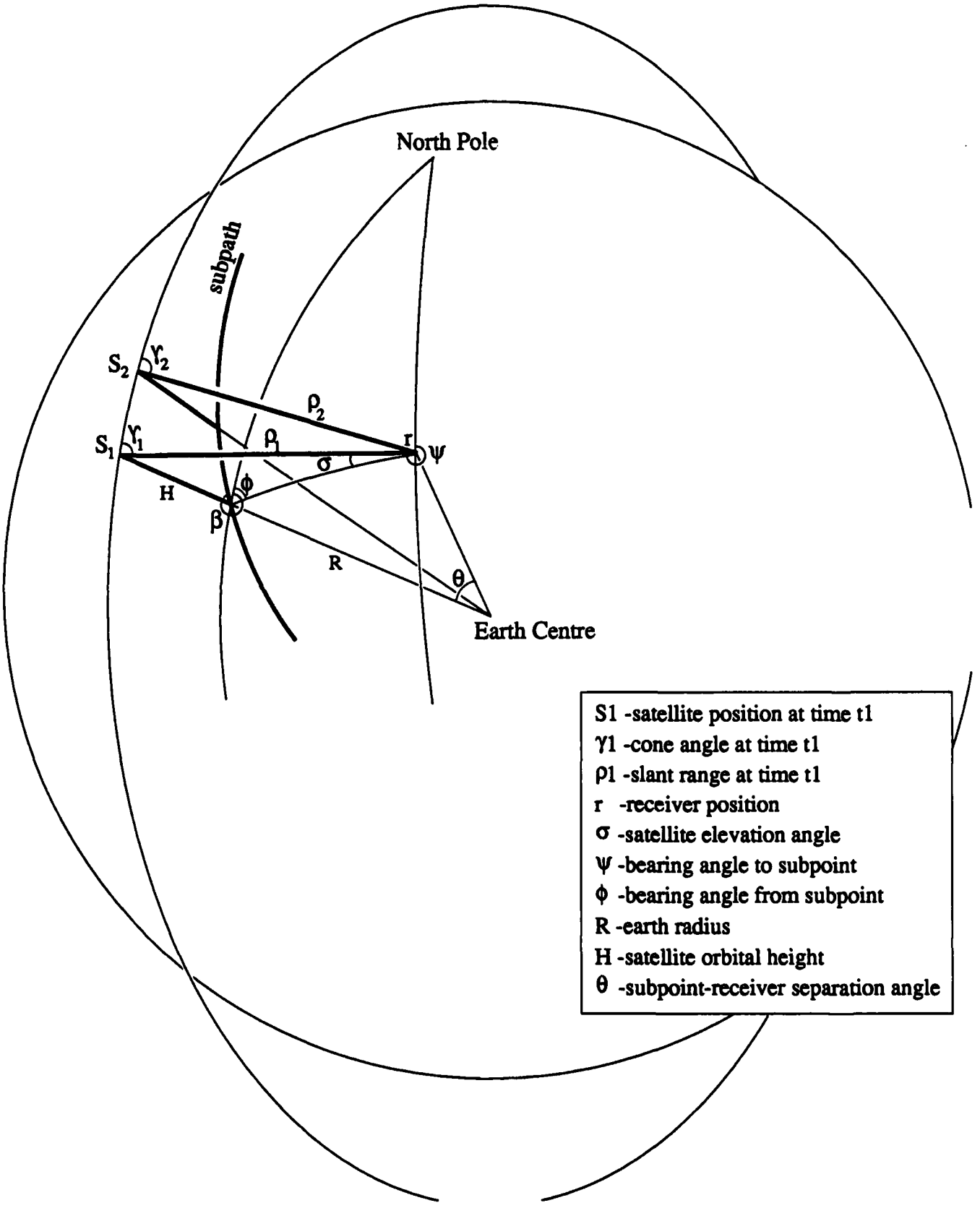

Table 2: Relevant Constants.

| | | |
|---|---|---|
| R | earth radius | = 6,370,000 metres |
| H | satellite orbital height | = 1,075,000 metres |
| Vs | satellite "speed" | = 7,290 m/s |
| $\omega$ | earth rate | = 0.0000729211585 radians/sec. |

This satellite "speed" Vs is constant in an earth centred non-rotating frame (not earth fixed). When earth rate at orbital height is added to this, the correct earth fixed speed is (since these velocity components are orthogonal):

$$V = \sqrt{Vs^2 + (R+H)^2\omega^2\cos^2\lambda p} \qquad (5)$$

$$= \sqrt{7{,}290^2 + 543^2\cos^2\lambda p} \qquad (6)$$

thus

$$7{,}290 \text{ m/s} \leq V \leq 7{,}310 \text{ m/s} \qquad (7)$$

All quantities (except Vs as just explained) are defined in an earth fixed reference frame. Figure 1 shows a receiver at point $\underline{r}$, moving with speed $\underline{v}$ and heading $\alpha$, a satellite moving south to north in a polar orbit. Two satellite positions are shown $\underline{s}1$ and $\underline{s}2$, for two points in time t1 and t2. The distance between the receiver and satellite is $\rho 1$ and $\rho 2$, and is called the slant range. Since the receiver velocity is assumed to be much smaller than the satellite velocity (as it would be in the marine and land vehicle applications of interest here), the change in receiver position between t1 and t2 is not visible here (a Transit satellite pass lasts less than 20 minutes, so that a land vehicle could not move more than about 30 to 40 kilometers, and in most cases would move much less).

The satellite subpoint is the point $\underline{p}$ on the surface of the earth directly below the satellite. Every satellite pass has a "point of closest approach" (PCA), which is the point (in time and space) at which the slant range is at its minimum. The path of the subpoint on the earth's surface is called the subpath. Since the satellite's orbit is fixed in an earth-centred

"inertial space" (ie. non-rotating) the subpath does not follow a meridian of longitude. The meridians are shown for the receiver and the subpoint, in order to define the bearing $\psi$ from the receiver to the subpoint, the bearing $\phi$ from the subpoint to the receiver, and the heading of the subpath $\beta$ (these are all clockwise angles from north). Also illustrated is the separation angle $\Theta$, at the centre of the earth between the receiver and the subpoint.

It will be seen that a very important variable is the "elevation angle" $\sigma$, which is the angle at the receiver from the slant range vector to the locally horizontal plane. As shall be seen, the maximum elevation angle corresponds to the PCA. Another important variable is the "satellite direction of travel" which is really two logical variables simply indicating whether the satellite is moving north to south or vice versa (NS), and whether the PCA is east or west of the receiver's meridian (EW). If the PCA is on (or very close to) the receiver's meridian then the geometry does not allow a position fix to be made.

Some symbolic conventions will be used: in general the error in a quantity x is represented by using the prefix $\Delta$, as in $\Delta x$, a differential error is represented by the prefix $\delta$, as in $\delta x$, and an infinitesimal time difference is represented by the prefix d, as in dx.

## 3.0 ASSUMPTIONS

In this mathematical derivation, all important assumptions shall be explicitly stated, and any approximations clearly pointed out.

In order to apply spherical trigonometry it shall be assumed that the satellites are all in circular polar orbits and that the earth is spherical. The earth is actually slightly oblate, with the best fitting ellipsoid (World Geodetic Survey 1984) having semi major axis A and semi minor axis B of lengths

$$A = 6{,}378{,}137 \text{ metres}$$
$$B = 6{,}356{,}752 \text{ metres} \qquad (8)$$

respectively, therefore having a small eccentricity of

$$e = \frac{\left(A^2 - B^2\right)^{1/2}}{A} = 0.08 \qquad (9)$$

This is close enough to being spherical for the purpose of determining the desired error relationship, which is essentially a local phenomenon. The eccentricity of a typical Transit satellite orbit is even smaller, at about 0.002. The deviation from a polar orbit is usually expressed as the orbital inclination angle, which is the angle between the orbital plane and the equatorial plane. For Transit this is typically well within half a degree of polar (90 degrees).

To obtain the linear relationship of equation (1), using differential techniques, it shall be assumed that the Transit position fix is made using relative velocity measurements (Doppler) in a neighbourhood of the point of closest approach (PCA). The PCA is a point in time that typically occurs near the centre of the satellite pass, when the distance between the satellite and the receiver is a minimum (hence the satellite velocity in the receiver reference frame is orthogonal to the receiver-satellite range vector). Receivers actually use Doppler measurements over the duration of the satellite pass, which is from 10 to 16 minutes, typically forming one Doppler count measurement every 23 seconds. Although this is the most serious simplifying assumption, it is justified on the grounds that the satellite pass is approximately symmetric about the PCA and therefore the effects of the different geometry on the two sides of the PCA should approximately cancel.

This appears to carry the implicit assumption that the velocity and height errors are constant over the satellite pass, but this is really not a restriction if we use the average error values in (1). The linearity of (1) permits averaging on both sides.

It is also necessary to assume that the receiver velocity error is small compared to the satellite velocity ( $v \ll V$ ) which in light of (7) is not a serious restriction for the usual terrestrial and marine applications. This is to ensure that the error relationship of equation (3) is linear, as in (1).

There are many equivalent ways to calculate receiver position, given the satellite position and Doppler measurements over an interval. In this report a largely geometric rather than analytic solution shall be used, where the various sources of error and the intermediate quantities that must be calculated, have clear physical interpretations that are easily understood. This also facilitates verification.

## 4.0 TRANSIT POSITIONING

### 4.1 Stationary Receiver

For a stationary receiver $\underline{r}$, in an earth fixed frame, Figure 2 illustrates geometrically how a Transit position fix can be obtained.

A Transit Doppler measurement gives the rate of change of the range from the receiver to the satellite. From the transmitted ephemerides data the receiver knows the satellite position $\underline{s}$, and velocity $\underline{V}$, in an earth fixed reference frame. If the receiver position $\underline{r}$ is not moving in this frame, then the measured relative velocity (the rate of change of the slant range) $d\rho/dt$ is due entirely to the satellite velocity $\underline{V}$, which must therefore be at an angle $\gamma$ to the range line, as shown in Figure 2, where

$$\dot{\rho} = -V \cos\gamma \qquad (10)$$

(where a dot $\dot{}$ indicates d/dt). Equation (10) can then be solved for $\gamma$. Then $\underline{r}$ must lie on the cone defined by the angle $\gamma$ and the satellite velocity vector $\underline{V}$. Two Doppler measurements therefore define two such cones, at angles $\gamma 1$ and $\gamma 2$ about the respective satellite velocity vectors $\underline{V1}$ and $\underline{V2}$. The intersection of these two cones is a curve C, which becomes circular about the satellite in the limit as the time between measurements becomes small (so that $\underline{V1}$ approaches colinearity with $\underline{V2}$).

Assuming that $\underline{r}$ is on the earth's surface, or a surface of known height, then $\underline{r}$ must lie on the intersection of this surface and the curve C.

This intersection (of a circle and a sphere) will generally consist of two points, (provided that the satellite does not pass directly over the receiver, in which case the circle will be tangent to the sphere). The ambiguity can be resolved by a third Doppler measurement, because the satellite path is not coplanar in the earth fixed reference frame. Since we are interested here only in the effect of receiver velocity error on the position fix, it shall be assumed that this ambiguity has been resolved.

In fact these multiple Doppler measurements can in principle be used to solve for receiver height above geoid as well by intersecting different curves C. However the vertical geometric dilution of precision (VDOP) is generally such that the

**Figure 2. Transit Positioning, Stationary Receiver.**

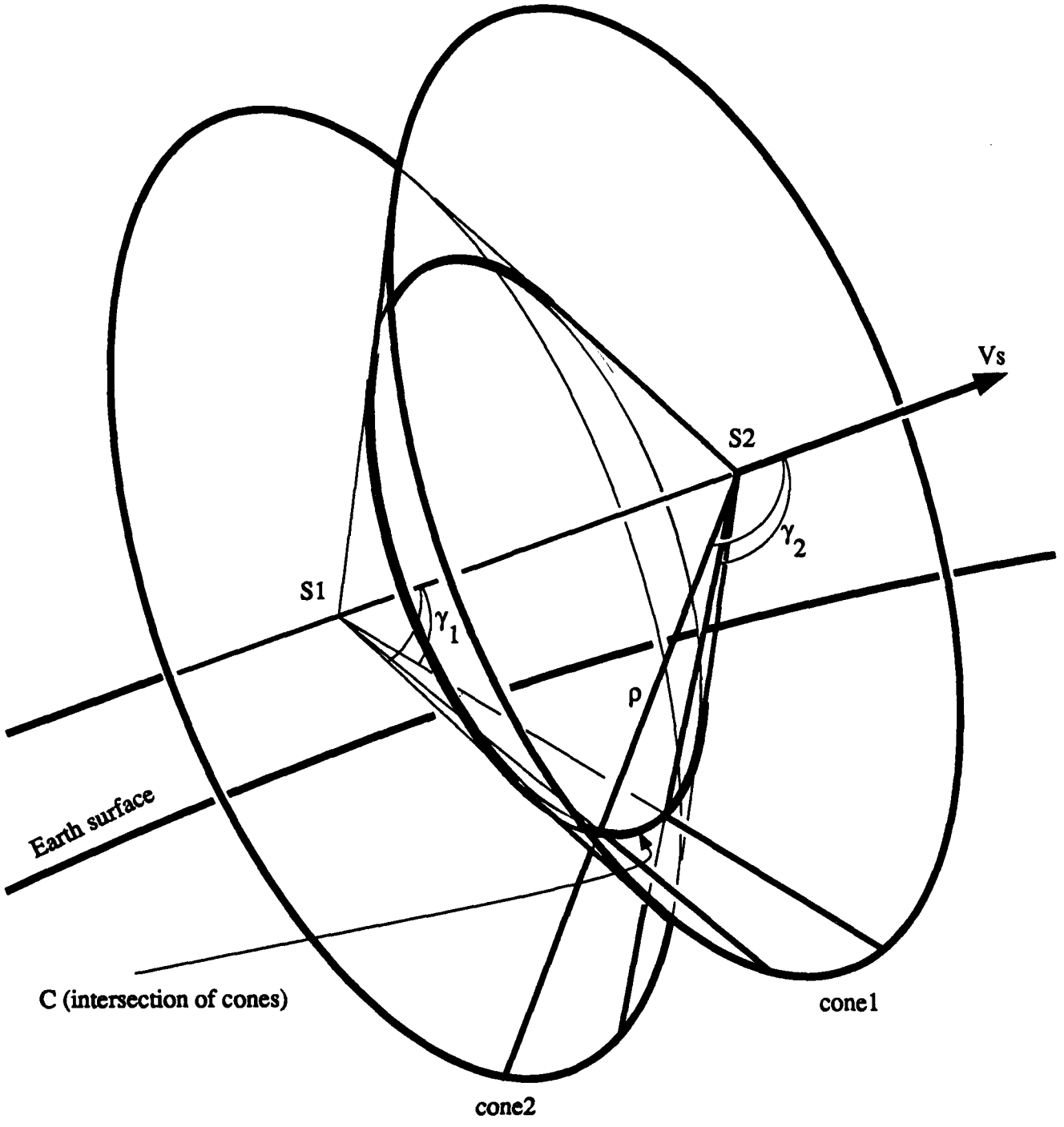

height obtained from a single pass would be very inaccurate since the curves C intersect at a sharp angle. This would degrade the horizontal solution since the curves C are not necessarily vertical. Therefore it is normal for Transit receivers to be given this height information from some external source.

## 4.2 Moving Receiver

If the receiver is moving in this earth fixed frame then there are several complications. First the measured Doppler shift must be compensated to remove the effect of receiver velocity before calculating the angles $\gamma 1$ and $\gamma 2$. This is accomplished by subtracting the component of the receiver's velocity in the direction of the slant range $v_r$ from the measured velocity $d\rho/dt$. Equation (10) then becomes:

$$-V \cos\gamma = \dot{\rho} - v_r \tag{11}$$

The receiver velocity component $v_r$ is shown in Figure 3 to be:

$$v_r = v \cos(\psi - \alpha)\cos\sigma \tag{12}$$

where v and $\alpha$ are the receiver speed and heading, and $\psi$ and $\sigma$ are as defined in Section 2.0 and shown in Figure 1 (the bearing to the subpoint and the elevation angle).

Secondly the receiver's position will have changed between times t1 and t2, and will therefore not be on the intersection of the cones. This can also be resolved by applying the appropriate translation to the first cone, as shown in Figure 4. The appropriate translation is of course the position change vector of the receiver, which for a small time interval is $v\Delta t$. This therefore also requires knowledge of the receiver velocity v, and in particular its component in the direction orthogonal to the slant range.

**Figure 3. Receiver Velocity Component $v_r$ in Satellite Direction.**

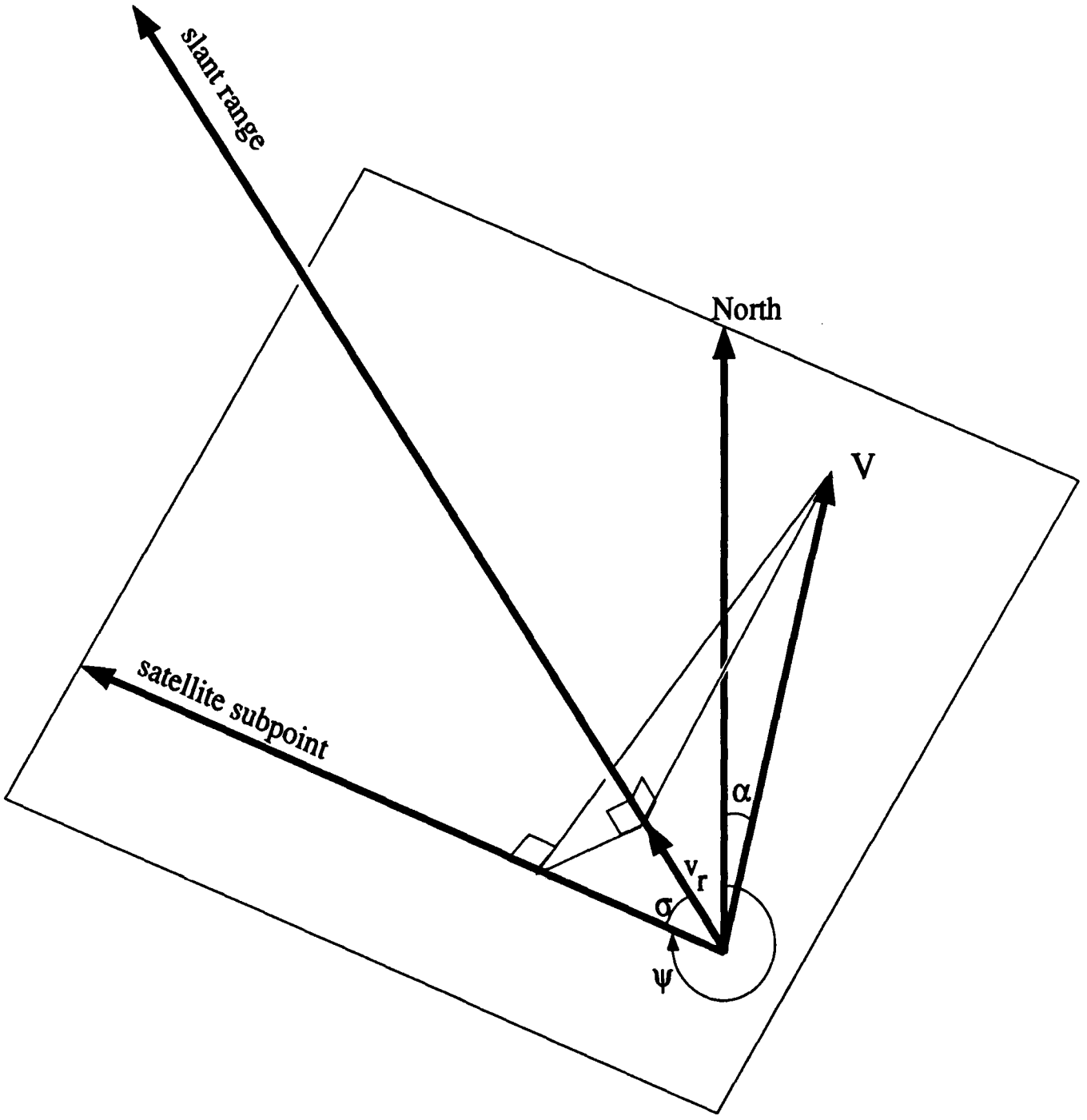

**Figure 4. Transit Positioning, Moving Receiver.**

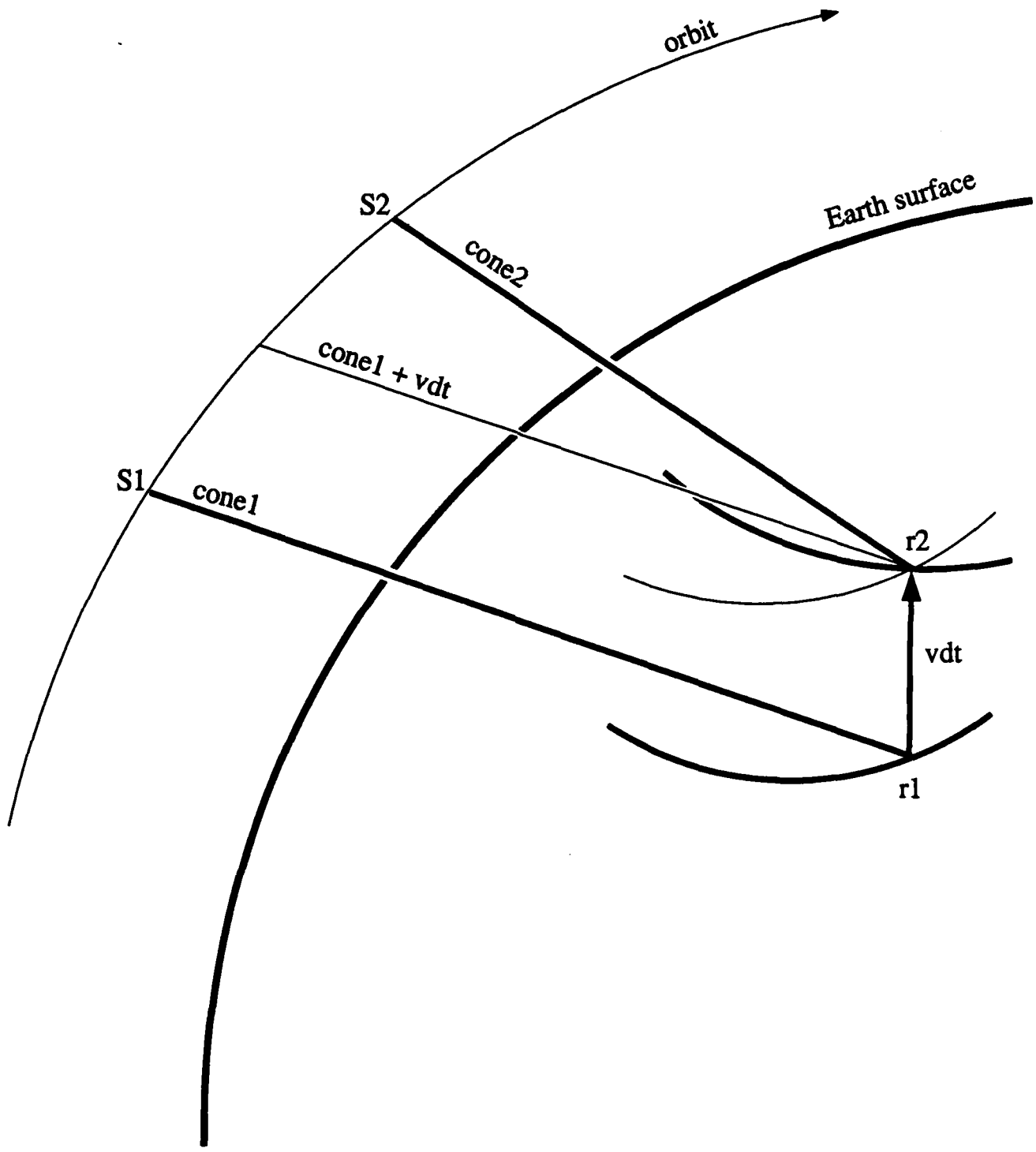

## 5.0 EFFECT OF ANTENNA HEIGHT ERROR

The position fix, as explained in Section 4.1, is found by intersecting the Doppler curve C (defined by the intersection of two Doppler cones as seen in Figure 2) with a surface of known height h above the earth's surface. The effect of an error in this height $\Delta h$, simply has the effect of moving the position fix along the curve C. If the height error is small compared to the satellite range, then this curve can be approximated by its tangent vector at the receiver location, as shown in Figure 5, where the correct position is r and the error in the estimated position is $\underline{\Delta r}$.

The effect of $\Delta h$ is then linear, in the direction of this tangent vector. Thus this simple geometric effect can be described in terms of the "bearing" and "elevation angle" of this tangent vector.

Assuming a circular orbit, the satellite velocity V is perpendicular to the vertical line sp from the satellite to its subpoint. At the PCA the satellite velocity V is also perpendicular to the slant range line sr from the satellite to the receiver (by definition of PCA). Therefore at the PCA, V is perpendicular to the plane srp containing the satellite, its subpoint and the receiver.

Since the Doppler curve C is perpendicular to V at PCA, and passes through r, it must also lie in the plane srp. Therefore, as shown in Figure 5 (where $\rho$, C and U are coplanar) the angle $\xi$ between the Doppler curve C and the vertical, is equal to the elevation angle $\sigma$ (since both are complementary to the angle between the slant range and the vertical). Also the bearing angle from $\underline{\Delta r}$ to north is $(\psi-\pi)$ (for a positive $\Delta h$, or just $\psi$ for a negative $\Delta h$), where $\psi$ is the bearing to the subpoint path.

Therefore the magnitude of the position error $\underline{\Delta r}$ caused by a height error $\Delta h$, satisfies:

$$\tan\sigma = \tan\xi = \Delta r/\Delta h \qquad (13)$$

(where this $\Delta r$ is defined to be positive away from the subpoint, and negative towards the subpoint, giving it the same sign as $\Delta h$). Thus

$$\Delta r = \Delta h \tan\sigma \qquad (14)$$

Taking components of $\underline{\Delta r}$ in the north and east direction, we have:

$$\Delta N = \Delta h \cos(\psi - \pi) \tan\sigma$$

$$= -\Delta h \cos\psi \tan\sigma \qquad (15)$$

$$\Delta E = \Delta h \sin(\psi - \pi) \tan\sigma$$

$$= -\Delta h \sin\psi \tan\sigma \qquad (16)$$

This gives us the first column of the H matrix of equation (2):

$$\begin{pmatrix} \Delta N \\ \Delta E \end{pmatrix} = \begin{pmatrix} -\cos\psi \tan\sigma \\ -\sin\psi \tan\sigma \end{pmatrix} \begin{pmatrix} \Delta h \end{pmatrix} \qquad (17)$$

(in the absence of velocity errors). The satellite elevation angle $\sigma$ is provided by the receiver. The bearing angle $\psi$ to the subpoint can be expressed in terms of the known quantities $(\lambda, \sigma, NS, EW)$ as shown in the appendices. Appendix A shows how $\psi$ can be expressed in terms of the intermediate variables $(\phi, \lambda p)$ and appendices A, B and C show how these intermediate variables can be expressed in terms of the known quantities.

**Figure 5. Effect of Height Error.**

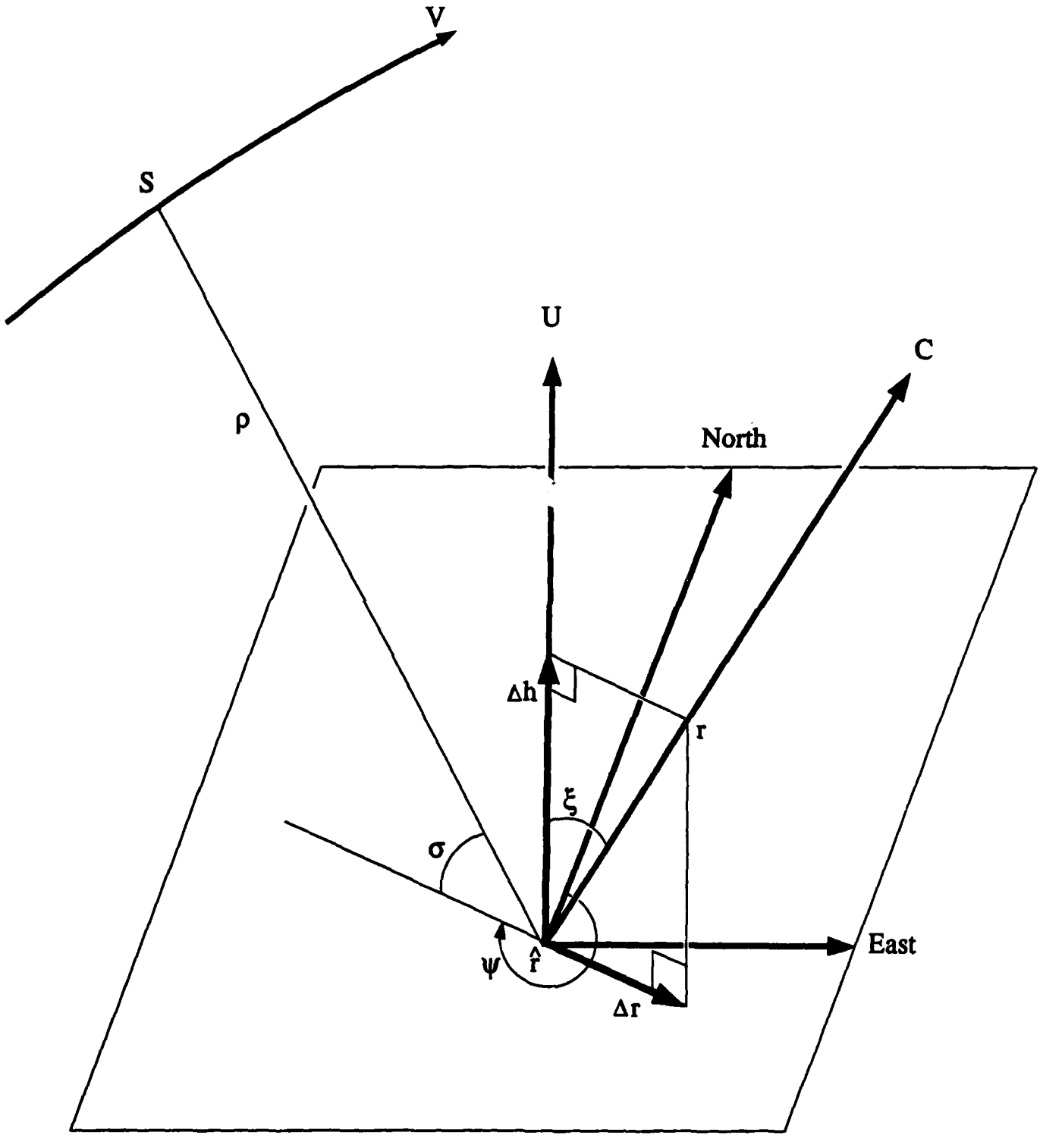

## 6.0 EFFECT OF VELOCITY ERROR

The error in the Transit position fix, due to the error in the receiver's estimate of its velocity, is decomposed into four separate and independent errors. As was explained in Section 4.2, the measured Doppler shift must be adjusted using the estimated receiver velocity component in the direction of the slant range, and the resulting lines of position (from successive Doppler measurements) must be subsequently adjusted using the receiver velocity in the direction orthogonal to the slant range. Any error in the estimates of these receiver velocity components will therefore lead to a position fix error. Two different effects arise from the velocity error parallel to the slant range (due to a constant error and a differential error) which are explained in detail in Sections 6.1 and 6.2 below. Two other effects arise from the velocity error orthogonal to the slant range, as described in detail in Section 6.3. Section 6.4 then summarizes the combined effect of the velocity error on Transit position.

### 6.1 Velocity Error Parallel to the Slant Range

The first error will be called $\Delta\underline{r}1$, and is due to the effect of a constant velocity error component in the direction of the slant range $\underline{\rho}$ from the satellite to the receiver. This component of the velocity error directly effects the Doppler measurement, and therefore introduces an error in the calculation of the cone angle $\gamma$ (between the slant range and the satellite velocity vector) as found from equations (10) and (11).

In this subsection we will find the relationship between this velocity error and the resulting position error, as in equation (2) (assuming zero height error). To do this we first express the position error ($\Delta N, \Delta E$) as a function of the Doppler cone angle error $\Delta\gamma$, and then we express the Doppler cone angle error as a function of the velocity error ($\Delta vn, \Delta ve$).

#### 6.1.1 Magnitude of $\Delta\underline{r}1(\Delta\gamma)$

In expressing the position error $\Delta\underline{r}1$ as a function of the cone angle error $\Delta\gamma$, we first find its magnitude, then its direction.

Figure 6a shows how a constant cone angle bias $\Delta\gamma$ (true - estimate) causes the position estimate to shift in the direction orthogonal to the slant range vector $\underline{\rho}$ in the locally horizontal

**Figure 6a. Error1: Due to Cone Angle Bias**
**(Velocity Error Parallel to Slant Range)**

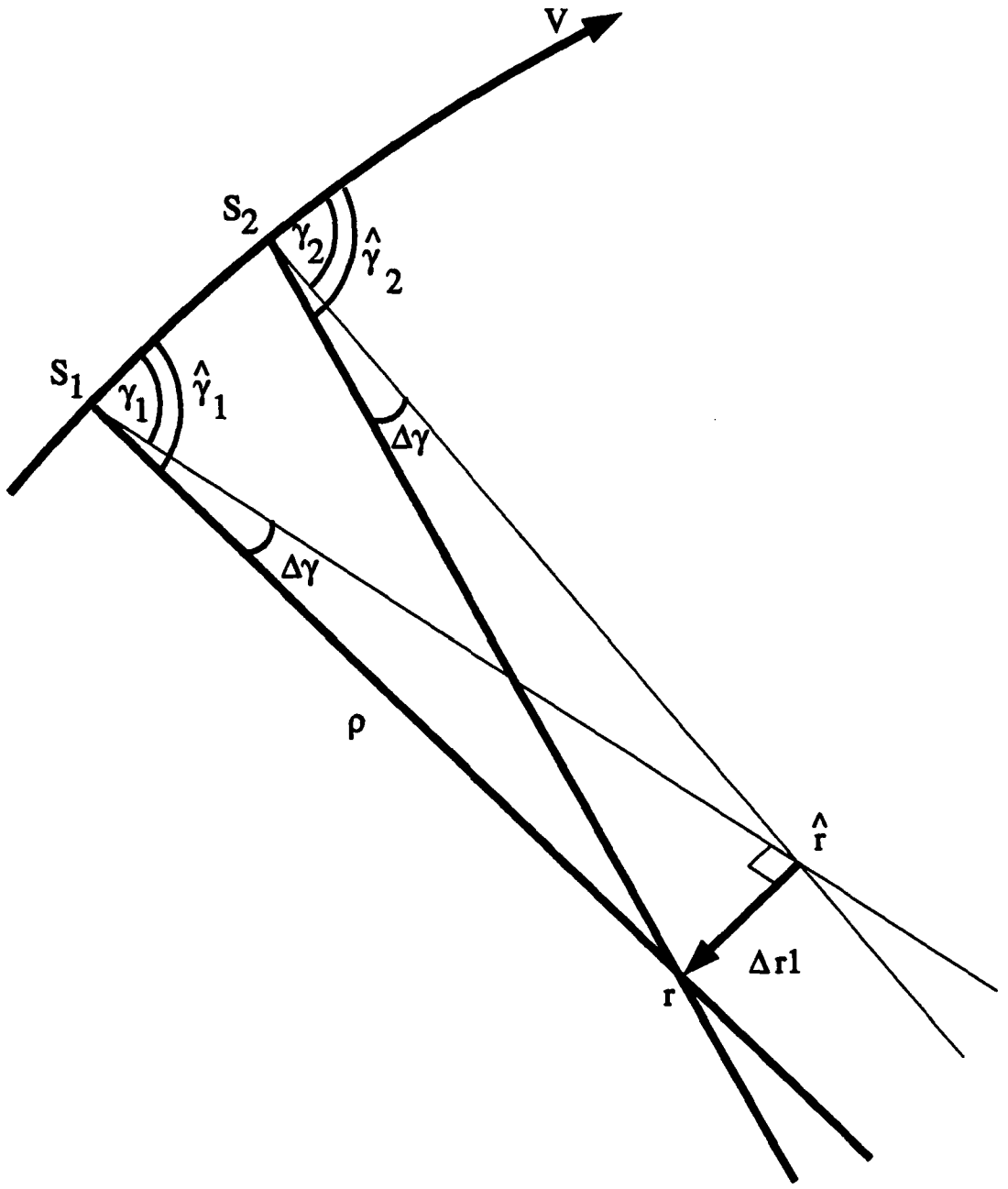

plane. From this we can see that for small errors $\Delta\gamma$, the position error vector

$$\underline{\Delta r1} \equiv \underline{r} - \underline{\hat{r}} \tag{18}$$

has magnitude

$$\Delta r1 \equiv |\underline{\Delta r1}| = \rho \sin|\Delta\gamma| \tag{19}$$

### 6.1.2 Direction of $\underline{\Delta r1}$

Figure 6a shows how a constant cone angle bias $\Delta\gamma$ (true - estimate) causes the position estimate to shift in the direction orthogonal to the slant range vector $\underline{\rho}$ (in the local horizontal plane at the receiver).

Figure 6b shows the situation at the receiver in more detail. Since the bearing to the subpoint is $\psi$, the horizontal projection of the slant range vector $\underline{\rho}$ is in the direction $\psi$. Thus the position error $\underline{\Delta r1}$, which is orthogonal to the direction $\psi$, is either in the direction $(\psi+\pi/2)$ or $(\psi-\pi/2)$.

Thus we can see that the north and east components of this position error are:

$$\begin{pmatrix}\Delta N\\ \Delta E\end{pmatrix}_1 = \begin{pmatrix}\Delta r1\cos(\psi\pm\pi/2)\\ \Delta r1\sin(\psi\pm\pi/2)\end{pmatrix} \tag{20}$$

where the actual sign of $\pm$ is yet to be determined.

At the point of closest approach $\underline{\rho}$ is also orthogonal to the satellite velocity vector $\underline{V}$ (which is approximately northward or southward, depending on the sign of the parameter NS). Again from Figure 6a we can see that the error $\underline{\Delta r1}$ (true - estimate) induced by a positive constant cone angle bias $\Delta\gamma$, is roughly in the direction $-\underline{V}$. Similarly a negative $\Delta\gamma$ would cause an error $\underline{\Delta r1}$ in the general direction of $\underline{V}$.

**Figure 6b. Geometry of Error1.**

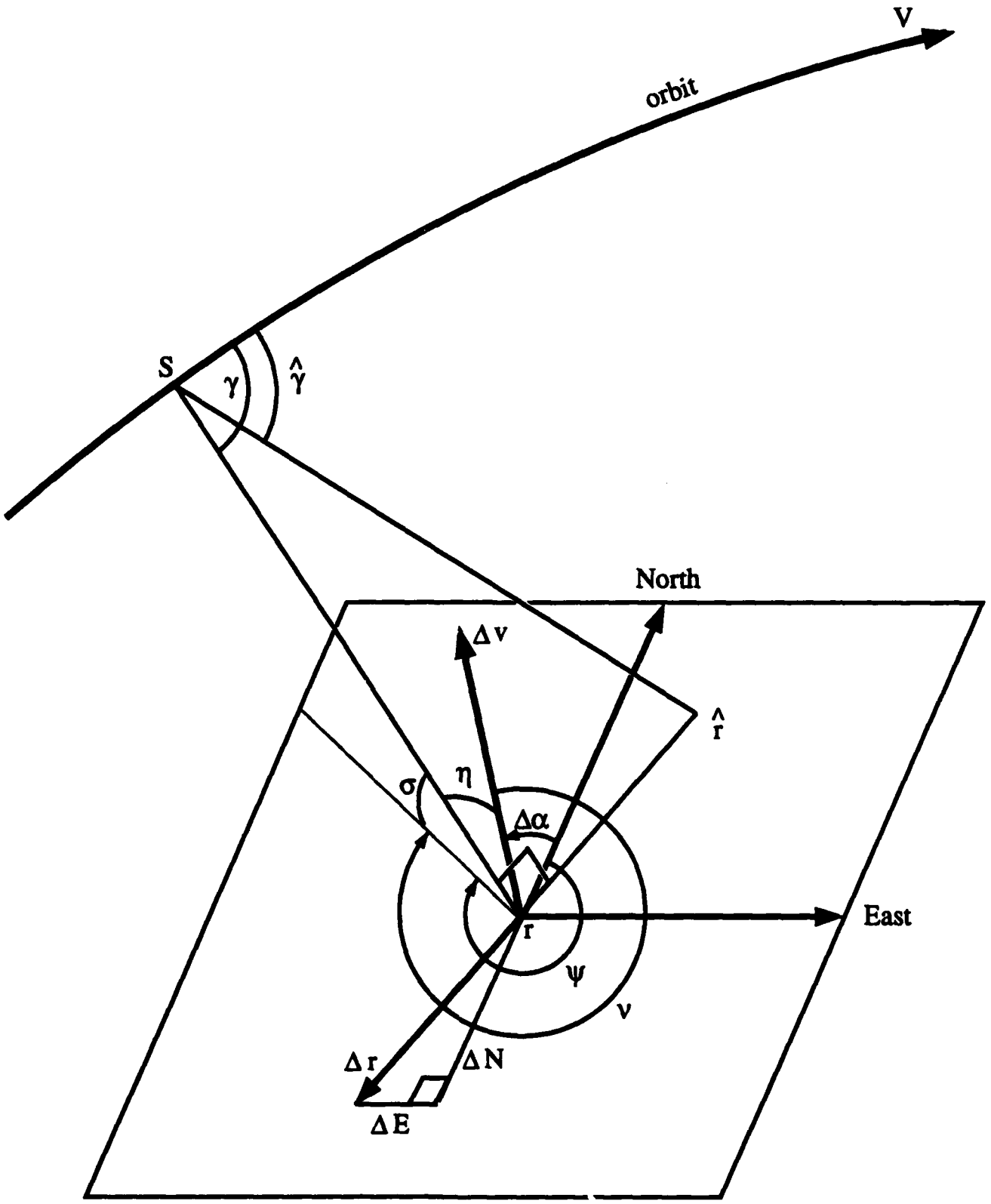

The actual direction of $\Delta\underline{r}1$, as seen from Figure 6b is $(\psi-\pi/2)$ rather than $-\underline{V}$ and $(\psi+\pi/2)$ rather than $\underline{V}$. This is the case where the satellite is west of the receiver. The situation is the reverse if the satellite is east of the receiver: the direction of $\Delta\underline{r}1$ is $(\psi+\pi/2)$ when $\Delta\gamma$ is positive, and $(\psi-\pi/2)$ when $\Delta\gamma$ is negative. This east-west relationship between the satellite and the receiver is contained in the parameter EW, which is provided by the receiver as part of the position fix data.

Thus the direction of $\Delta\underline{r}1$ (the sign of $\pi/2$ in (20)), is determined entirely by $\psi$, the sign of $\Delta\gamma$, the direction of $\underline{V}$, and EW. Appendix D provides the expressions needed to find $\psi$ (actually only $\sin\psi$ and $\cos\psi$ are needed). The sign of $\Delta\gamma$ will be derived in the next section, and for now can be expressed as $\Delta\gamma/|\Delta\gamma|$. The direction of $\underline{V}$ for this purpose is contained in the variable NS (which is +1 if the satellite is moving southward and -1 if moving northward).

A change in sign of NS corresponds to a change in direction of $\underline{V}$ and hence a change in direction of $\Delta\underline{r}1$. A change in sign of $\Delta\gamma$ has the same effect on $\Delta\underline{r}1$. Therefore we can write

$$\mu = \psi \pm \frac{NS\cdot EW\cdot\Delta\gamma}{|\Delta\gamma|}\,\pi/2 \qquad (21)$$

where now the $\pm$ has a constant value.

Careful consideration of the example shown in Figure 6b indicates that the correct value is negative. In the case illustrated by Figure 6b a receiver velocity error $\Delta\underline{v}$, with a component towards the satellite, has caused a positive cone angle error $\Delta\gamma$ (the Doppler cone angle estimated is too small, as seen from equation 11). This positive $\Delta\gamma$ moves the position fix, $\underline{f}$, in the direction $\psi+\pi/2$. This corresponds to a position error vector, $\Delta\underline{r}1$, in the opposite direction, $\psi-\pi/2$.

Thus the sign in (20) should be negative in the situation illustrated by Figure 6b. In this case the satellite is on the south-to-north half of its orbit (NS=-1) and the receiver is east of the satellite subpoint (EW=-1). The cone angle error $\Delta\gamma$ here is positive. Thus the sign in (21) must be negative, so that (20) can be rewritten:

$$\begin{pmatrix}\Delta N\\ \Delta E\end{pmatrix}_1 = \begin{pmatrix}\Delta r1\,\cos\left(\psi - \frac{NS\cdot EW\cdot\Delta\gamma}{|\Delta\gamma|}\,\pi/2\right)\\ \Delta r1\,\sin\left(\psi - \frac{NS\cdot EW\cdot\Delta\gamma}{|\Delta\gamma|}\,\pi/2\right)\end{pmatrix} \qquad (22)$$

Careful use of reduction formulae reduces (22) to

$$\begin{pmatrix} \Delta N \\ \Delta E \end{pmatrix}_1 = NS \cdot EW \cdot \frac{\Delta\gamma}{|\Delta\gamma|} \begin{pmatrix} \Delta r1 \sin\psi \\ -\Delta r1 \cos\psi \end{pmatrix} \qquad (23)$$

In the last subsection we found the magnitude of the position error $\Delta r1$, given by equation (19). Substituting this into (23) yields:

$$\begin{pmatrix} \Delta N \\ \Delta E \end{pmatrix}_1 = NS \cdot EW \cdot \frac{\Delta\gamma}{|\Delta\gamma|} \begin{pmatrix} \rho \sin|\Delta\gamma| \sin\psi \\ -\rho \sin|\Delta\gamma| \cos\psi \end{pmatrix} \qquad (24)$$

or

$$\begin{pmatrix} \Delta N \\ \Delta E \end{pmatrix}_1 = NS \cdot EW \begin{pmatrix} \rho \sin\Delta\gamma \sin\psi \\ -\rho \sin\Delta\gamma \cos\psi \end{pmatrix} \qquad (25)$$

It remains now to find $\Delta\gamma$ as a function of the velocity error.

### 6.1.3 Cone Error as a Function of Velocity Error

Now to find the relationship between the velocity error ($\Delta vn$, $\Delta ve$) and the cone angle error, $\Delta\gamma$, we use equation (10), which relates the range rate $d\rho/dt$ to the cone angle. We can see how their errors are related by differentiating (10) with respect to $\gamma$:

$$\frac{\partial\dot{\rho}}{\partial\gamma} = V \sin\gamma \qquad (26)$$

so that for small $\Delta\dot{\rho}$

$$\Delta\dot{\rho} \simeq V \sin\gamma \, \Delta\gamma \tag{27}$$

$$\therefore \quad \Delta\gamma \simeq \frac{\Delta\dot{\rho}}{V \sin\gamma} \tag{28}$$

This shows the expected change in $\gamma$ due to satellite motion along a straight line, as a function of the expected change in $d\rho/dt$ (a purely geometric relationship).

Now the error (true - estimate) in range rate $\Delta\dot{\rho}$ caused by a velocity error $\Delta\underline{v}$, is the projection of the velocity error $\Delta\underline{v}$ along the slant range vector, as seen from Figure 6b (where the angle $\nu$ is in the locally horizontal plane, and $\sigma$ is in a locally vertical plane):

$$\Delta\dot{\rho} = \Delta v \cos\eta \tag{29}$$

where $\Delta v \equiv |\Delta\underline{v}|$ is the magnitude of the velocity error.

The sign in (29) arises from careful consideration of Figure 6b, where it can be seen that when $\Delta\underline{v}$ (true - estimate) is towards the satellite (ie. $\cos\eta$ is positive), then the magnitude of the range rate estimate $|d\rho/dt|$ will be too large. Since $d\rho/dt$ is negative, this implies that the range rate error $\Delta\dot{\rho}$ (true - estimate) is positive.

For example, if the true velocity were zero and the estimated velocity was away from the satellite (so that $\Delta\underline{v}$ is towards the satellite as in Figure 6b), then the estimated range rate would be incorrectly compensated to give it a larger negative value (to counter the effect of the estimated velocity, which would have decreased the Doppler shift since it is away from the satellite). This therefore leads to an estimated range rate that is too small (or too large in a negative sense). In this case the range rate error (true - estimate) would be positive.

Since $\sigma$, $\eta$ and $(2\pi-\nu)$ form a right spherical triangle, with $\eta$ the hypotenuse, equation (29) can be written:

$$\Delta\dot{\rho} = \Delta v \cos\sigma \cos\nu \tag{30}$$

Now from (28) and (30), the Doppler error can be written as:

$$\Delta\gamma = \frac{\Delta v \cos\sigma \cos\nu}{V \sin\gamma} \tag{31}$$

Since we have assumed that the velocity error is much smaller than the satellite velocity ( $\Delta v << V$ ) equation (31) produces a small $\Delta\gamma$ angle (if we keep in mind that near the point of closest approach $\sin\gamma \simeq 1$). Thus we have $\sin\Delta\gamma \simeq \Delta\gamma$ and from (25) and (31):

$$\begin{pmatrix}\Delta N \\ \Delta E\end{pmatrix}_1 = NS\cdot EW \frac{\rho\, \Delta v \cos\sigma \cos\nu}{V\sin\gamma}\begin{pmatrix}\sin\psi \\ -\cos\psi\end{pmatrix} \tag{32}$$

At the PCA $\gamma=\pi/2$, so that $\sin\gamma=1$, and this simplifies slightly. The effect of the velocity components is resolved through the angle $\nu$. From Figure 6b we see that (since $\Delta\alpha$ here is a negative angle)

$$\nu = \psi - \Delta\alpha \tag{33}$$

and so

$$\cos\nu = \cos(\psi-\Delta\alpha) \tag{34}$$

$$= \cos\Delta\alpha \cos\psi + \sin\Delta\alpha \sin\psi \tag{35}$$

$$= ( \Delta vn \cos\psi + \Delta ve \sin\psi )/\Delta v \tag{36}$$

Substituting this into equation (32) now allows us to relate the position error components $\Delta N$ and $\Delta E$ to the receiver's north and east velocity error components $\Delta vn$ and $\Delta ve$ at the PCA (where $\sin\gamma=1$):

$$\begin{pmatrix}\Delta N\\ \Delta E\end{pmatrix}_1 = NS\cdot EW\ \frac{\rho\cos\sigma}{V}\begin{pmatrix}(\cos\psi\ \Delta vn + \sin\psi\ \Delta ve)\sin\psi\\ -(\cos\psi\ \Delta vn + \sin\psi\ \Delta ve)\cos\psi\end{pmatrix} \quad (37)$$

$\therefore$

$$\boxed{\begin{pmatrix}\Delta N\\ \Delta E\end{pmatrix}_1 = NS\cdot EW\ \frac{\rho\cos\sigma}{V}\begin{pmatrix}\cos\psi\sin\psi & \sin^2\psi\\ -\cos^2\psi & -\cos\psi\sin\psi\end{pmatrix}\begin{pmatrix}\Delta vn\\ \Delta ve\end{pmatrix}} \quad (38)$$

In the appendices it will be shown how $\rho$, $\psi$ and V can be expressed as functions of the known quantities $\lambda, L, \sigma$, NS and EW. Appendix A gives $\rho(\sigma)$ and $\Theta(\sigma)$. Appendices A, B, C and D together give $\psi(\sigma, \lambda, NS, EW)$. Appendices A and C with equation (5) give $V(\sigma, \lambda, NS, EW)$.

### 6.1.4 Qualitative Verification

Since the Transit satellites are in polar orbits, we can see from Figure 1 that $\psi$ is generally close to $\pm 90°$, in which case $|\sin\psi| >> |\cos\psi|$ and the dominant term in equation (38) is the $\sin^2\psi$ term, which implies that $\Delta\underline{r}1$ is largely in the north-south direction, due to the east velocity error (as would be expected from the physics).

A simple thought experiment can verify that the sign of this dominant term in equation (38) is correct. If we consider the situation where :

$$NS = EW = 1$$

$$vn = \hat{v}n = 0$$

$$ve = |\varepsilon|$$

$$\hat{v}_e = 0$$

then

$$\Delta ve = |\varepsilon|$$

In this case the satellite is moving southward, and is east of the receiver. Since the true velocity here is towards the satellite (ie. to the east), the measured Doppler shift will greater than would be received by a stationary receiver. This causes a smaller cone angle, moving the position estimate south of the true position. Therefore $\Delta N$ will be positive in this situation. Thus a positive $\Delta ve$ produces a positive $\Delta N$ when NS=EW=1, which is consistent with equation (38).

Another way to arrive at the same conclusion in this situation is to consider that the Doppler shift will be zero after the true point of closest approach (in the earth fixed locally level frame), at which time the satellite will be south of the true PCA. This again implies that the position estimate will be south of the true position, so that $\Delta N$ will be positive.

## 6.2 Effect of Differential Cone Angle Error

From equation (31) we can see how the cone angle error $\Delta\gamma$ changes as a function of $\gamma$ and $\nu$. Figure 6a showed how a constant cone angle error $\Delta\gamma$ causes a cross-range error $\Delta\underline{r}1$. Figure 7 illustrates how a change in this cone angle error of $\delta\gamma$ causes an error in range $\Delta\rho$, which projected on the ground becomes an along-range position error $\Delta\underline{r}2$. In this section we will find the expression for this position error. As before, we first find the magnitude $\Delta r2$ and then the direction.

### 6.2.1 Magnitude of $\Delta\underline{r}2$

In Figure 7 we let $\hat{\gamma}1$ and $\hat{\gamma}2$ (where $\hat{\gamma}2 = \pi/2$ is at the apparent point of closest approach) be the cone angle estimates, taken a short time apart (dt seconds). From Figure 7 we can see that the differential cone angle error $\delta\gamma$ (the change in the error over the interval dt) causes an error in the slant range $\Delta\rho$. From the right angle triangles in Figure 7, we have:

$$\tan\hat{\gamma}1 = \frac{\rho}{Vdt} \tag{39}$$

and

$$\tan(\hat{\gamma}1 - \delta\gamma) = \frac{\rho - \Delta\rho}{Vdt} \tag{40}$$

where the slant range error $\Delta\rho$ is related to the horizontal error magnitude $\Delta r2$ by:

$$\Delta\rho = \Delta r2 \cos\sigma \tag{41}$$

Substituting (39) and (41) into (40) yields:

$$\tan(\hat{\gamma}1 - \delta\gamma) = \tan\hat{\gamma}1 - \frac{\Delta r2 \cos\sigma}{Vdt} \tag{42}$$

**Figure 7. Error2: Due to Differential Cone Angle Error.**

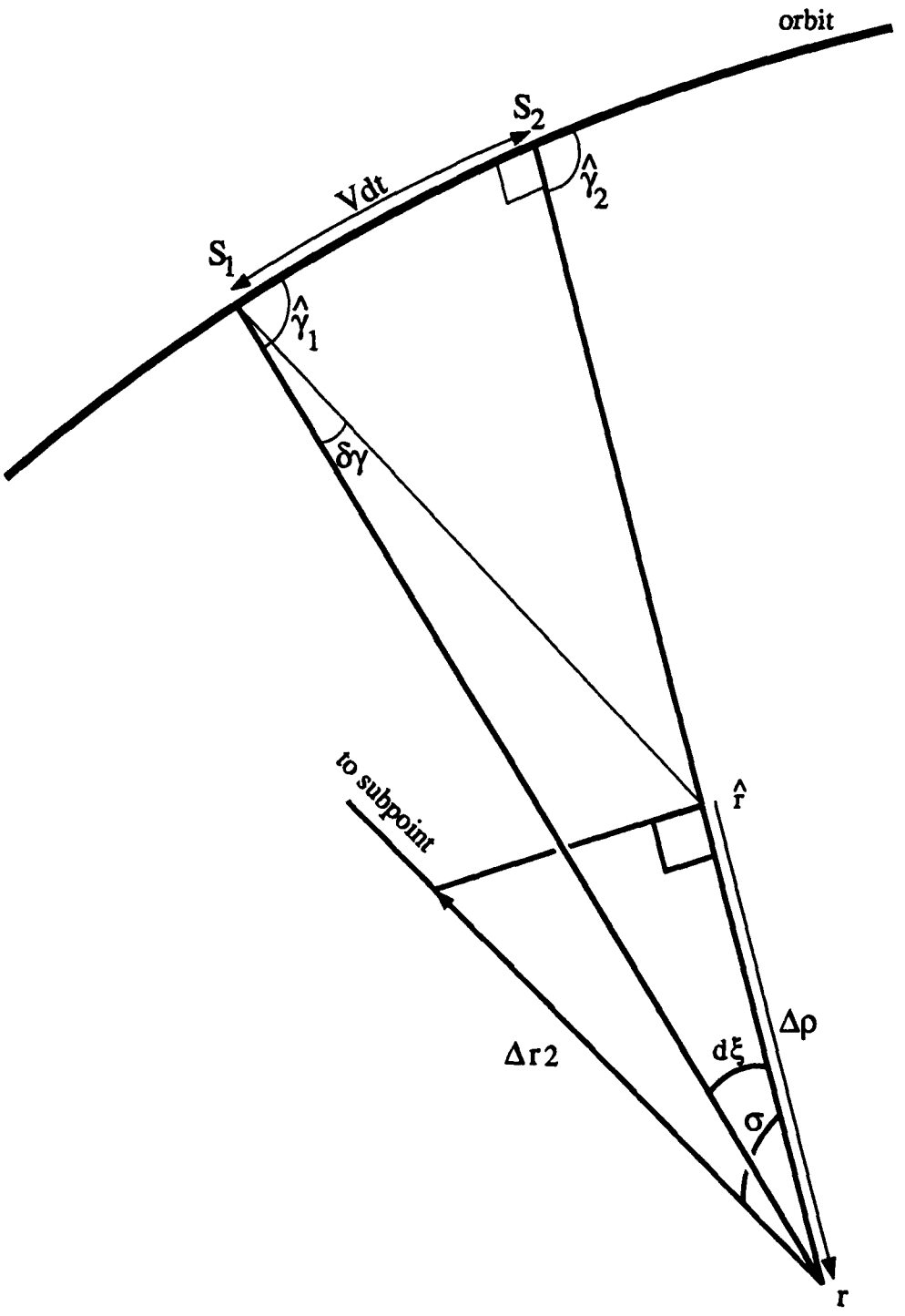

which can be written

$$\frac{\Delta r2 \cos\sigma}{Vdt} = \tan\hat{\gamma}1 - \tan(\hat{\gamma}1 - \delta\gamma) \tag{43}$$

$$= \frac{\sin(\delta\gamma)}{\cos\hat{\gamma}1 \cos(\hat{\gamma}1 - \delta\gamma)} \tag{44}$$

$$= \frac{\sin\hat{\gamma}1}{\cos\hat{\gamma}1} \left( \frac{\sin(\delta\gamma)}{\sin\hat{\gamma}1 \cos(\hat{\gamma}1-\delta\gamma)} \right) \tag{45}$$

From (39) this becomes:

$$\frac{\Delta r2 \cos\sigma}{Vdt} = \frac{\rho}{Vdt} \left( \frac{\sin(\delta\gamma)}{\sin\hat{\gamma}1 \cos(\hat{\gamma}1-\delta\gamma)} \right) \tag{46}$$

Therefore the range error magnitude can be expressed as:

$$\boxed{\Delta r2 = \frac{\rho \sin\delta\gamma}{\sin\hat{\gamma}1 \cos(\hat{\gamma}1 - \delta\gamma) \cos\sigma}} \tag{47}$$

To eliminate $\hat{\gamma}1$ from (47), we use equation (39), which gives us:

$$\frac{Vdt}{\rho} = \cot(\hat{\gamma}1) \tag{48}$$

$$= \tan(\pi/2 - \hat{\gamma}1)$$

Since the cone angle $\gamma$ is taken from the satellite velocity vector to the slant range vector, it is always increasing in time. Therefore $\hat{\gamma}1 < \hat{\gamma}2 \equiv \pi/2$, and the denominator of equation (46) cannot be zero. For small dt, (in the neighbourhood of the PCA) $\hat{\gamma}1 \simeq \pi/2$, so that (48) can be written

$$\frac{Vdt}{\rho} \simeq \pi/2 - \hat{\gamma}1 \tag{49}$$

Thus the cone angle estimate at a short time, dt, before the point of closest approach (ie. for small dt) is:

$$\hat{\gamma}1 \simeq \pi/2 - Vdt/\rho \tag{50}$$

Thus, to eliminate $\hat{\gamma}1$ in (47) we keep the first order terms in dt, which are:

$$\sin\hat{\gamma}1 \simeq 1 \tag{51}$$

and

$$\cos(\hat{\gamma}1-\delta\gamma) \simeq \cos(\pi/2 - Vdt/\rho - \delta\gamma) \tag{52}$$

$$= \sin(Vdt/\rho + \delta\gamma) \tag{53}$$

$$\simeq Vdt/\rho + \delta\gamma \tag{54}$$

Using this in (47) gives:

$$\Delta r2 \simeq \frac{\rho \sin\delta\gamma}{(\delta\gamma + Vdt/\rho)\cos\sigma} \tag{55}$$

Now we need the differential expression for $\delta\gamma$ (as a function of dt). To obtain this we use (31), and recognize that $\nu$ also changes. (Since we are at the maximum elevation angle, $d\sigma/dt = 0$, and $\sigma$ can be considered constant. It can also be shown that this is the point of closest approach, so that $\rho$ is at a minimum and $d\rho/dt = 0$. Thus $\rho$ can also be considered constant.)

$$\delta\gamma \equiv \hat{\Delta\gamma}2 - \hat{\Delta\gamma}1 \tag{56}$$

$$= \frac{\Delta v \cos\sigma}{V}\left(\frac{\cos\nu 2}{\sin\hat{\gamma}2} - \frac{\cos\nu 1}{\sin\hat{\gamma}1}\right) \tag{57}$$

where $\Delta v$ is the velocity error which induced these cone angle errors. Using (50) for $\hat{\gamma}1$, and since $\hat{\gamma}2 = \pi/2$, this becomes:

$$\delta\gamma \simeq -\frac{\Delta v \cos\sigma}{V}\left(\frac{\cos\nu 1}{\sin(\pi/2 - Vdt/\rho)} - \cos\nu 2\right) \tag{58}$$

$$= -\frac{\Delta v \cos\sigma}{V}\left(\frac{\cos\nu 1}{\cos(Vdt/\rho)} - \cos\nu 2\right) \tag{59}$$

From Figure 8 we will see that the angle $d\xi$ between slant ranges, is simply related to the angle in the horizontal plane:

$$d\nu \equiv \nu 2 - \nu 1 \tag{60}$$

which is the difference in bearing from the velocity error to the horizontal projection of the slant ranges (as can be seen from Figure 6b). Since these bearings are defined by the geodesics (which are great circles if a spherical earth model is used) from the receiver to the subpoints, and these great circles are the intersection of vertical planes with the earth's surface, we therefore must project down from the slant ranges using vertical

**Figure 8. Vertical Projection From Slant Range to Horizontal.**

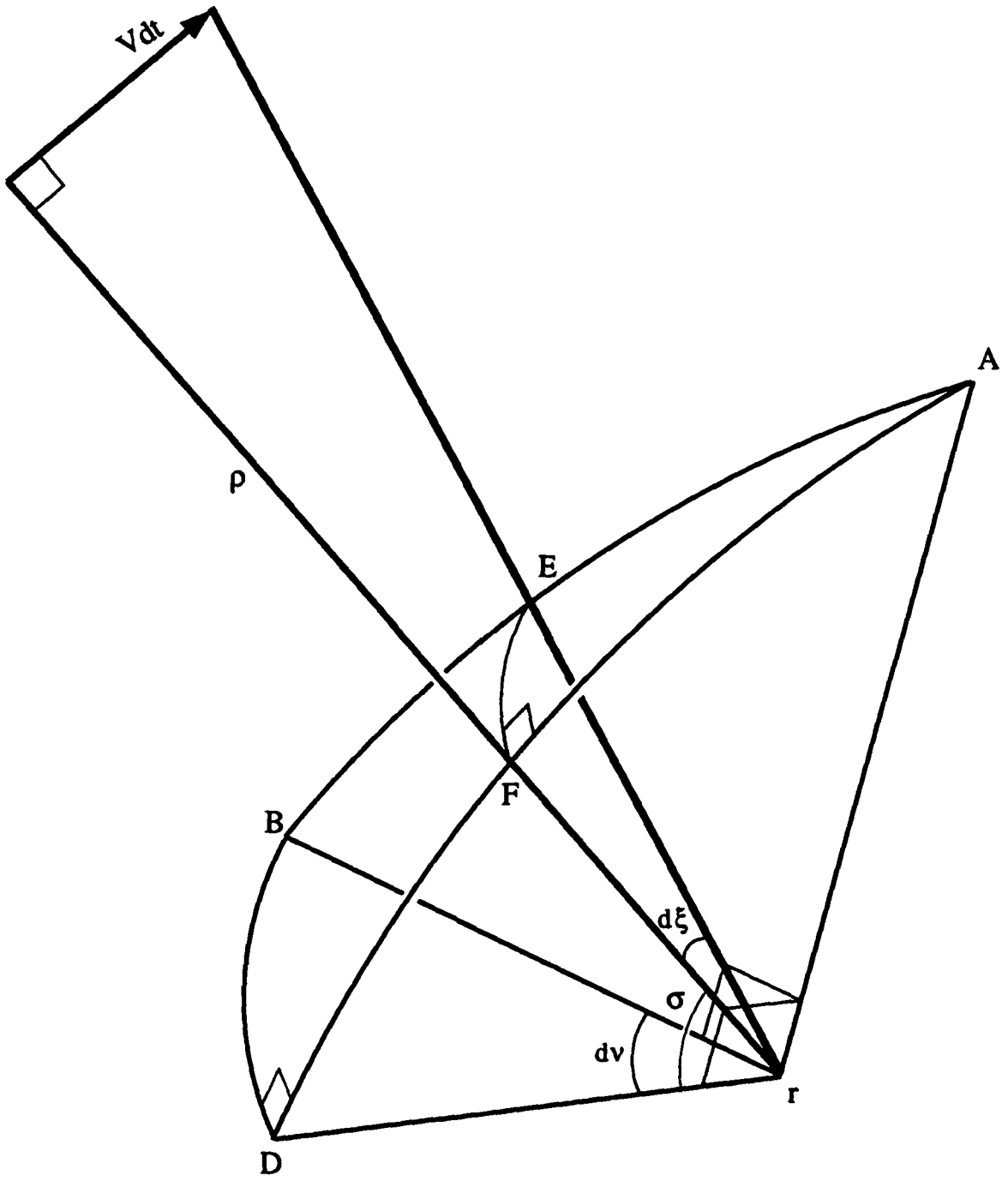

planes, as shown in Figure 8.

Consider the small right spherical triangle ΔAEF in Figure 8. A trigonometric identity gives the relationship

$$\sin(\pi/2-\sigma) = \tan|d\xi|\cdot\cot A \qquad (61)$$

which can be rearranged as

$$\tan|d\xi| = \cos\sigma\cdot\tan A \qquad (62)$$

Now, by considering the large right spherical triangle ΔABD, the same trigonometric identity yields:

$$\sin(\pi/2) = \tan|d\nu|\cdot\cot A \qquad (63)$$

$$\therefore \quad \tan|d\nu| = \tan A \qquad (64)$$

From (62) and (64) we therefore have

$$\tan|d\nu| = \frac{\tan|d\xi|}{\cos\sigma} \qquad (65)$$

Therefore, for small $d\nu$ we have (and since $0 < \sigma < \pi/2$ )

$$|d\nu| \simeq \frac{|d\xi|}{\cos\sigma} \qquad (66)$$

From Figure 6b we can see that $\nu$ is increasing in time ($d\nu$ is positive) if the satellite is to the east moving south or to the west moving north, otherwise $d\nu$ is negative. In other words, the sign of $d\nu$ is NS·EW. Thus equation (66) can be rewritten:

$$d\nu = \frac{NS \cdot EW \cdot |d\xi|}{\cos\sigma} \tag{67}$$

From Figure 7 we can see that

$$|d\xi| = \pi/2 - \gamma 1 \tag{68}$$

From (50) this gives, to first order in dt:

$$|d\xi| \simeq Vdt/\rho \tag{69}$$

Thus, from (60), (66) and (69) we have:

$$\nu 2 = \nu 1 + \frac{NS \cdot EW \cdot |d\xi|}{\cos\sigma} \tag{70}$$

$$\simeq \nu 1 + \frac{NS \cdot EW \cdot Vdt}{\rho\cos\sigma} \tag{71}$$

Therefore

$$\cos\nu 2 \simeq \cos\left(\nu 1 + \frac{NS \cdot EW \cdot Vdt}{\rho\cos\sigma}\right) \tag{72}$$

$$\simeq \cos\nu 1 \cos\left(\frac{Vdt}{\rho\cos\sigma}\right) - NS \cdot EW \cdot \sin\nu 1 \sin\left(\frac{Vdt}{\rho\cos\sigma}\right) \tag{73}$$

Now the term $Vdt/\rho$ is very small, since the slant range $\rho$ is greater than the orbital height (1,075,000 metres) and the satellite velocity V is less than 7,310 m/s (from (7)). Thus for small dt we can approximate, to first order in dt:

$$\cos\nu 2 \simeq \cos\nu 1 - NS \cdot EW \cdot \sin\nu 1 \cdot \frac{Vdt}{\rho\cos\sigma} \tag{74}$$

This can now be used in (59) to express $\delta\gamma$ in terms of dt, keeping only the first order terms in dt, (also, since we have eliminated the $\nu 2$ terms, we can just use $\nu$ for $\nu 1$):

$$\delta\gamma = -\frac{\Delta v \cos\sigma}{V}\left(\frac{\cos\nu}{1} - \cos\nu + NS\cdot EW\cdot\sin\nu\cdot\frac{Vdt}{\rho\cos\sigma}\right) \qquad (75)$$

$$\boxed{\delta\gamma = -NS\cdot EW\ \Delta v\ \sin\nu\ dt/\rho} \qquad (76)$$

This can now be used in (55) to express the position error independently of dt:

$$\Delta r2 \simeq \frac{\rho\ (-NS\cdot EW\ \Delta v\ \sin\nu\ dt/\rho)}{[(-NS\cdot EW\ \Delta v\ \sin\nu\ dt/\rho) + Vdt/\rho]\cos\sigma} \qquad (77)$$

$$\simeq \frac{-NS\cdot EW\ \rho\ \Delta v\ \sin\nu}{-NS\cdot EW\ \Delta v\ \cos\sigma\ \sin\nu + V\cos\sigma} \qquad (78)$$

Now for velocity errors $\Delta v$ much smaller than the satellite velocity V, this can be written:

$$\boxed{\Delta r2 \simeq \frac{-NS\cdot EW\ \rho}{V\cos\sigma}\sin\nu\ \Delta v} \qquad (79)$$

This can be expressed in terms of the components of the velocity error vector $\underline{\Delta v}$ by using the fact that $\nu = \psi - \Delta\alpha$ (see equation (33)), where $\Delta\alpha$ is the bearing of $\underline{\Delta v}$.

$$\sin\nu = \sin(\psi-\Delta\alpha) \tag{80}$$

$$= \sin\psi\cos\Delta\alpha - \cos\psi\sin\Delta\alpha \tag{81}$$

$$\therefore \quad \Delta v \sin\nu = \sin\psi(\Delta v \cos\Delta\alpha) - \cos\psi(\Delta v \sin\Delta\alpha) \tag{82}$$

$$= \sin\psi\,\Delta vn - \cos\psi\,\Delta ve \tag{83}$$

Thus from (79) we have:

$$\Delta r2 = \frac{-NS\cdot EW\ \rho}{V\cos\sigma}(\sin\psi\,\Delta vn - \cos\psi\,\Delta ve) \tag{84}$$

### 6.2.2 Direction of $\underline{\Delta r}2$

Now we must express the components of the position error ($\Delta N, \Delta E$) in terms of the position error magnitude $\Delta r2$. From Figure 9 it can be seen that a positive differential cone angle error $\delta\gamma$ (defined by (56)) causes the position estimate to move in the direction away from the subpoint (at bearing $\psi+\pi$). Thus a positive $\delta\gamma$ creates a position error vector $\underline{\Delta r}2$ (true-estimate) with bearing $\psi$. From (76) and (79) we can see that $\delta\gamma$ has the same sign as $\Delta r2$ (both are determined by the sign of $\sin\nu$). Therefore $\underline{\Delta r}2$ has bearing $\psi+\pi$ if $\delta\gamma$ (given by (76)) is positive, and has bearing $\psi$ if $\delta\gamma$ is negative. Since

$$\cos(\psi+\pi) = -\cos\psi$$
$$\sin(\psi+\pi) = -\sin\psi \tag{85}$$

we can therefore write:

$$\begin{pmatrix}\Delta N\\ \Delta E\end{pmatrix}_2 = \Delta r2 \begin{pmatrix}\cos\psi\\ \sin\psi\end{pmatrix} \tag{86}$$

**Figure 9. Direction of Δr2.**

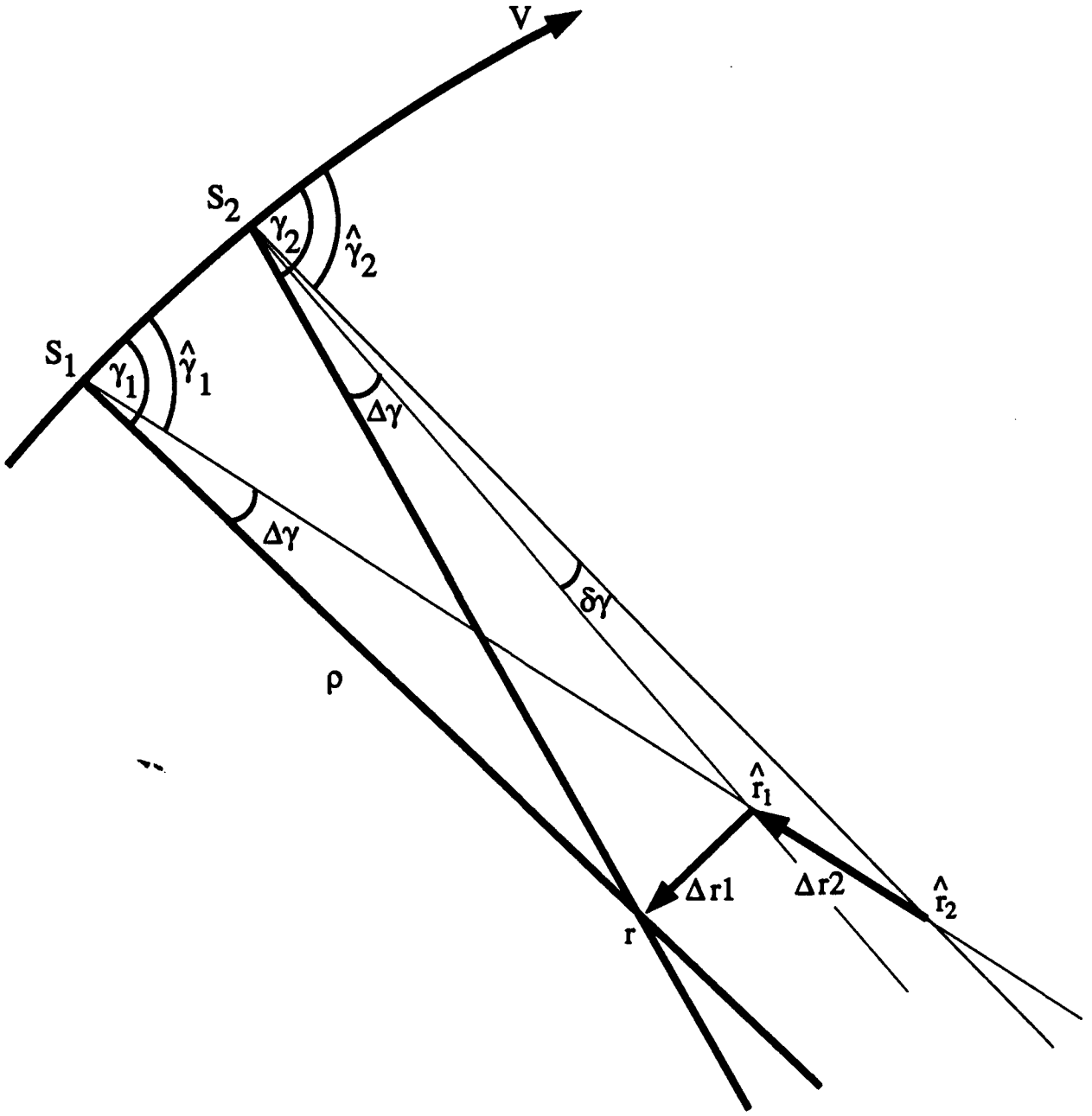

Finally we can use (84) to substitute for $\Delta r2$ in (86) to obtain:

$$\begin{pmatrix}\Delta N\\ \Delta E\end{pmatrix}_2 = \frac{NS\cdot EW\ \rho}{V\cos\sigma}\begin{pmatrix}(\sin\psi\ \Delta vn\ -\ \cos\psi\ \Delta ve)\cos\psi\\ (\sin\psi\ \Delta vn\ -\ \cos\psi\ \Delta ve)\sin\psi\end{pmatrix} \qquad (87)$$

or

$$\boxed{\begin{pmatrix}\Delta N\\ \Delta E\end{pmatrix}_2 = \frac{NS\cdot EW\ \rho}{V\cos\sigma}\begin{pmatrix}-\sin\psi\cos\psi & \cos^2\psi\\ -\sin^2\psi & \cos\psi\sin\psi\end{pmatrix}\begin{pmatrix}\Delta vn\\ \Delta ve\end{pmatrix}} \qquad (88)$$

## 6.3 Velocity Error Orthogonal to the Slant Range

The remaining velocity induced position errors are due to the effect of the velocity error component orthogonal to the slant range. In Section 6.3.1 we will see how this affects the individual cone angle calculations, and in Section 6.3.2 we will see how it causes an additional error when cones are translated to remove the effect of receiver motion between successive cone angle measurements (prior to intersecting the cones).

### 6.3.1 Cone Angle Error

A velocity error $\Delta\underline{v}$ which is orthogonal to the slant range will be parallel to the satellite velocity vector $\underline{V}$ (at the point of closest approach). This will not affect the cone angle at the point of closest approach (as seen in Section 6.1 above), but it will effect the cone angle measurement on either side of the PCA, where there will be a component of $\Delta\underline{v}$ along the slant range. More importantly, this component of $\Delta\underline{v}$ will be positive on one side of the PCA and negative on the other, which will cause the cone angle to increase on one side of the PCA and decrease on the other. This will move the intersection of the cones towards or away from the satellite, introducing a position error. The situation is illustrated in Figure 10.

#### 6.3.1.1 Magnitude of $\Delta\underline{r3}$

Figure 10 illustrates the situation where the satellite is at S1, a short time dt before the point of closest approach (PCA), and therefore is at a distance of Vdt from the PCA. We let D be the slant range at S1, and $\gamma$ be the cone angle. Then the cone angle error $\Delta\gamma$ at S1 causes a slant range error $\Delta\rho$, as shown. Simple trigonometry gives us:

$$\Delta\rho \cos(\gamma+\Delta\gamma) = D \sin\Delta\gamma \qquad (89)$$

and

$$D = \rho/\sin\gamma \qquad (90)$$

so that

**Figure 10. Error3: Due To Assymetric Cone Angle Error.**
**(Velocity Error Orthogonal to Slant Range)**

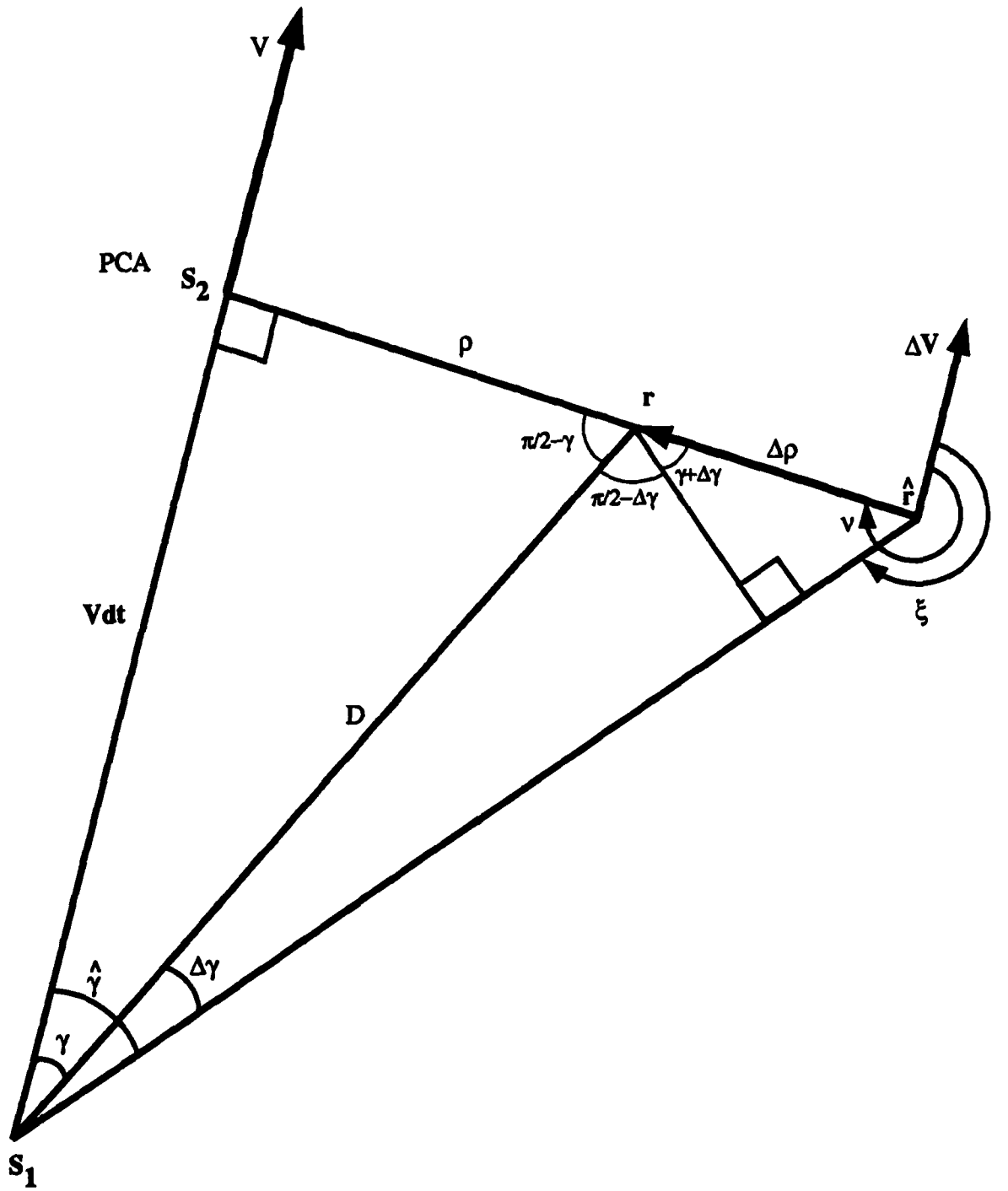

$$\Delta\rho = \frac{\rho \sin\Delta\gamma}{\sin\gamma\cos(\gamma+\Delta\gamma)} \tag{91}$$

Now equation (31) of Section 6.1.3 gives us the expression for the cone angle error $\Delta\gamma$ caused by a velocity error $\Delta v$:

$$\Delta\gamma = \frac{\Delta v \cos\sigma \cos\xi}{V \sin\gamma} \tag{92}$$

where $\sigma$ is the satellite elevation angle and $\gamma$ is the cone angle at S1. Here we use $\xi$ for the angle between the velocity error $\Delta v$ and the bearing to the subpoint for S1, so that we can reserve $\nu$ (as shown in Figure 6b) for the angle between $\Delta v$ and the bearing line to the subpoint at PCA.

From equations (67) and (69) we saw that the bearing angle $\xi = \nu - d\nu$, a time dt before the PCA, is related to the angle $\nu$ at the PCA by

$$\xi \simeq \nu - \frac{NS \cdot EW \, V dt}{\rho \cos\sigma} \tag{93}$$

so that

$$\cos\xi \simeq \cos\nu \cos\left(\frac{V dt}{\rho\cos\sigma}\right) + NS \cdot EW \cdot \sin\nu \sin\left(\frac{V dt}{\rho\cos\sigma}\right) \tag{94}$$

$$\simeq \cos\nu + NS \cdot EW \cdot \sin\nu \cdot \left(\frac{V dt}{\rho\cos\sigma}\right) \tag{95}$$

Using this in (92) gives:

$$\Delta\gamma = \frac{\Delta v \cos\sigma}{V\sin\gamma}\left(\cos\nu + NS \cdot EW \cdot \frac{\sin\nu \, V dt}{\rho\cos\sigma}\right) \tag{96}$$

$$= \frac{\Delta v \cos\sigma \cos\nu}{V\sin\gamma} + \frac{NS \cdot EW \cdot \Delta v \sin\nu \, dt}{\rho \sin\gamma} \tag{97}$$

Now the first term is from the component of $\Delta\underline{v}$ parallel to the

slant range ($\Delta v\cos\nu$), and is symmetric in the cone angle $\nu$. This gives rise to a position error orthogonal to the slant range, (and in fact is the error $\Delta\gamma$ described in equation (31), which led to $\Delta\underline{r}1$), which does not contribute to the error described by Figure 10. The second term however, is antisymmetric in the cone angle $\nu$ ( since $\sin(-\nu) = -\sin\nu$ ), causing an along-range error which we call $\Delta\underline{r}3$.

Using this second term of equation (97) in (91), (and since $\Delta\gamma$ is a small angle: $\sin\Delta\gamma\simeq\Delta\gamma$ and $\cos(\gamma+\Delta\gamma)\simeq\cos\gamma$ ), we obtain

$$\Delta\rho = \frac{NS\cdot EW\cdot\Delta v\,\sin\nu\,dt}{\sin^2\gamma\,\cos\gamma} \qquad (98)$$

From equation (50) we saw that near the PCA

$$\gamma \simeq \pi/2 - Vdt/\rho \qquad (99)$$

so that, since $Vdt/\rho \ll 1$

$$\sin\gamma \simeq 1$$
$$\cos\gamma \simeq Vdt/\rho \qquad (100)$$

Using this in (98) gives

$$\Delta\rho = \frac{NS\cdot EW\cdot\rho\,\Delta v\,\sin\nu}{V} \qquad (101)$$

Projecting this into the horizontal plane, as illustrated in Figure 7 for $\Delta\underline{r}2$, we obtain the magnitude of $\Delta r3$:

$$\Delta r3 = \frac{NS\cdot EW\cdot\rho\,\Delta v\,\sin\nu}{V\,\cos\sigma} \qquad (102)$$

Note that this position error is independent of the time dt before (or after) the point of closest approach, so that the cone

error described by (97) does lead to a constant position error.

Furthermore, this error $\Delta r3$ can be seen to have exactly the same magnitude as $\Delta r2$ (by comparing equation (102) to equation (79)). We could therefore similarly express $\Delta r3$ in terms of $\psi$ rather than $\nu$ by following the same derivation, given by equations (79) to (84).

### 6.3.1.2 Direction of $\Delta r3$

As shown in Figure 10, the direction of $\underline{\Delta r}3$ is towards the subpoint (bearing $\psi$) if the velocity error $\underline{\Delta v}$ has a positive component in the satellite direction of travel $\underline{V}$. Conversely $\underline{\Delta r}3$ is away from the subpoint if $\underline{\Delta v}$ is towards $-\underline{V}$. Thus $\underline{\Delta r}3$ can be expressed as in equation (88), with a possible sign change. Using Figure 10 to test the sign, we see that with NS = EW = -1, a positive $\Delta vn$ should cause a negative $\Delta E$, which equation (88) does. Therefore $\underline{\Delta r}3$ is identical to $\underline{\Delta r}2$, and is therefore given by:

$$\begin{pmatrix}\Delta N\\ \Delta E\end{pmatrix}_3 = \frac{NS\cdot EW\ \rho}{V\cos\sigma}\begin{pmatrix}-\sin\psi\cos\psi & \cos^2\psi\\ -\sin^2\psi & \cos\psi\sin\psi\end{pmatrix}\begin{pmatrix}\Delta vn\\ \Delta ve\end{pmatrix} \qquad (103)$$

### 6.3.2 Translation Error

Since the receiver moves between Doppler measurements, the Doppler cones must be translated by the displacement vector ($\underline{v}$ dt) in the direction of the receiver velocity to form these intersections. Figure 11a, showing the "slant range plane", illustrates how an error in this velocity $\Delta\underline{v}$ over an interval $\Delta t$, moves the cone by an excess amount ($\Delta\underline{v}$ dt) which moves the cone intersection in the direction of the slant range by an excess amount $\Delta\rho$. The resulting position error $\Delta\underline{r}4$ is the projection of this slant range error $\Delta\rho$ into the local horizontal plane (perpendicular to the slant range, as shown in Figure 7). The position r and its estimate are more properly shown in the horizontal plane as in Figure 11b, which shows the quantities of interest, assuming zero true velocity for simplicity.

In the receiver's horizontal plane, as shown in Figure 11b, the cones (on intersection with the horizontal plane) reduce to lines of position (LOPs). In this plane, in the neighbourhood of the receiver, these LOPs are just the projections of the slant range vectors into the horizontal plane, as shown in Figure 12. This projection is in the direction of the line of intersection of the two cones (orthogonal to both the slant range $\underline{\rho}$ and the satellite velocity $\underline{V}$, as seen in Figure 2).

#### 6.3.2.1 Magnitude of $\Delta\underline{r}4$

From Figure 11b we can see that the magnitude $\Gamma$ of the component of the velocity error ($\Delta\underline{v}$ dt) orthogonal to the LOP is found by projecting with the included angle $\nu$ (where $\nu$ is defined as shown in Figure 6b). Thus the effective LOP displacement $\Gamma$ (orthogonal to the LOP) due to this velocity error has magnitude:

$$\Gamma = \Delta v \, dt \, |\sin\nu| \qquad (104)$$

Now the resulting position error $\Delta\underline{r}4$ can be seen from Figure 11b to be parallel to the slant range and of magnitude $\Delta r4$ related to the displacement error by:

$$\Delta r4 \, |\sin(d\zeta)| = \Gamma \qquad (105)$$

where $d\zeta$ is the change in the angle between lines of position (intersection of Doppler cones with the horizontal plane) over

**Figure 11a. Error4: Due to Incorrect Translation of Cone1.**
**(Velocity Error Orthogonal to Slant Range)**

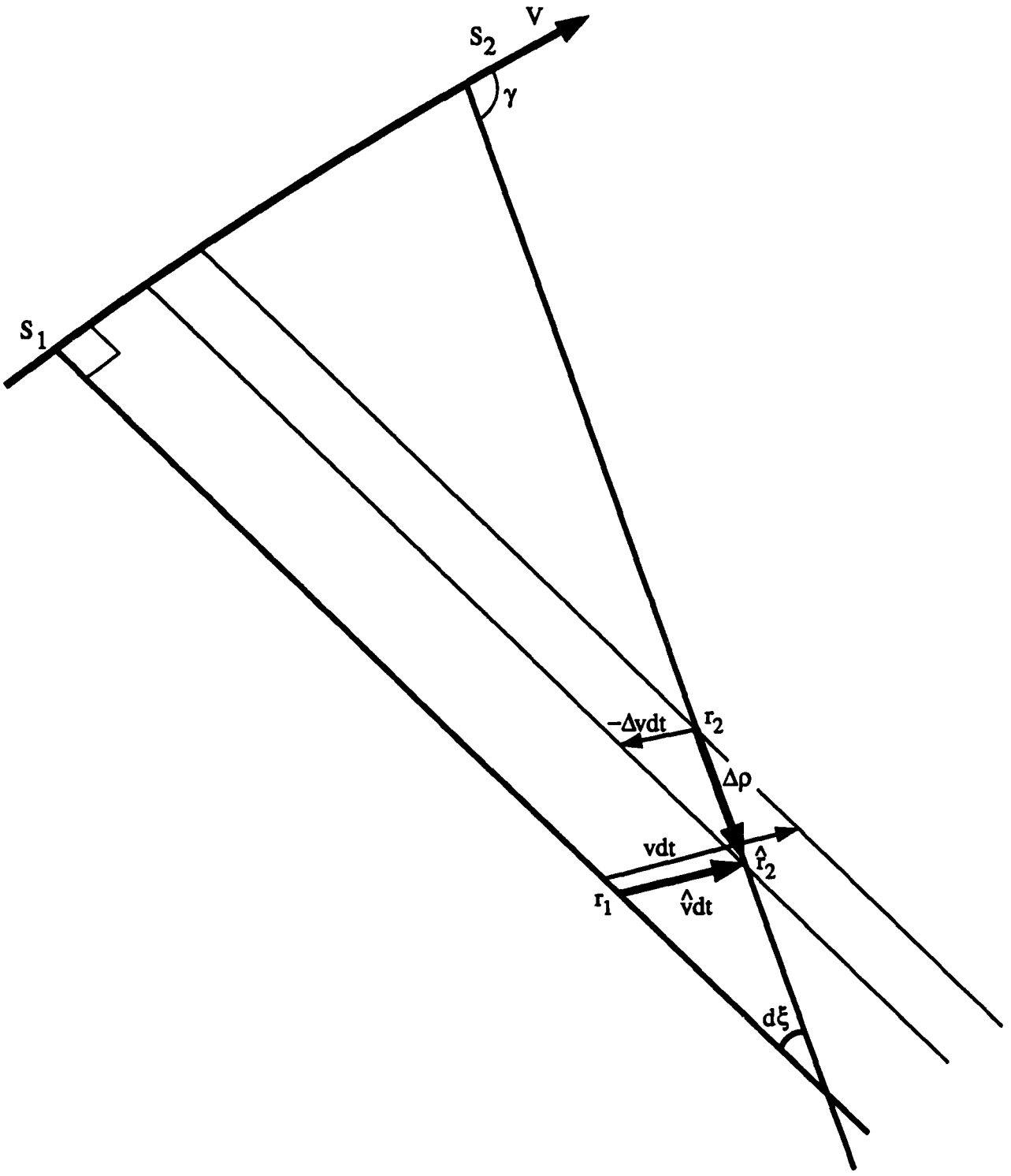

**Figure 11b. Error4 in the Horizontal Plane.**

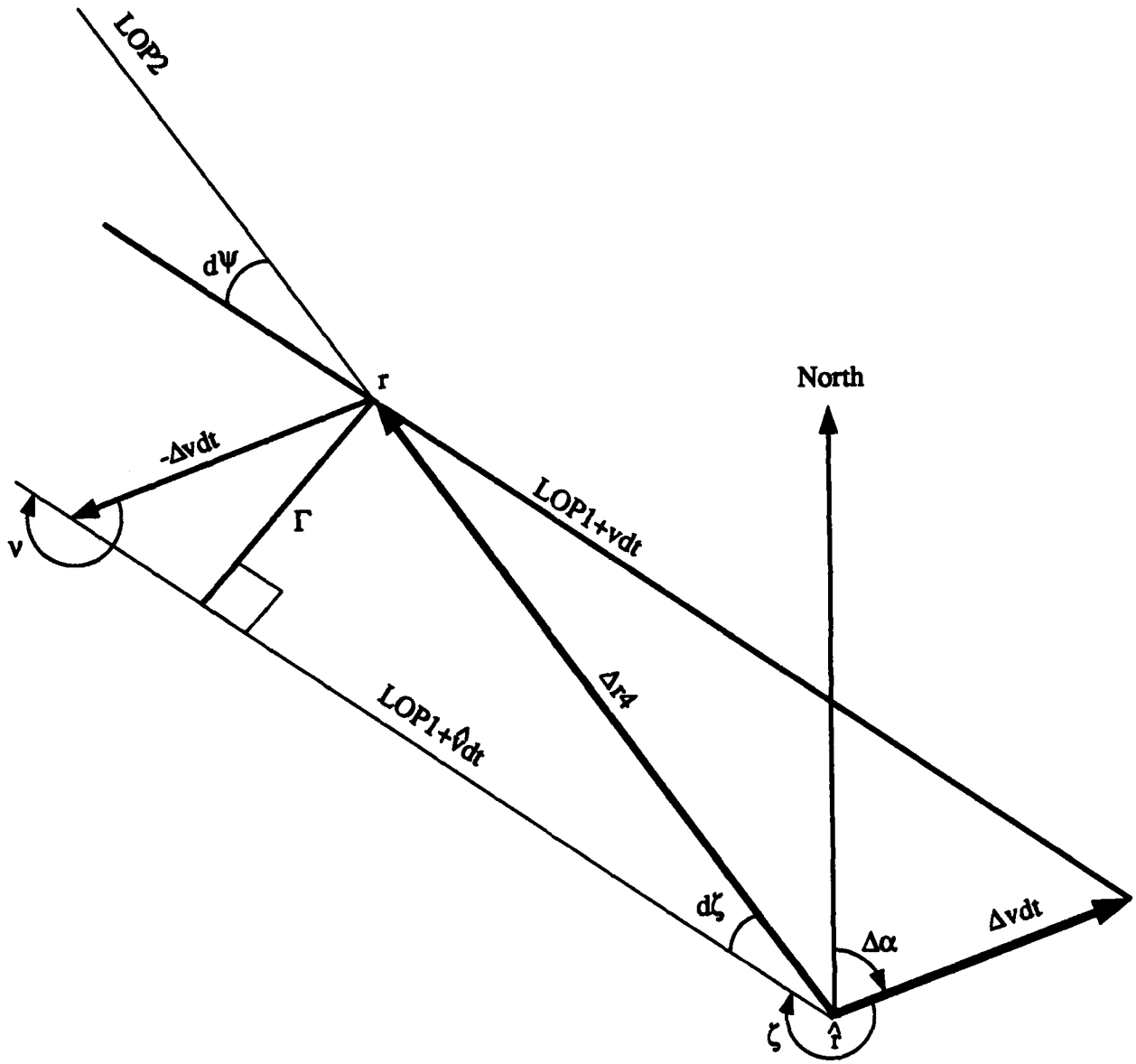

the time interval dt (assuming a constant velocity error $\Delta\underline{v}$ over this interval). From (104) and (105) we have:

$$\Delta r4 \; |\sin(d\zeta)| \; = \; \Delta v \; dt \; |\sin\nu| \qquad (106)$$

For small intervals dt, clearly $d\zeta$ is also very small, so that we can use $\sin(d\zeta) \simeq d\zeta$, and write (106) as

$$\Delta r4 \; = \; \frac{\Delta v \; |\sin\nu|}{(|d\zeta|/dt)} \qquad (107)$$

which relates the velocity error magnitude $\Delta v$ to the magnitude of the position error $\Delta r4$.

Consider the spherical triangle $\Delta GBD$ in Figure 12. This spherical triangle is formed by approximating the Doppler cones at the receiver, near the point of closest approach, as planes (tangent to the cone along the slant range). This is valid since the cone at the PCA does reduce to a plane, and in any case the curvature will be very small compared to the position error $\Delta r4$. Note that since the circle of intersection of the Doppler cones, $\underline{C}$, is orthogonal to the slant range $\underline{\rho}$:

$$\mu = d\xi \qquad (108)$$

Note also that the smaller spherical triangle $\Delta GEF$ is a hemisphere slice, so that its angles E and F are $\pi/2$ and the sides GE and GF subtend $\pi/2$ at the centre $\underline{r}$. Therefore the law of cosines applied to $\Delta GEF$ gives us

$$\cos(d\zeta) \; = \; \cos^2(\pi/2+\sigma) \; + \; \sin^2(\pi/2+\sigma) \; \cos\mu \qquad (109)$$

$$= \; \sin^2\sigma \; + \; \cos^2\sigma \; \cos(d\xi) \qquad (110)$$

Thus for small $d\zeta$ (using $\cos\varepsilon \simeq 1-\varepsilon^2/2$):

$$1 - (d\zeta)^2/2 \; = \; \sin^2\sigma \; + \; \cos^2\sigma \; ( \; 1 - (d\xi)^2/2 \; ) \qquad (111)$$

**Figure 12. Projection Parallel to Cone Intersection.**

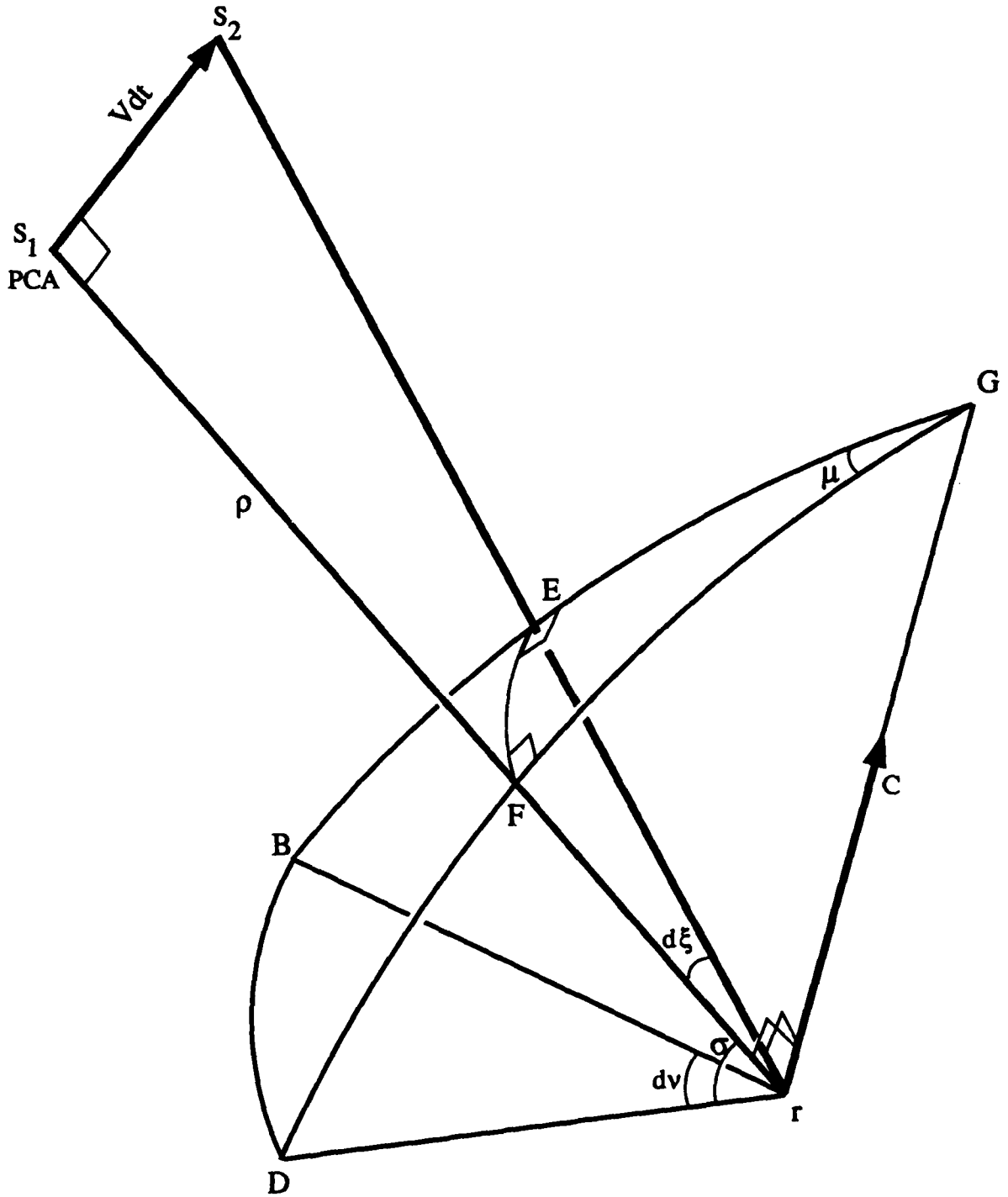

$$\therefore \quad (d\zeta)^2 = \cos^2\sigma\,(d\xi)^2 \tag{112}$$

and so

$$|d\zeta| = |d\xi|\cos\sigma \tag{113}$$

Using (69) for $|d\xi|$ this becomes

$$|d\zeta| \simeq \frac{Vdt}{\rho}\cos\sigma \tag{114}$$

This can now be used in (107) to express the relationship between the position error magnitude $\Delta r4$ and the velocity error $\underline{\Delta v}$ in terms of "known" quantities.

$$\Delta r4 = \frac{\Delta v\,|\sin\nu|\,\rho}{V\cos\sigma} \tag{115}$$

### 6.3.2.2 Direction of $\underline{\Delta r}4$

Now we must express the components of the position error $(\Delta N, \Delta E)$ in terms of the position error magnitude $\Delta r4$. From careful consideration of Figures 11a and 11b, it can be seen that in general $\underline{\Delta r}4$ is in the direction towards the subpoint (bearing $\psi$) if the projection of the velocity error $\underline{\Delta v}$ in the satellite direction of travel $\underline{V}$ is positive, and conversely that $\underline{\Delta r}4$ is away from the subpoint (bearing $\psi+\pi$) if this projection is negative. Since

$$\begin{aligned} \cos(\psi+\pi) &= -\cos\psi \\ \sin(\psi+\pi) &= -\sin\psi \end{aligned} \tag{116}$$

we can therefore write:

$$\begin{pmatrix}\Delta N\\ \Delta E\end{pmatrix}_4 = \pm\Delta r4 \begin{pmatrix}\cos\psi\\ \sin\psi\end{pmatrix} \qquad (117)$$

or, using equation (115)

$$\begin{pmatrix}\Delta N\\ \Delta E\end{pmatrix}_4 = \pm\frac{\Delta v \sin\nu\ \rho}{V\cos\sigma} \begin{pmatrix}\cos\psi\\ \sin\psi\end{pmatrix} \qquad (118)$$

where the $\pm$ has absorbed the absolute value sign from (115), and hence the $\pm$ of equation (118) may not be the same as in equation (117).

In the particular situation shown in Figure 11a ( NS=-1, EW=-1, $\sin\nu<0$ ), the velocity error $\Delta\underline{v}$ has a positive component in the satellite direction of travel $\underline{V}$ ($\underline{V}$ and $\Delta\underline{v}$ are both to the north), so that the resulting position error $\Delta\underline{r}4$ has bearing $\psi$ (towards the satellite subpoint). Therefore the sign of the first term in equation (118) should be positive, to produce a vector in the direction of $\psi$. Since $\sin\nu$ in this case is negative, the $\pm$ in equation (118) should also be negative.

To generalize this: there are two factors which determine whether or not $\Delta\underline{v}$ has a component in the direction of $\underline{V}$. These are:

-the direction of $\underline{V}$, as determined by NS
-the direction of $\Delta\underline{v}$

The second factor here can in turn be determined by two factors:

-the angle $\nu$ between $\Delta\underline{v}$ and the subpoint vector,
-the direction to subpoint vector, as determined by EW

We can see therefore that the sign in equation (118) should change with NS, since the direction of $\underline{V}$ does. We can also see that the sign in equation (118) should change with the relative direction of $\Delta\underline{v}$, which can be accounted for by the sign of $\sin\nu$ and by EW. We can therefore express (118) as:

$$\begin{pmatrix}\Delta N\\ \Delta E\end{pmatrix}_4 = \frac{-NS\cdot EW\ \rho\ \Delta v\ \sin\nu}{V\cos\sigma}\begin{pmatrix}\cos\psi\\ \sin\psi\end{pmatrix} \qquad (119)$$

Finally we can use (83) to substitute for $\Delta v \sin\nu$ in (119) to obtain:

$$\begin{pmatrix}\Delta N\\ \Delta E\end{pmatrix}_4 = \frac{-NS\cdot EW\ \rho\ (\sin\psi\ \Delta vn - \cos\psi\ \Delta ve)}{V\cos\sigma}\begin{pmatrix}\cos\psi\\ \sin\psi\end{pmatrix} \qquad (120)$$

or

$$\boxed{\begin{pmatrix}\Delta N\\ \Delta E\end{pmatrix}_4 = NS\cdot EW\frac{\rho}{V\cos\sigma}\begin{pmatrix}-\sin\psi\cos\psi & \cos^2\psi\\ -\sin^2\psi & \cos\psi\sin\psi\end{pmatrix}\begin{pmatrix}\Delta vn\\ \Delta ve\end{pmatrix}} \qquad (121)$$

Comparing this to (88) and (103) we can see that this error is in fact identical in magnitude and direction to $\Delta\underline{r}2$ and $\Delta r3$. If there is a simple reason for this it is not immediately apparent.

## 6.4 Combined Effect of Velocity Error

Equations (38), (88), (103) and (121) can be combined to express the total effect of the error in the velocity provided to a Transit receiver on the Transit position fix error:

$$\Delta N = \frac{NS \cdot EW\rho}{V}\Big( [\ \cos\sigma - 3/\cos\sigma\ ]\cos\psi\sin\psi\ \Delta vn + [\ \cos\sigma\sin^2\psi + (3/\cos\sigma)\cos^2\psi\ ]\Delta ve \Big) \qquad (122)$$

$$\Delta E = \frac{NS \cdot EW\rho}{V}\Big( [\ -\cos\sigma\cos^2\psi - (3/\cos\sigma)\sin^2\psi\ ]\Delta vn + [\ -\cos\sigma + 3/\cos\sigma\ ]\cos\psi\sin\psi\ \Delta ve \Big) \qquad (123)$$

or

$$\Delta N = \frac{NS \cdot EW\rho}{V\cos\sigma}\Big( -(3-\cos^2\sigma)\cos\psi\sin\psi\ \Delta vn + [\ \cos^2\sigma\sin^2\psi + 3\cos^2\psi\ ]\Delta ve \Big) \qquad (124)$$

$$\Delta E = \frac{NS \cdot EW\rho}{V\cos\sigma}\Big( [-\cos^2\sigma\cos^2\psi - 3\sin^2\psi\ ]\Delta vn + (3-\cos^2\sigma)\cos\psi\sin\psi\ \Delta ve \Big) \qquad (125)$$

Now if we let

$$A \equiv \cos^2\sigma \qquad (126)$$

$$B \equiv 3 - \cos^2\sigma \qquad (127)$$

then

$$\begin{pmatrix} \Delta N \\ \Delta E \end{pmatrix} = \frac{NS \cdot EW \rho}{V \cos\sigma} \begin{pmatrix} -B\cos\psi\sin\psi & A\sin^2\psi + 3\cos^2\psi \\ -A\cos^2\psi - 3\sin^2\psi & B\cos\psi\sin\psi \end{pmatrix} \begin{pmatrix} \Delta vn \\ \Delta ve \end{pmatrix} \qquad (128)$$

Together with equation (17) for the height sensitivity components, this gives us all components of the Transit position measurement sensitivity matrix H, of equation (1), as needed by a Kalman filter to properly process a Transit fix. These components are given here as functions of $\rho$, $\sigma$, $\psi$, NS, EW and V. The receiver generally provides $\sigma$, NS and EW (as well as $\lambda$ and L). The remaining variables $\rho$, $\psi$ and V can be expressed as functions of these receiver supplied quantities.

As mentioned earlier, it is noteworthy that in most cases the bearing to the subpoint $\psi$ is approximately $\pm\pi/2$, so that $\cos\psi$ is of small magnitude relative to $\sin\psi$. Note also that at high satellite elevation angles ($\sigma \approx \pi/2$) the $1/\cos\sigma$ factor becomes very large.

## 7.0 COMBINED EFFECT OF VELOCITY AND HEIGHT ERRORS

Equations (17) and (128) can be combined to express the total effect of the error in the velocity and height provided to a Transit receiver on the Transit position fix error:

$$H = \begin{pmatrix} -\cos\psi\tan\sigma & -\frac{NS\cdot EW\rho B\cos\psi\sin\psi}{V\cos\sigma} & \frac{NS\cdot EW\rho\,(A\sin^2\psi+3\cos^2\psi)}{V\cos\sigma} \\ -\sin\psi\tan\sigma & -\frac{NS\cdot EW\rho(A\cos^2\psi+3\sin^2\psi)}{V\cos\sigma} & \frac{NS\cdot EW\rho B\cos\psi\sin\psi}{V\cos\sigma} \end{pmatrix} \tag{129}$$

where

$$A \equiv \cos^2\sigma \tag{130}$$

$$B \equiv 3 - \cos^2\sigma \tag{131}$$

so that

$$\begin{pmatrix} \Delta N \\ \Delta E \end{pmatrix} = \begin{pmatrix} -\cos\psi\tan\sigma & -C\cdot B\cos\psi\sin\psi & C(A\sin^2\psi+3\cos^2\psi) \\ -\sin\psi\tan\sigma & -C(A\cos^2\psi+3\sin^2\psi) & C\cdot B\cos\psi\sin\psi \end{pmatrix} \begin{pmatrix} \Delta h \\ \Delta vn \\ \Delta ve \end{pmatrix} \tag{132}$$

where

$$C \equiv \frac{NS\cdot EW\rho}{V\cos\sigma} \tag{133}$$

This provides all of the components of the Transit position measurement sensitivity matrix H, of equation (1), as needed by a Kalman filter to properly process a Transit fix. Notice from (133) that C diverges as the elevation angle $\sigma$ approaches 90° (while A goes to 0 and B goes to 3), reflecting the fact that high elevation angle satellite passes cannot

provide a useful fix (due to $\Delta r2$, $\Delta r3$ and $\Delta r4$).

The H components are given here as functions of $\rho$, $\sigma$, $\psi$, NS, EW and V. The receiver generally provides $\sigma$, NS and EW (as well as $\lambda$). The remaining variables $\rho$, $\psi$ and V can be expressed as functions of these receiver supplied quantities.

Section 8 below provides an algorithm by which these H components can be evaluated.

## 8.0 ALGORITHM

In this section we assemble all of the relevant equations needed to calculate the H matrix from the four input quantities that are assumed to be known:

1/ receiver latitude $\lambda$
2/ satellite maximum elevation angle $\sigma$
3/ satellite north-to-south direction of travel NS
4/ satellite east-to-west direction of travel EW

Since these are needed after the fix is made, the fix latitude can be used for $\lambda$, and modern receivers usually do supply $\sigma$, NS and EW.

The following set of equations, gathered from throughout this paper and its appendices, have all been derived herein and are sufficient for evaluating the components of H as functions of $(\lambda, \sigma, NS, EW)$. These equations can be solved in the order presented here. It is also important to apply the consistency check (A15), which limits $\Theta$ at high latitudes $\lambda$. If this limit is violated (because of an elevation angle $\sigma$ that is too low for the given latitude $\lambda$) then the square root in (C15) may not have a real value.

$$\Theta = \cos^{-1}\left( \frac{R}{R+H}\cos^2\sigma + \sin\sigma \sqrt{1 - \left(\frac{R}{R+H}\right)^2\cos^2\sigma} \right) \qquad \text{(A12)}$$

$$\cos\Theta \geq \sin|\lambda| \qquad \text{(A15)}$$

$$\rho = [\,(R+H)\cos\Theta - R\,]/\sin\sigma \qquad \text{(A5)}$$

$$K \equiv (R+H)\omega/V_S = .0744716 \qquad \text{(C11)}$$

$$\lambda_p = \sin^{-1}\left(\frac{\cos\theta - \sqrt{\cos^2\theta - 4K\sin\theta(NS\cdot EW\sin\lambda - K\sin\theta)}}{2NS\cdot EW\cdot K\sin\theta}\right) \quad \text{(C15)}$$

$$V = \sqrt{Vs^2 + (R+H)^2\omega^2\cos^2\lambda_p} \quad \text{(5)}$$

$$\sin\phi = \frac{-EW}{\left(1 + \left(\frac{(R+H)\omega\cos\lambda_p}{V_s}\right)^2\right)^{1/2}} \quad \text{(B13)}$$

$$\sin\psi = -\frac{\sin\phi\cos\lambda_p}{\cos\lambda} \quad \text{(D3)}$$

$$\cos\psi = \frac{\sin\lambda_p - \cos\theta\sin\lambda}{\sin\theta\cos\lambda} \quad \text{(D6)}$$

$$H = \begin{pmatrix} -\cos\psi\tan\sigma & -\frac{NS\cdot EW\rho B\cos\psi\sin\psi}{V\cos\sigma} & \frac{NS\cdot EW\rho}{V\cos\sigma}(A\sin^2\psi + 3\cos^2\psi) \\ -\sin\psi\tan\sigma & -\frac{NS\cdot EW\rho}{V\cos\sigma}(A\cos^2\psi + 3\sin^2\psi) & \frac{NS\cdot EW\rho B\cos\psi\sin\psi}{V\cos\sigma} \end{pmatrix} \quad \text{(129)}$$

$$A \equiv \cos^2\sigma \quad \text{(130)}$$

$$B \equiv 3 - \cos^2\sigma \quad \text{(131)}$$

The tree structure shown in Figure 13 illustrates graphically how the these equations can be used to find the components of H. Each node in Figure 13 shows the equation number followed by the variable which that equation expresses as a function of known quantities and the unknown variables attached to the node from below. Thus for example equation B13 expresses $\phi$ in terms of known quantities and the unknowns $\lambda_p$ and EW. To evaluate any variable in this figure one must therefore solve for all variables below its node.

Figure 13. Appendix Use Flow Diagram.

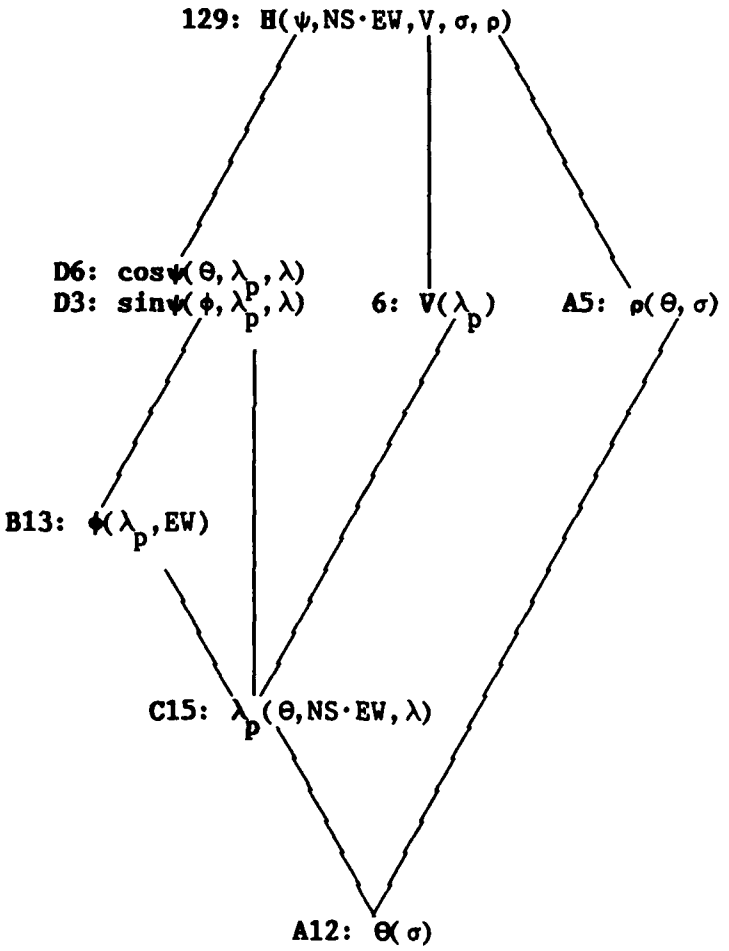


The following is a pseudo code algorithm which uses these equations to evaluate the components of the measurement matrix H, given the Transit satellite pass information ($\sigma$,NS,EW) and a receiver latitude estimate $\lambda$.

```
                                                                  Equation
input variables:        λ,NS,EW,σ
output variables:       H(2,3)
constants:              R  = 6370000.
                        H  = 1075000.
                        Vs = 7290
                        K  = .0744716          ω(R+H)/Vs    (C11)
                        K1 = .855608                 R/(R+H)
                        π  = 3.14159265
intermediate variables: ρ,V,cscphi
                        csig,c2sig,s2sig, clat,slat,
                        cthe,sthe,s2the, cpsi,spsi
dummy variables:        A,B,C,D


if( σ < .1  or  σ > 1.4 )  return error condition

csig = cos(σ)
c2sig = csig*csig
s2sig = 1 - c2sig
cthe = K1*c2sig + sqrt( s2sig*(1 - K1*K1*c2sig) )                 (A12)

if( cthe < abs(sin(λ)) ) return error condition                   (A15)

ρ = ( (R+H)*cthe - R )/sin(σ)                                     (A5)

s2the = 1 - cthe*cthe
sthe = sqrt(s2the)
D = sqrt( cthe*cthe - 4*K*(NS*EW*sthe*sin(λ) - K*s2the) )
slat = (cthe - D)/(2*NS*EW*K*sthe)                                (C15)
clat = sqrt(1 - slat*slat)

D = K*clat
cscphi = -EW*sqrt(1 + D*D)                                        (B13)

spsi = -clat/(cos(λ)*cscphi)                                       (D3)
cpsi = (slat - cthe*sin(λ))/(sthe*cos(λ))                          (D6)

V = Vs*sqrt(1 + K*K*clat*clat)                                      (5)

D = sin(σ)/csig
HH(1,1) = -cpsi*D                                                  (17)
HH(2,1) = -spsi*D

A = c2sig                                                         (130)
B = 3 - c2sig                                                     (131)
C = NS*EW*ρ/(V*csig)                                              (133)
HH(1,2) = -C*B*cpsi*spsi
HH(2,2) = -C*(A*cpsi*cpsi + 3*spsi*spsi)
HH(1,3) =  C*(A*spsi*spsi + 3*cpsi*cpsi)
HH(2,3) =  C*B*cpsi*spsi
```

## 9.0 NUMERICAL RESULTS

From Section 8.0 above, we see that the Transit error sensitivity model, as embodied in the H matrix of (129), is a function of four variables: ($\sigma$,NS,EW,$\lambda$). This model can therefore be illustrated by showing the numerical values of the H matrix as functions of the satellite elevation angle $\sigma$, for each of the four possible directions of travel (NS=$\pm$1,EW=$\pm$1), at a fixed receiver latitude $\lambda$. Section 8.0 above provides the explicit equations necessary to do this. In Section 9.2 below the six elements of H are plotted, along with three intermediate geometric quantities of interest, for each of the four directions of travel, at a receiver latitude of 45°. The latitude dependence is illustrated in Section 9.3, by considering the receiver latitude to be a parameter defining a family of curves for each of the curves shown in Section 9.2.

In Section 9.1 it is shown that, except for a change in sign, there are actually only four different height error sensitivity functions (out of a potential 8, from 2 H elements times 4 directions of travel), and there are only six different velocity error sensitivity functions (out of the potential 16, from four H elements times 4 directions of travel). From the plots of Section 9.3 it can be seen that in fact one of these four different height sensitivity functions (clockwise H(2,1)) is actually very close to an other (counter-clockwise H(2,1)), and two of the velocity sensitivity functions (clockwise H(2,2) and H(1,3)) are very close to two others, (counter-clockwise H(2,2) and H(1,3)) so that there are in effect only three "basic" height sensitivity functions and four "basic" velocity error sensitivity functions (except for a change in sign).

### 9.1 Direction of Travel Dependence

By inspecting the equations of Section 8.0 above, which express the H components explicitly in terms of the variables ($\sigma$,NS,EW,$\lambda$p), it can be seen that the direction of travel variables, NE and EW, appear only in equations (C15), (B13) and (107). In two of these equations they appear only as the product NE·EW, which has only two possible values. These two cases can conveniently be labelled the "clockwise" case, for NS·EW=1 (i.e. NS=EW=1 and NS=EW=-1) and the "counterclockwise" case, for NS·EW=-1 (ie. NS=1,EW=-1 and NS=-1,EW=1), describing the satellite direction relative to the receiver looking down from above. In the remaining equation (B13), only EW appears, and its effect is simply to change the sign of $\phi$, the effect of which can

be easily followed through to see that it simply changes the sign of $\psi$ (via (D3)), which in turn changes the sign of H(2,1), H(1,2) and H(2,3).

Therefore we can conclude that all terms for NS=EW=1 will be exactly the same as the corresponding term when NS=EW=-1 (the "clockwise" terms), except for a change in sign of H(2,1), H(1,2) and H(2,3). The same can be said for the "counterclockwise" terms with NS=1, EW=-1 as compared to those with NS=-1, EW=1.

$$\begin{aligned}
H(1,1)_{NS,EW=1} &= H(1,1)_{NS,EW=-1} \\
H(2,1)_{NS,EW=1} &= -H(2,1)_{NS,EW=-1} \\
H(1,2)_{NS,EW=1} &= -H(1,2)_{NS,EW=-1} \\
H(2,2)_{NS,EW=1} &= H(2,2)_{NS,EW=-1} \\
H(1,3)_{NS,EW=1} &= H(1,3)_{NS,EW=-1} \\
H(2,3)_{NS,EW=1} &= -H(2,3)_{NS,EW=-1}
\end{aligned} \tag{134}$$

$$\begin{aligned}
H(1,1)_{NS=-1,EW=1} &= H(1,1)_{NS=1,EW=-1} \\
H(2,1)_{NS=-1,EW=1} &= -H(2,1)_{NS=1,EW=-1} \\
H(1,2)_{NS=-1,EW=1} &= -H(1,2)_{NS=1,EW=-1} \\
H(2,2)_{NS=-1,EW=1} &= H(2,2)_{NS=1,EW=-1} \\
H(1,3)_{NS=-1,EW=1} &= H(1,3)_{NS=1,EW=-1} \\
H(2,3)_{NS=-1,EW=1} &= -H(2,3)_{NS=1,EW=-1}
\end{aligned} \tag{135}$$

This reduces by half (to 12) the number of different functional forms needed to describe this model. Furthermore, from the expressions (129) it can be seen that generally

$$H(1,2) = -H(2,3) \tag{136}$$

Thus, for a given latitude and satellite direction of travel, the velocity error sensitivity of a Transit fix can be described by three functions: H(1,2), H(1,3) and H(2,2). This reduces the number of independent functions (of $\sigma$ and $\lambda$) to 10 (four for

height sensitivity and six for velocity sensitivity).

At first glance of the numerical results shown in Section 9.2 below, it appears that changing the direction of travel (from clockwise to counterclockwise) also only changes the sign of H(2,1), H(2,2) and H(1,3). Closer inspection reveals that this is not exactly true however, and the difference arises from equation (C15), which is not homogeneous in NS·EW. The difference however is not significant, even at extreme latitudes, as seen in Section 9.3 below. Therefore we have

$$\begin{aligned} H(1,3)_{\text{clockwise}} &\simeq -H(1,3)_{\text{counterclockwise}} \\ H(2,1)_{\text{clockwise}} &\simeq -H(2,1)_{\text{counterclockwise}} \\ H(2,2)_{\text{clockwise}} &\simeq -H(2,2)_{\text{counterclockwise}} \end{aligned} \qquad (137)$$

This reduces the number of substantially different functions (again this is only if the sign is ignored) to 7, with 3 for height error sensitivity and 4 for velocity error sensitivity. Representative functions are:

$$\begin{aligned} &H(1,1)_{\text{clockwise}} \\ &H(2,1)_{\text{clockwise}} \\ &H(1,2)_{\text{clockwise}} \\ &H(2,2)_{\text{clockwise}} \\ &H(1,3)_{\text{clockwise}} \\ &H(1,1)_{\text{counterclockwise}} \\ &H(1,2)_{\text{counterclockwise}} \end{aligned} \qquad (138)$$

## 9.2 Elevation Angle Dependence

Figures 14 to 16 illustrate the six components of the H matrix (the Transit velocity and height error sensitivity model) as functions of the maximum satellite elevation angle $\sigma$, for a latitude of 45° N, and a satellite direction of travel NS=EW=1 (satellite rising in the north and passing east of the receiver). Figures 17 to 19 illustrate intermediate geometric quantities of interest, namely the latitude of the satellite subpoint $\lambda p$, the

bearing $\phi$ from the satellite subpoint to the receiver and the bearing $\psi$ from the receiver to the subpoint (all at the point of closest approach).

Figures 20 to 37 give the same set of plots for the other three satellite directions of travel. From these plots it can be seen that the primary effect of changing the direction of travel is simply to change the sign of the error, as discussed in Section 9.1 above.

Furthermore, from Figures 14 to 37, it can be seen that at this latitude the effect of changing the satellite direction of travel is to change the sign of, but not appreciably change the form of, the dominant terms H(1,3) and H(2,2). Only the smaller term H(1,2) significantly changes its form with different directions of travel, having a "clockwise" form (with NE,EW = 1,1 or -1,-1) and a "counterclockwise" form (with NS,EW = -1,1 or 1,-1).

Figure 14. Effect of 1m/s North Velocity Error (NS=EW=1, lat=45)

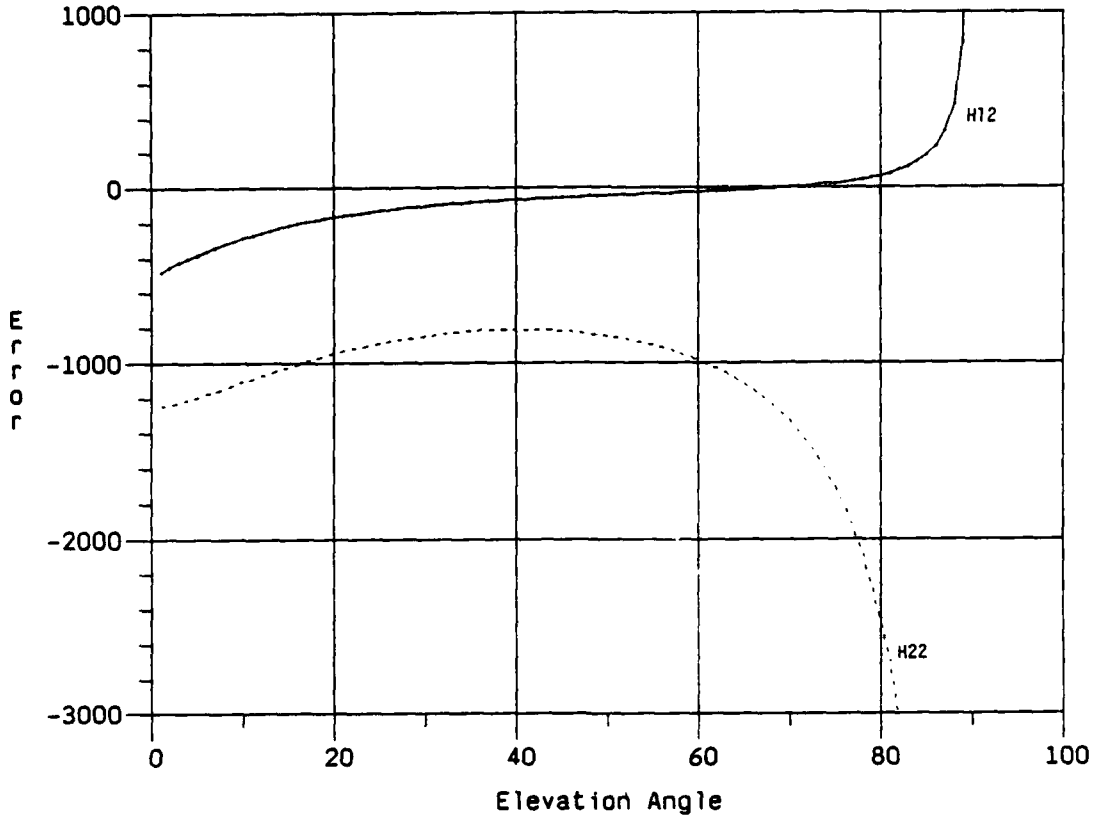


Figure 15. Effect of 1m/s East Velocity Error (NS=EW=1, lat=45)

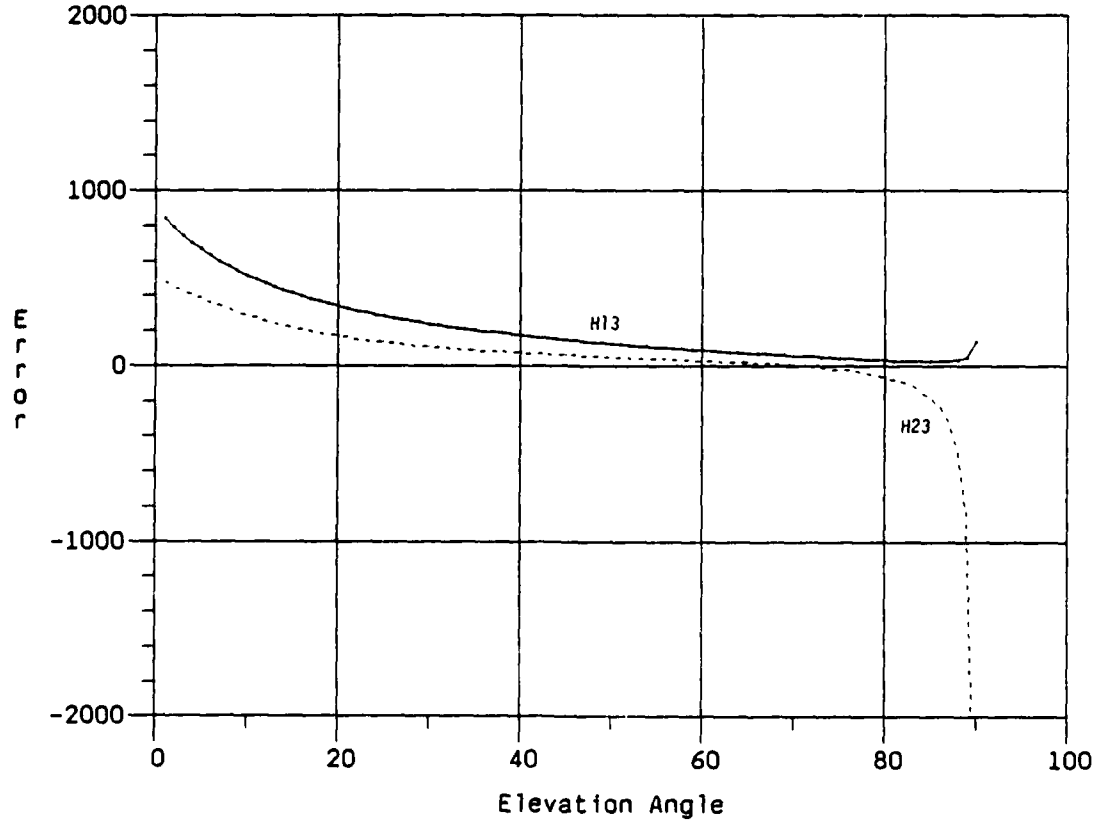

Figure 16. Effect of 1 metre Height Error (NS=EW=1, lat=45)

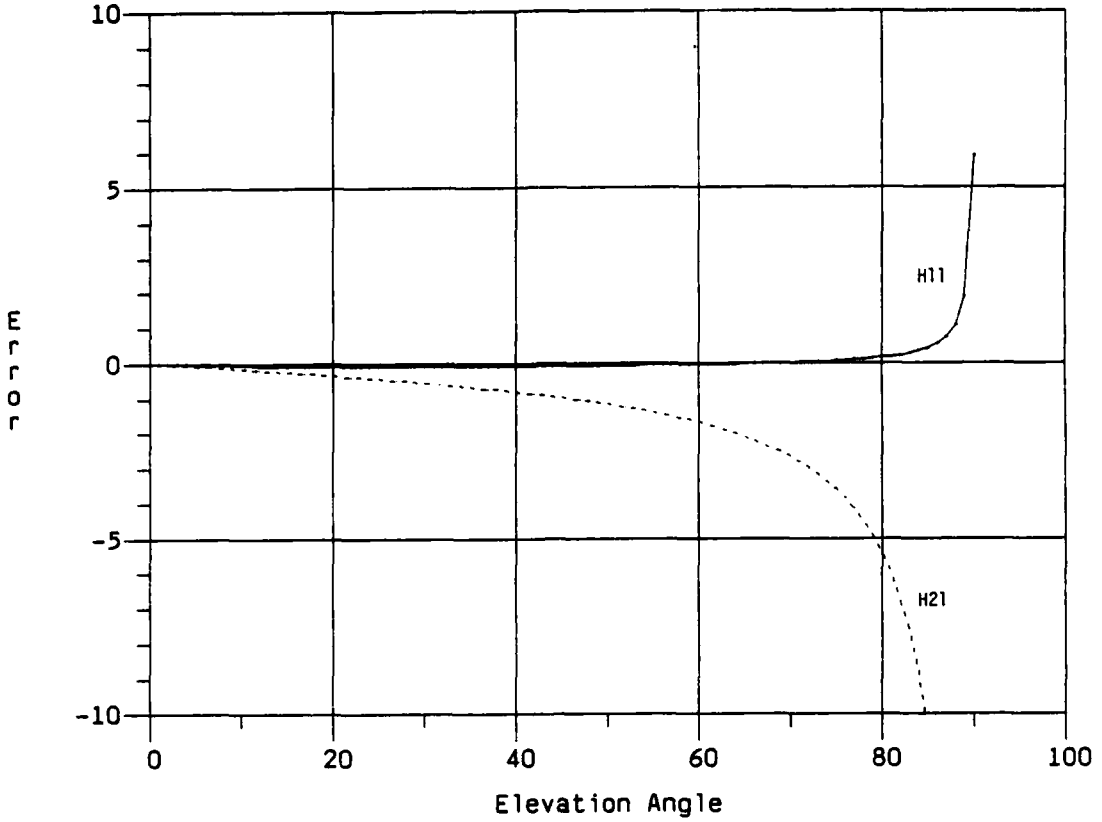


Figure 17. Subpoint Latitude (NS=EW=1, lat=45)

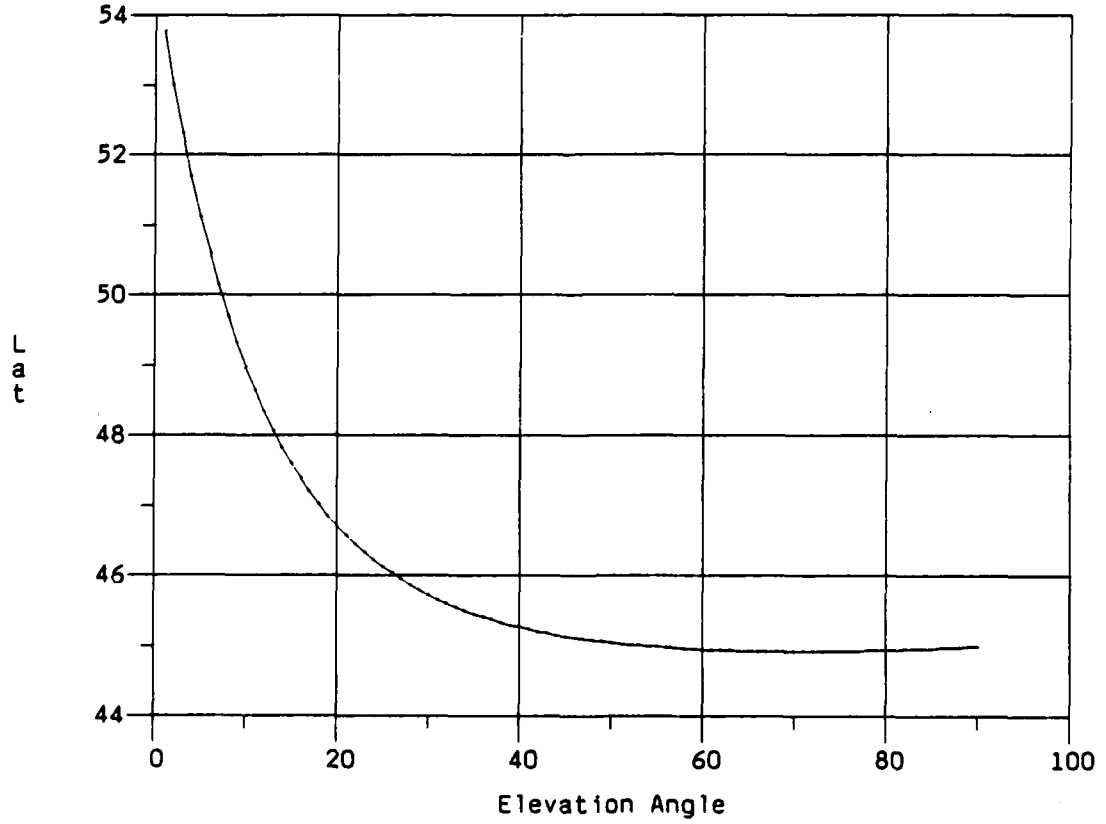

Figure 18. Bearing From Subpoint to Receiver (NS=EW=1,lat=45)

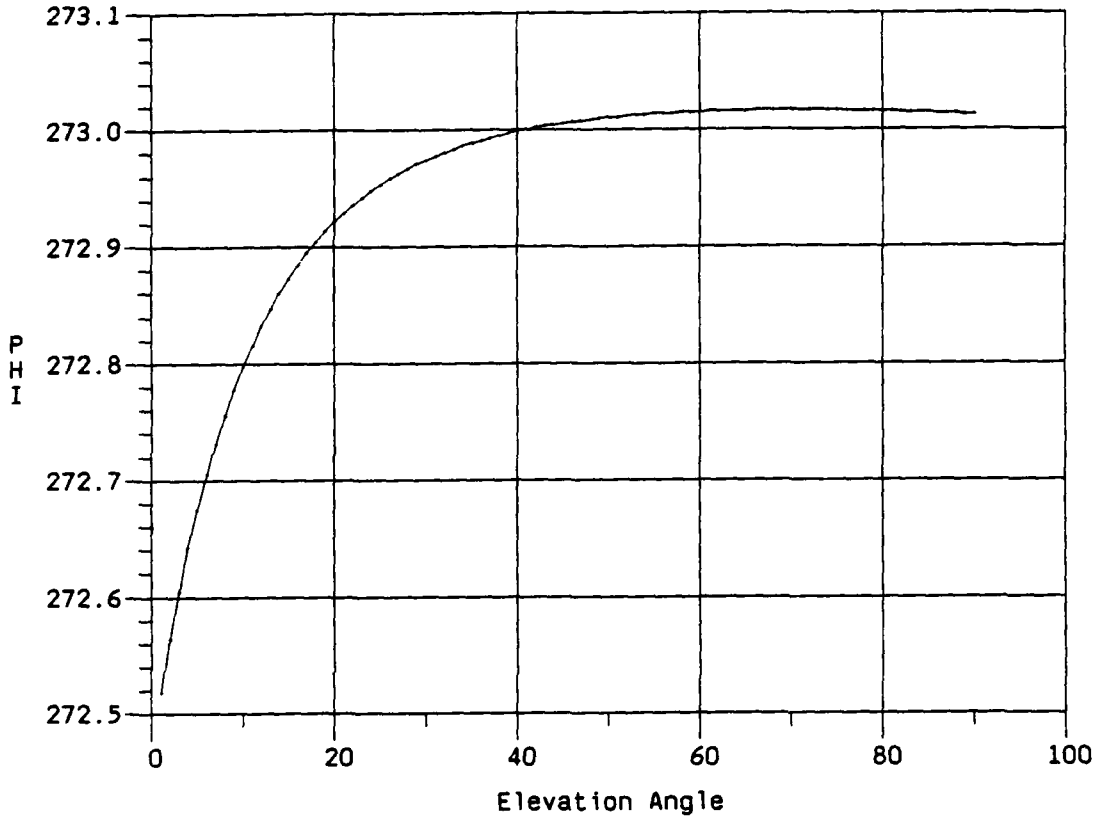


Figure 19. Bearing From Receiver to Subpoint (NS=EW=1,lat=45)

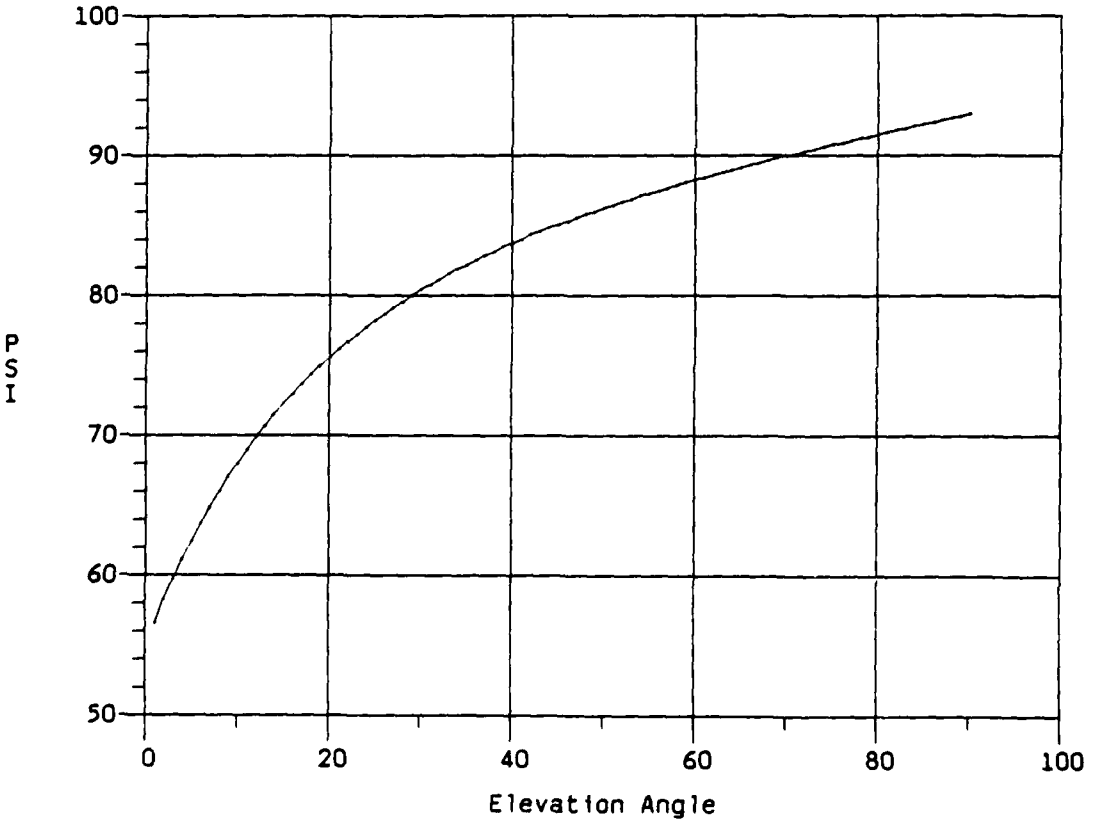

Figure 20. Effect of 1m/s North Velocity Error (NS=1,EW=-1, lat=45)

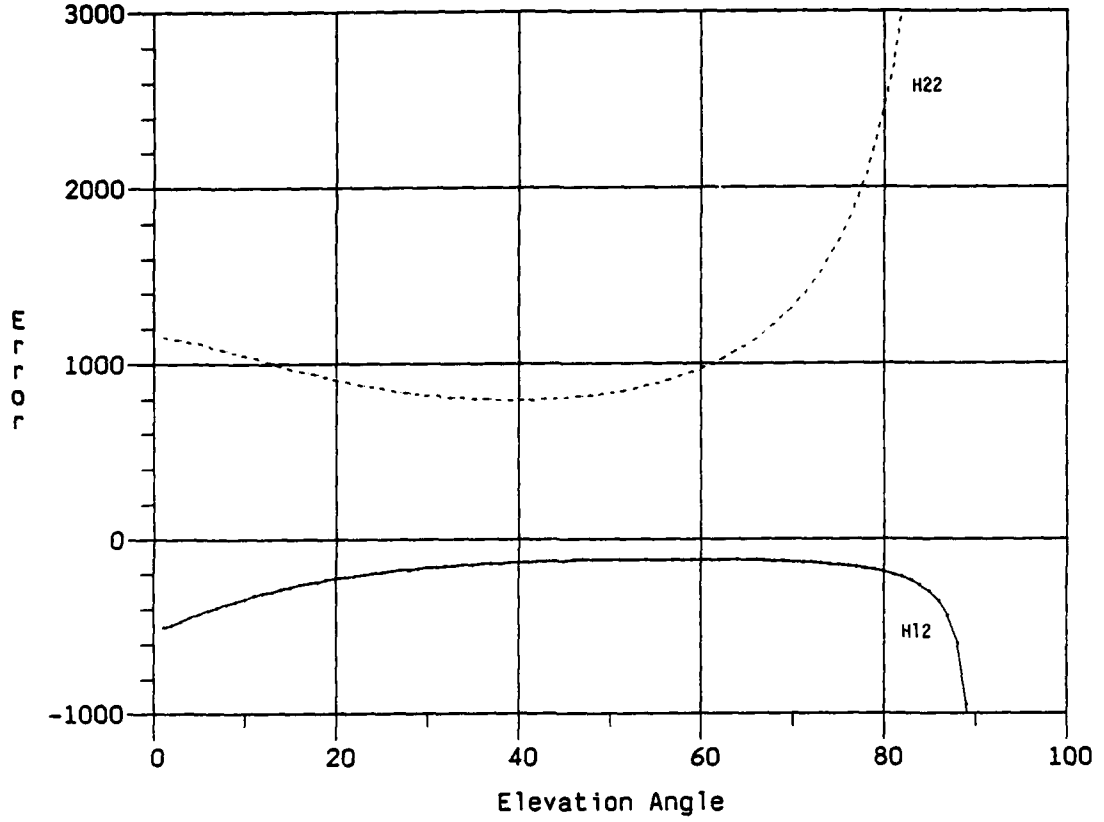


Figure 21. Effect of 1m/s East Velocity Error (NS=1,EW=-1,lat=45)

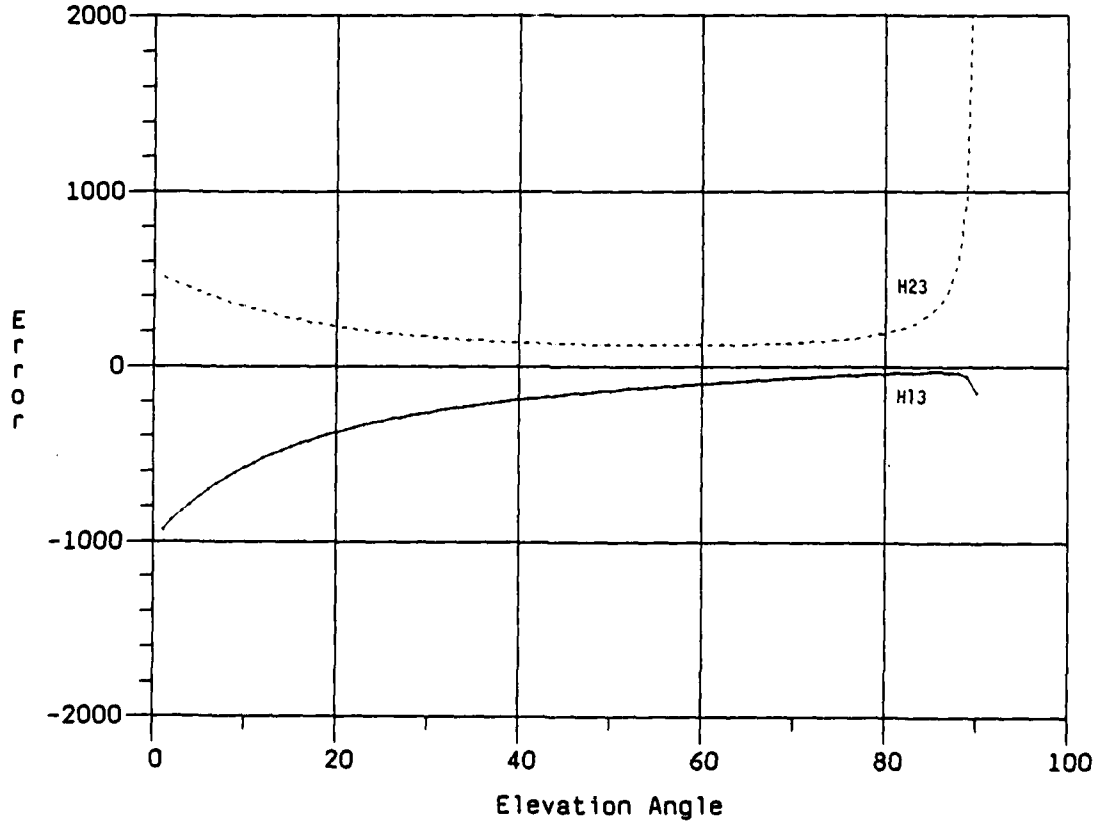

Figure 22. Effect of 1 metre Height Error (NS=1,EW=-1,lat=45)

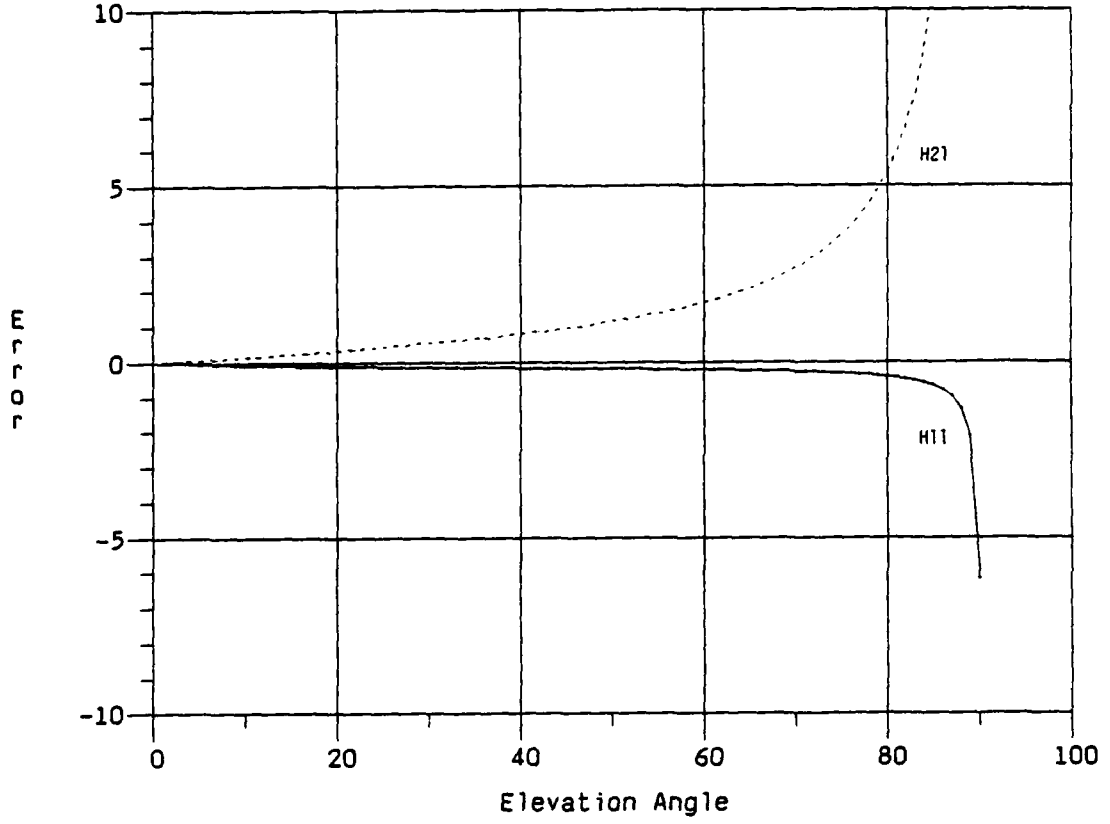


Figure 23. Subpoint Latitude (NS=1,EW=-1,lat=45)

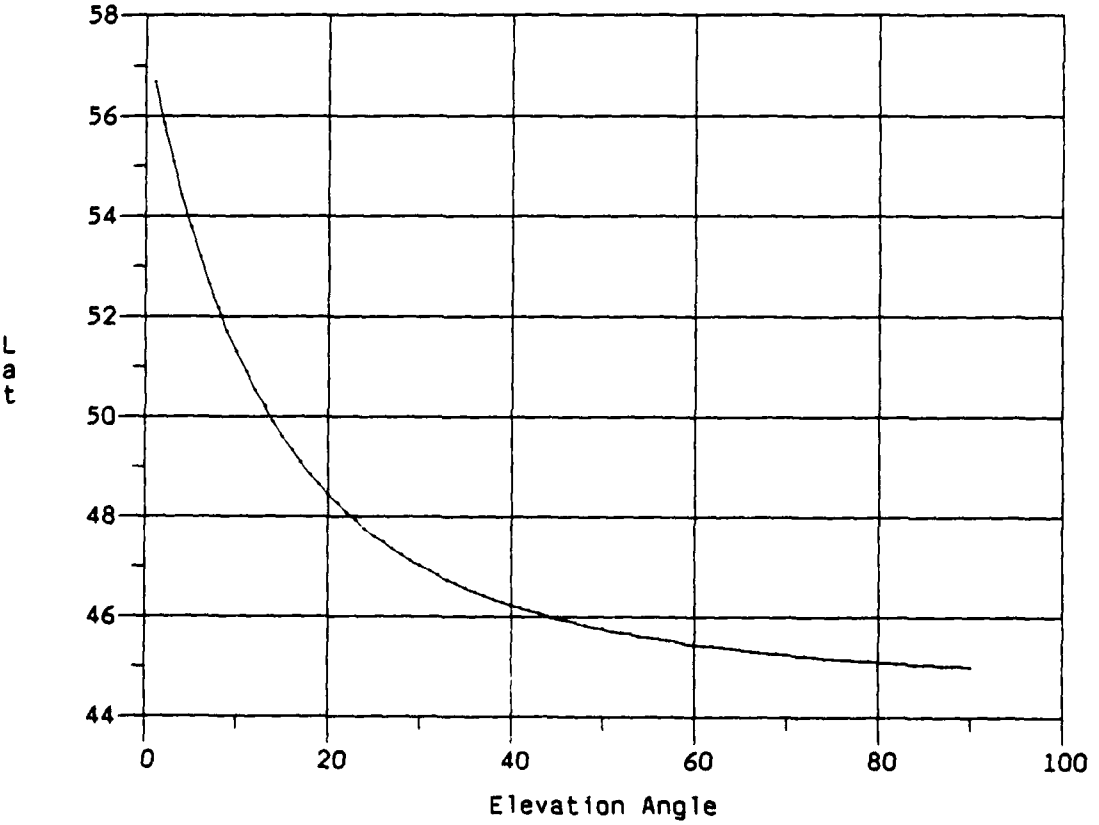

Figure 24. Bearing From Subpoint to Receiver (NS=1,EW=-1,lat=45)

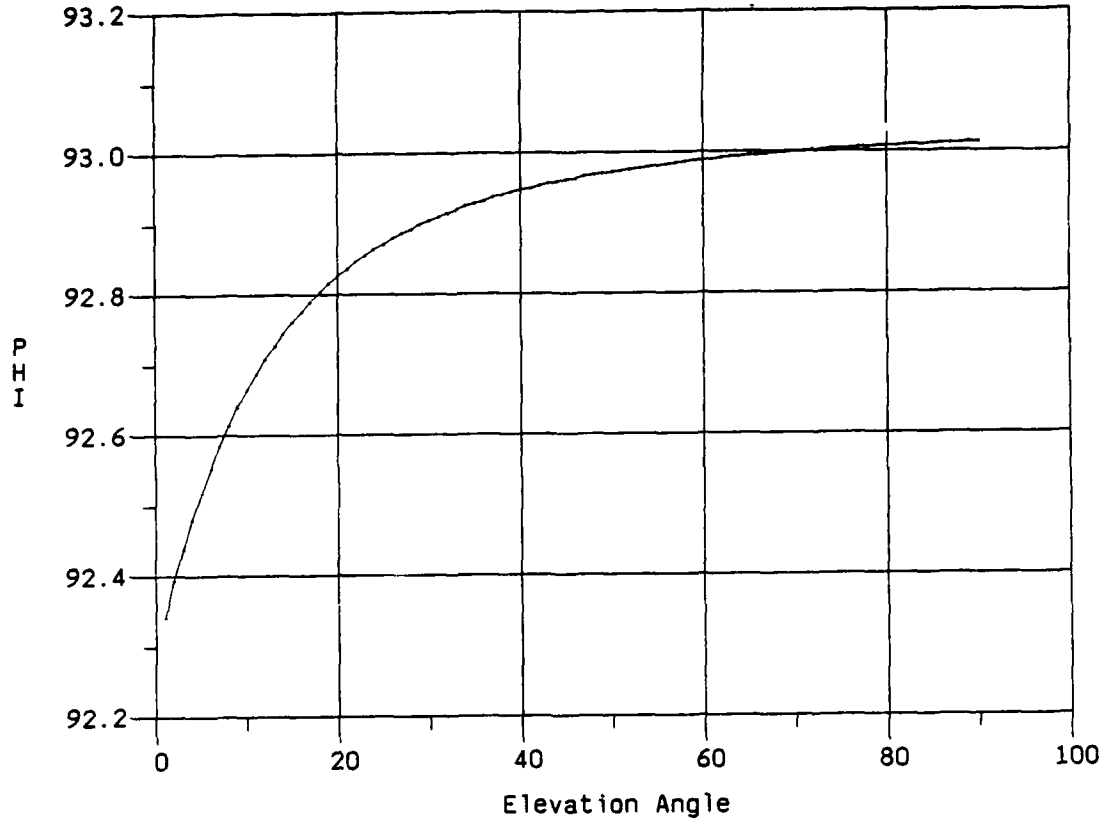


Figure 25. Bearing From Receiver to Subpoint (NS=1,EW=-1,lat=45)

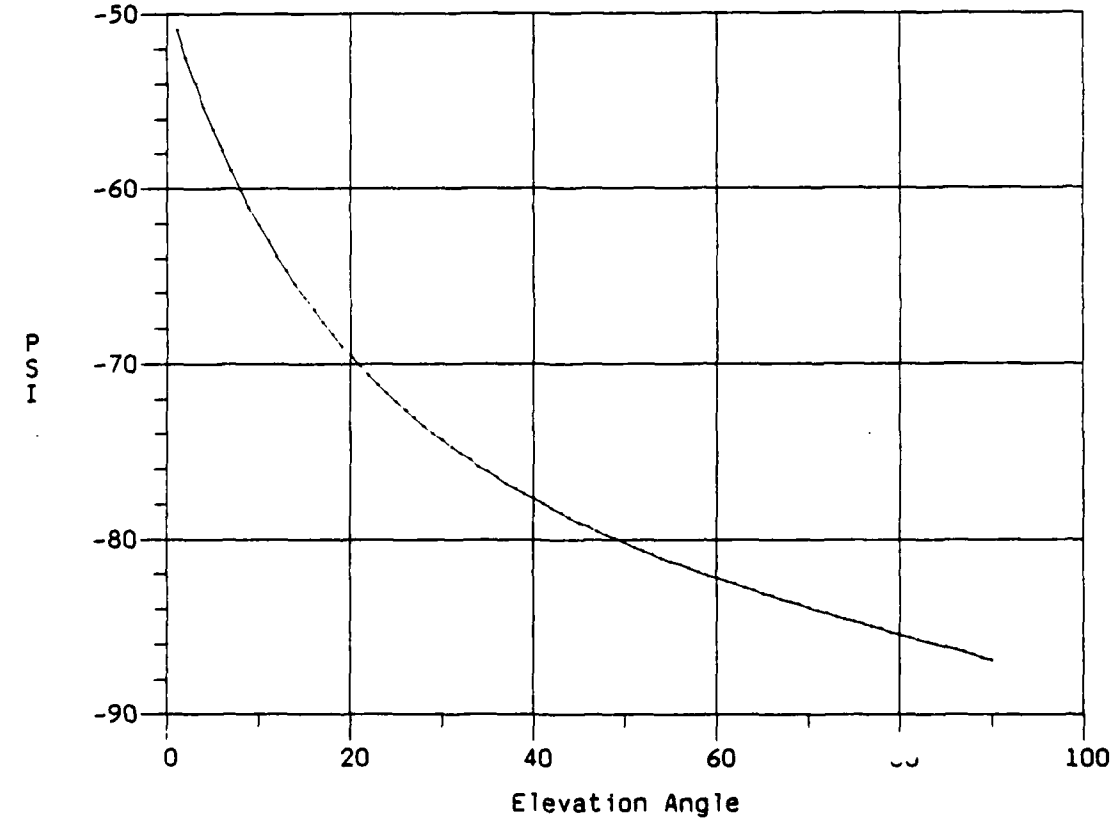

Figure 26. Effect of 1m/s North Velocity Error (NS=-1,EW=1, lat=45)

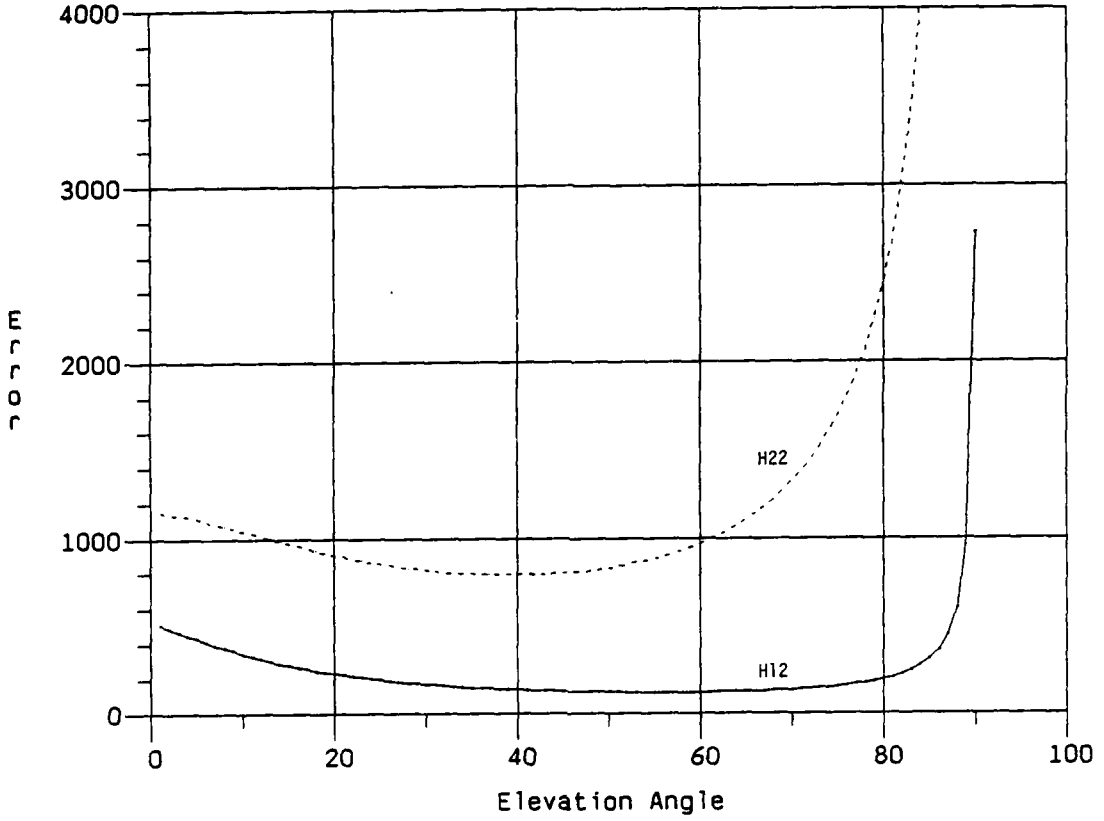


Figure 27. Effect of 1m/s East Velocity Error (NS=-1,EW=1,lat=45)

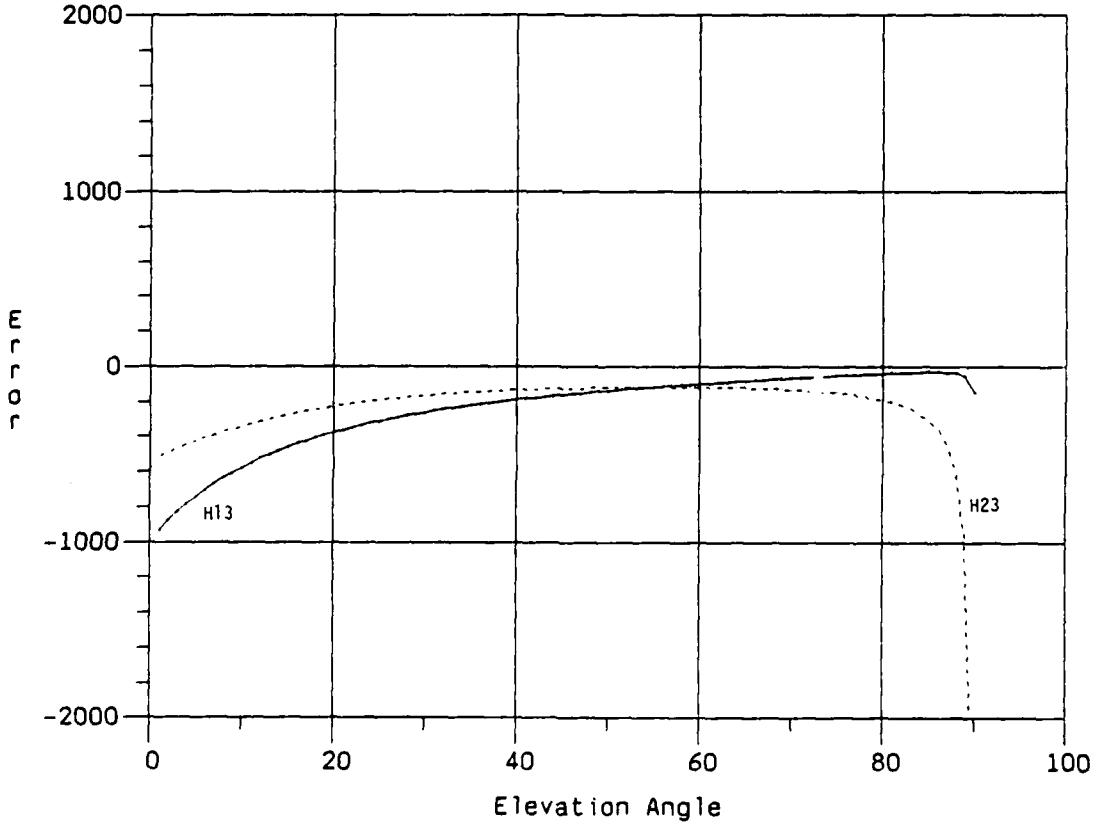

Figure 28. Effect of 1 metre Height Error (NS=-1,EW=1,lat=45)

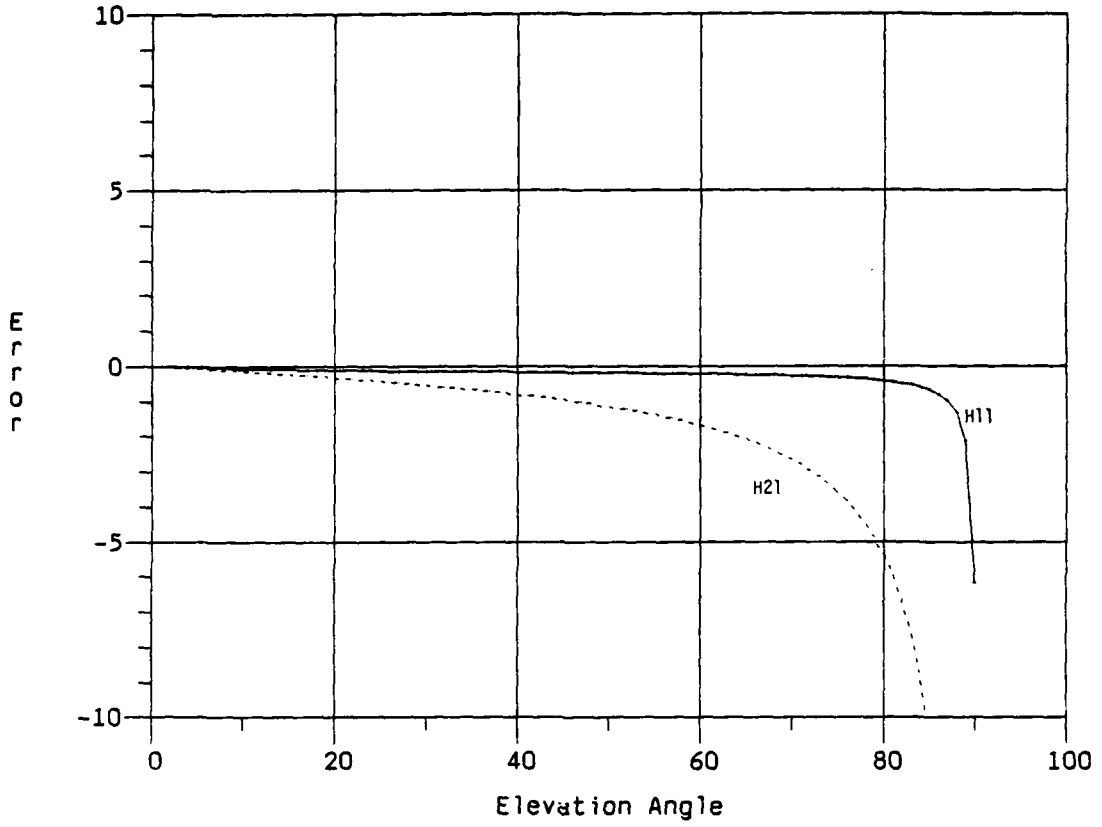


Figure 29. Subpoint Latitude (NS=-1,EW=1,lat=45)

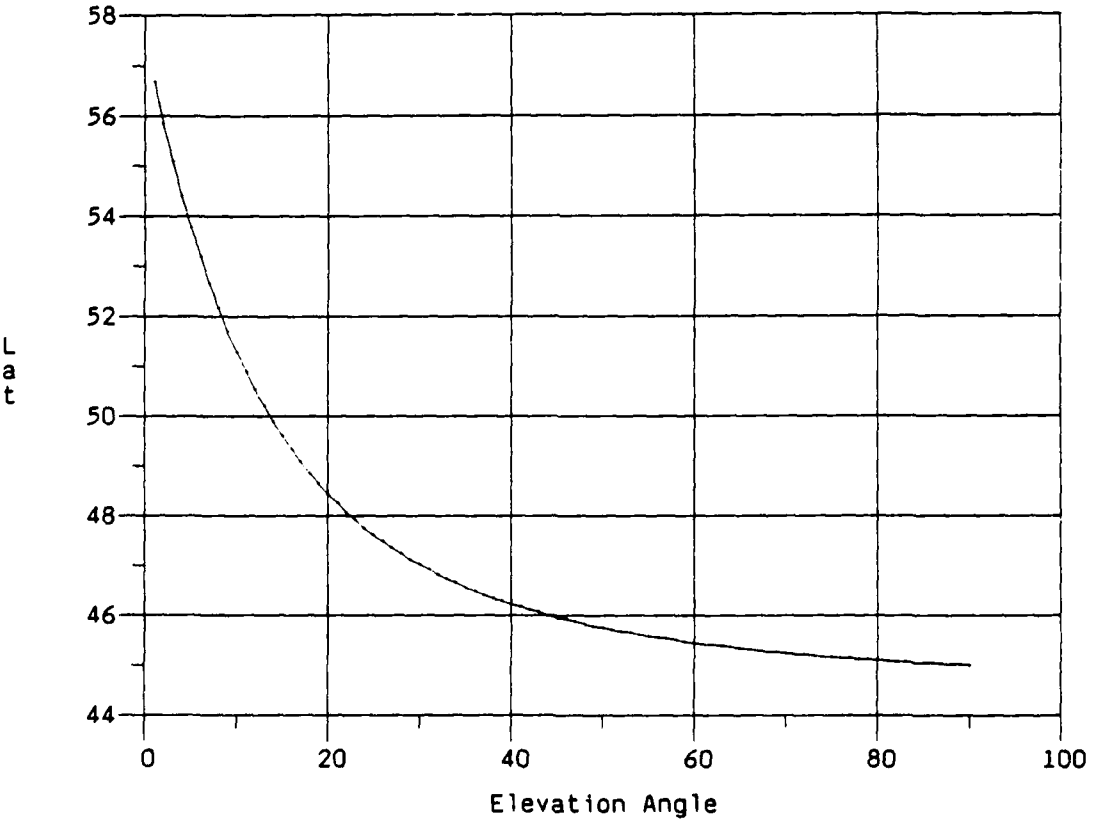

Figure 30. Bearing From Subpoint to Receiver (NS=-1,EW=1,lat=45)

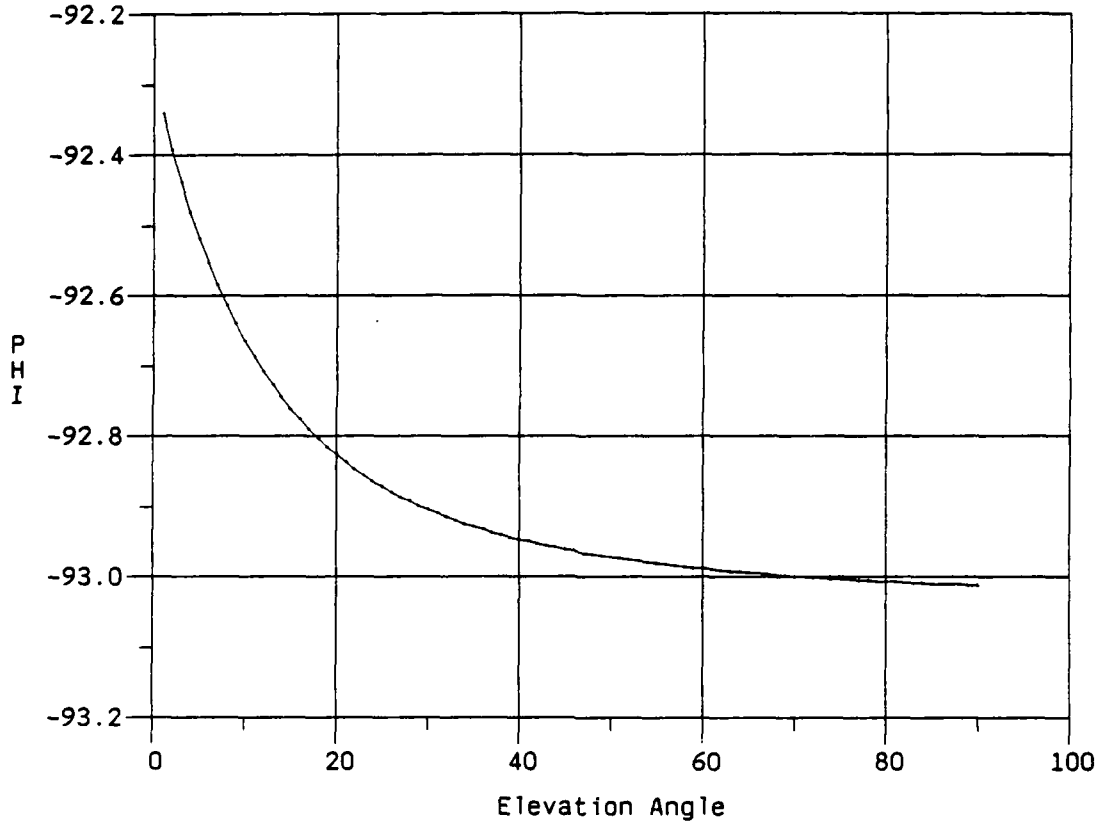


Figure 31. Bearing From Receiver to Subpoint (NS=-1,EW=1,lat=45)

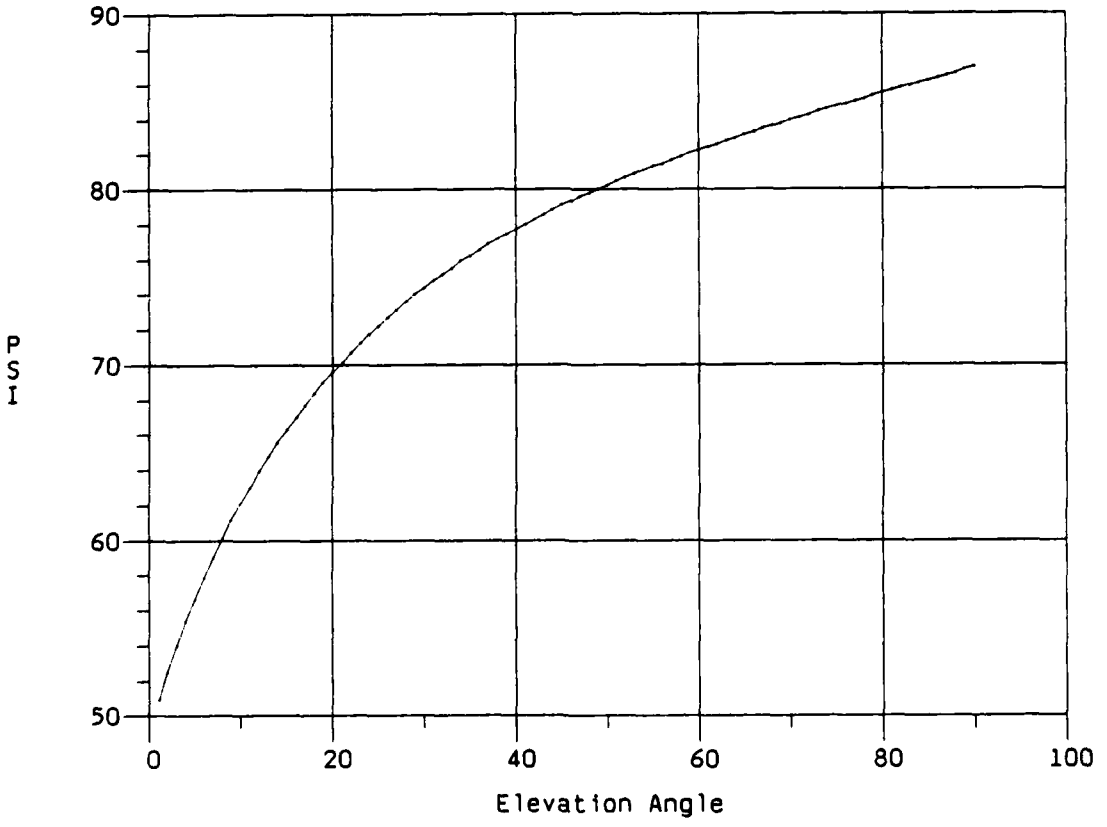

Figure 32. Effect of 1m/s North Velocity Error (NS=EW=-1, lat=45)

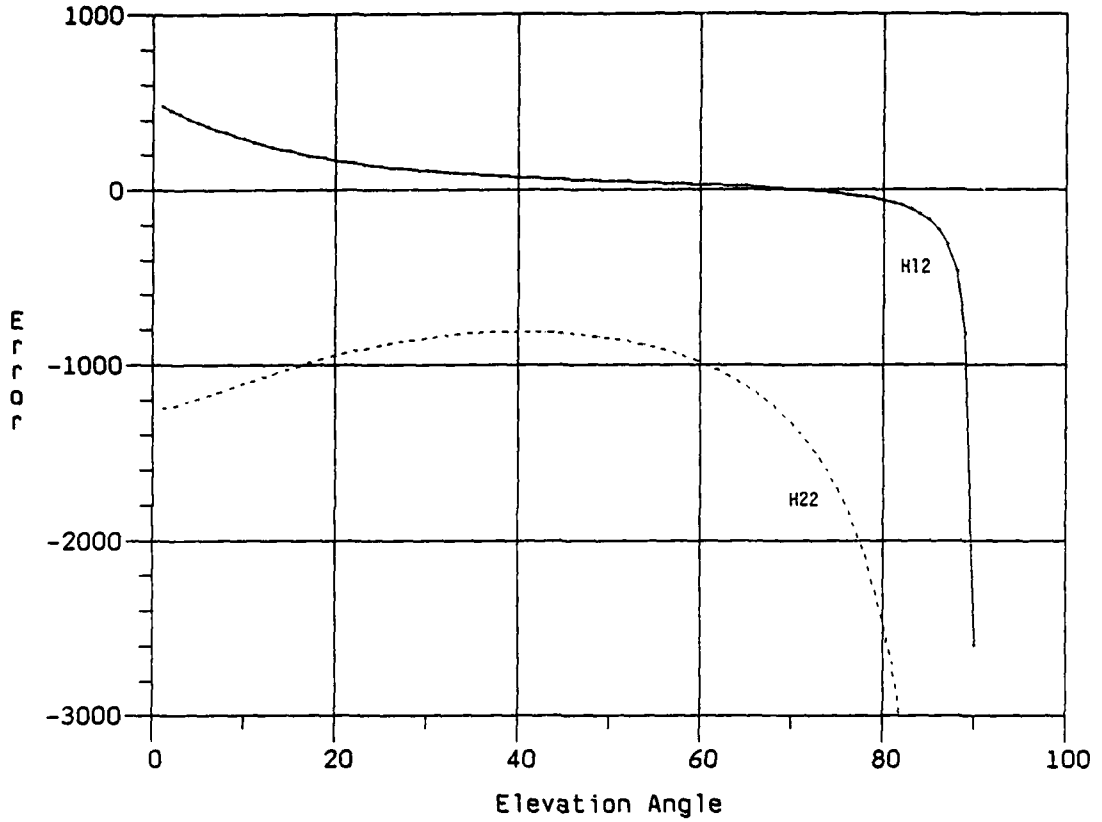


Figure 33. Effect of 1m/s East Velocity Error (NS=EW=-1, lat=45)

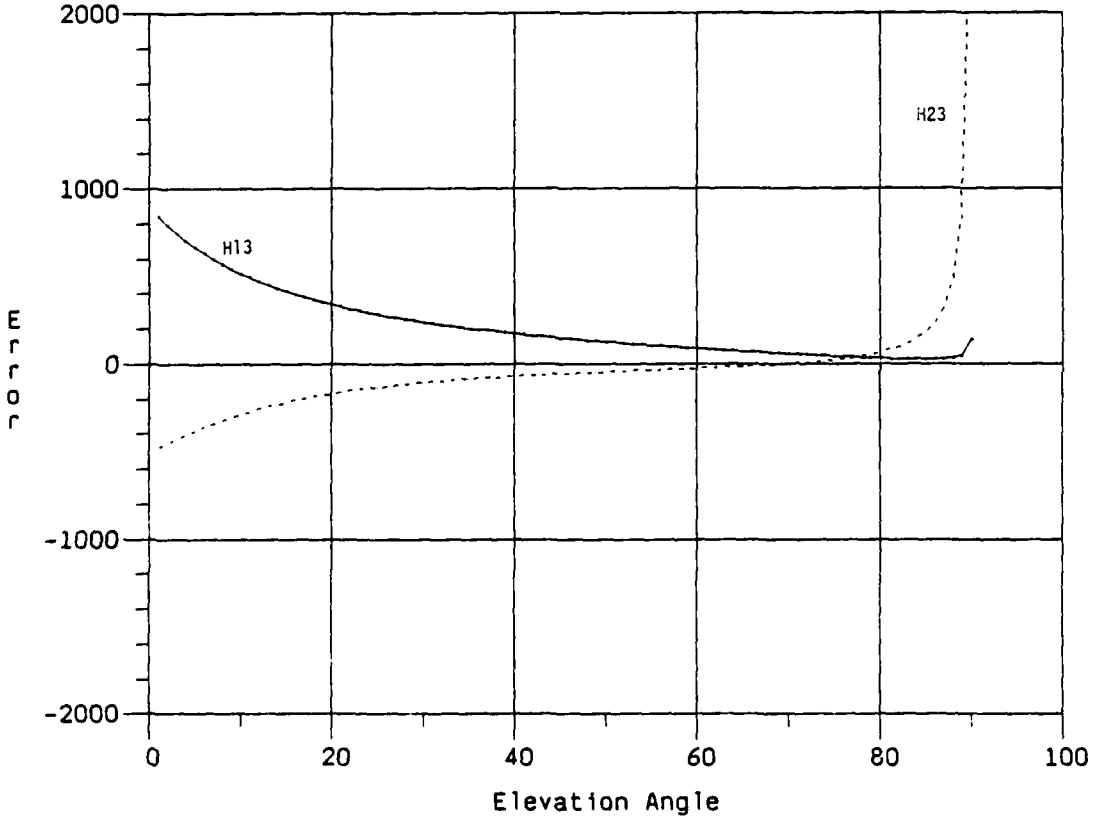

Figure 34. Effect of 1 metre Height Error (NS=EW=-1,lat=45)

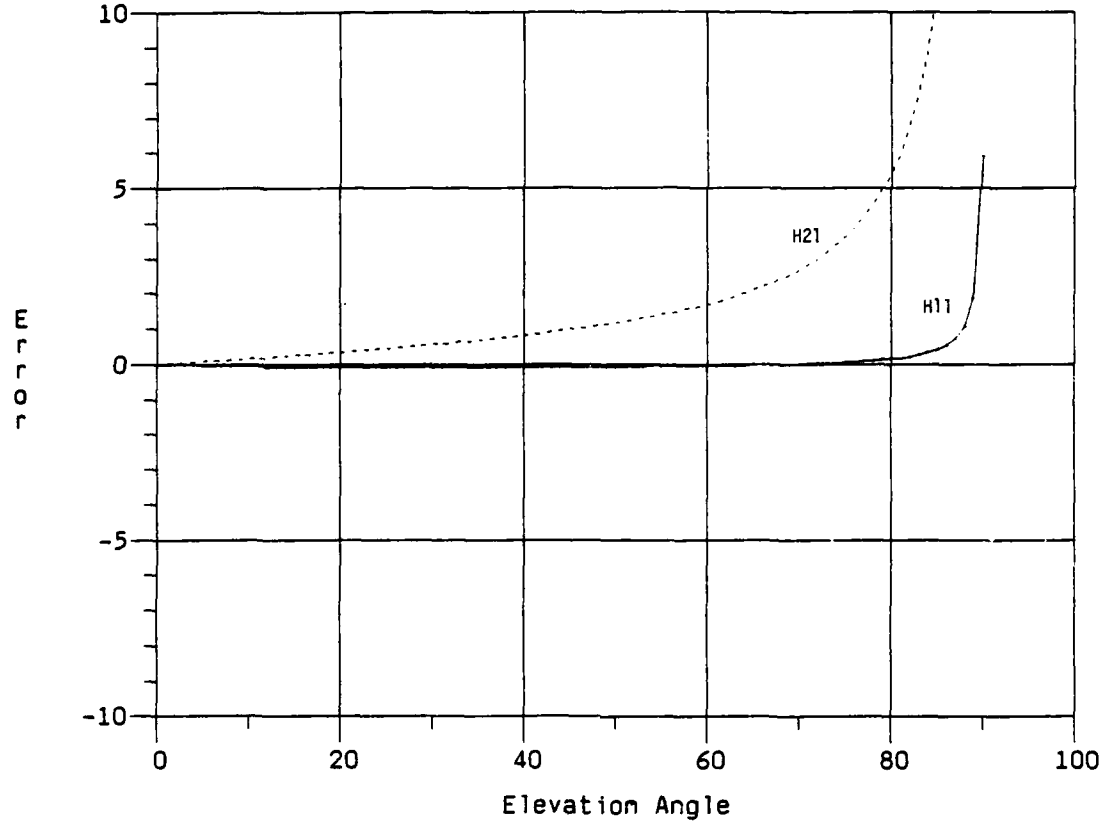


Figure 35. Subpoint Latitude (NS=EW=-1,lat=45)

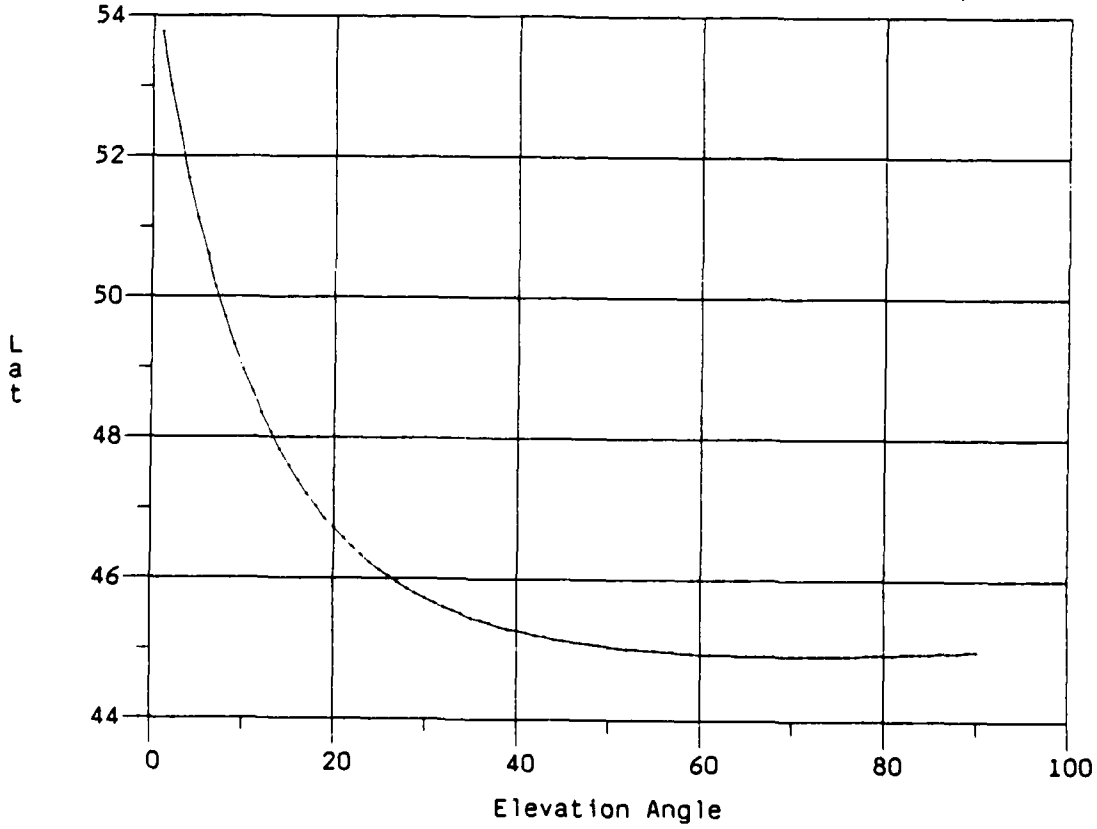

Figure 36. Bearing From Subpoint to Receiver (NS=EW=-1, lat=45)

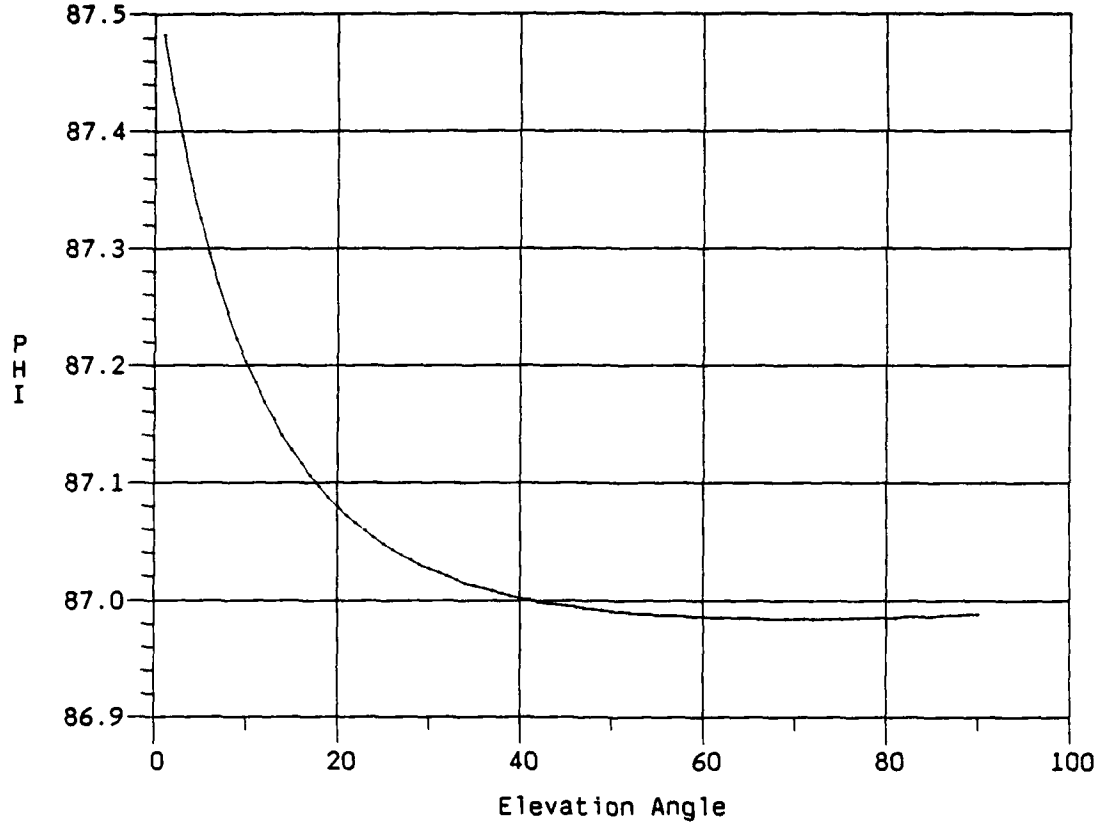


Figure 37. Bearing From Receiver to Subpoint (NS=EW=-1, lat=45)

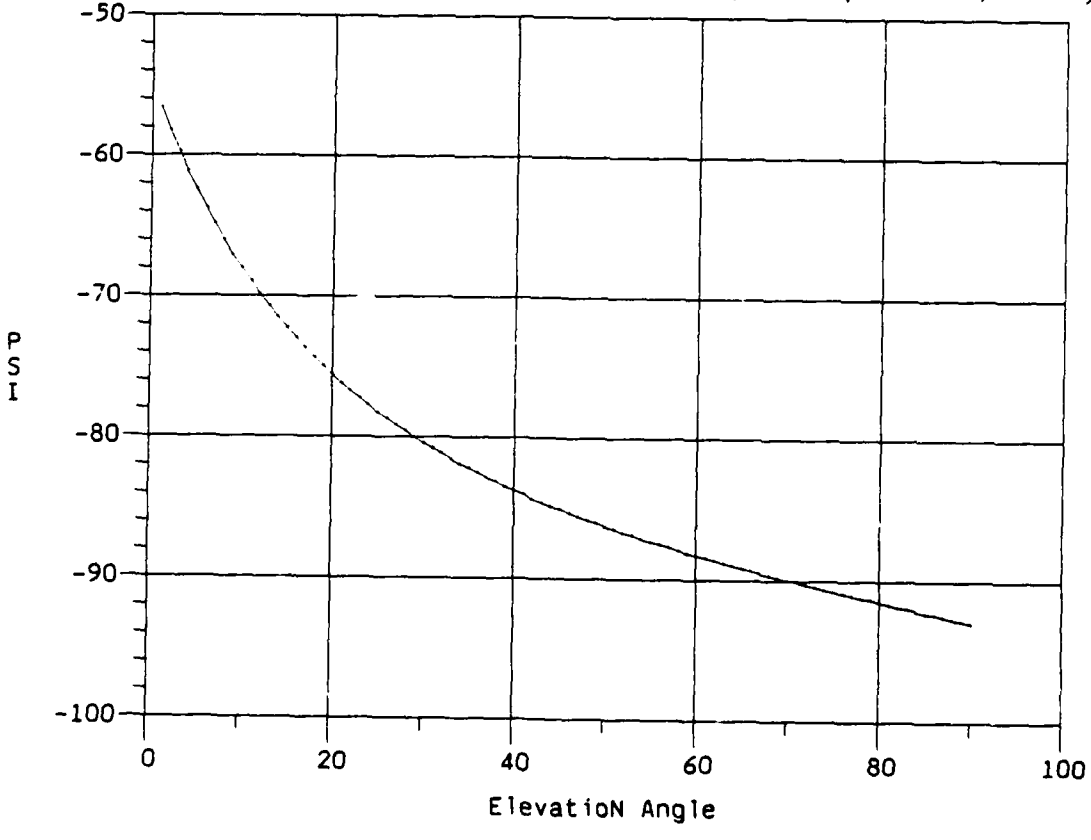

## 9.3 Latitude Dependence

Figures 38 to 69 illustrate the dependence of the H matrix elements (along with $\phi$ and $\psi$ ) on the receiver latitude. This is done by showing families of curves where each curve represents the elevation angle dependence of the variable of interest, at a fixed latitude. The discrete latitudes chosen for the different curves of each set are 0°, 20°, 40°, 60°, 70°, 80° and 85° (north and south for Figures 38 to 45, north only for Figures 46 to 69). Notice that the latitude spacing used is greater at low latitudes. This is because the effect of changing latitude is much less at low latitude, and in fact for some figures the 0° and 20° curves cannot be clearly separated.

The most notable difference at high latitudes is that the lower satellite elevation passes do not exist. The reason for this is that the polar point in the Transit orbit places a lower limit on the maximum elevation angle $\sigma$ (all Transit satellites are in polar orbits). This limit on $\sigma$ is greater than zero for all receiver latitudes above 59° (as shown in Appendix A).

From Figures 38 to 69 it can be confirmed that the H(2,2) function has essentially the same form (except for a change of sign) for all directions of travel at all latitudes, and that the same can be said of H(1,3). It can also be verified that, as predicted in Section 9.1 above, the terms H(1,2)=-H(2,3) have only two different forms (except for a change of sign) for all directions of travel at all latitudes.

When negative latitudes are examined an additional symmetry appears. Although it is only illustrated here explicitly for Figures 38 to 45 (the NS=EW=1 case) the general symmetry is easy to imagine from the remaining Figures 46 to 69, and can be proven using the equations of Section 8.0. That is: the clockwise families of curves at negative latitudes are of exactly the same form (ie. is the same except for possibly a change of sign) as the corresponding counterclockwise families for positive latitudes:

$$H(i,j)\ (\lambda)_{clockwise} = \pm H(i,j)\ (-\lambda)_{clockwise} \qquad (139)$$

for all i,j. We can see this by following through the equations of Section 8.0, where simultaneously changing the sign of $\lambda$ and NS·EW simply:

1-changes the sign of $\lambda_p$ in (C15) (because of NS·EW on the denominator)

2-leaves V unchanged in (5)

3-changes the sign of cos$\psi$ in (D6) (because $\lambda$ and $\lambda_p$ both change sign)

4-either changes the sign of $\phi$ in (B13) or leaves it unchanged (depending on whether or not EW changes sign)

5-either changes the sign of sin$\psi$ in (D3) or leaves it unchanged (depending on whether or not $\phi$ changes sign)

In the final equation (129) for the components of H, the net effect is to change:

$$\begin{aligned} \cos\psi &\rightarrow -\cos\psi \\ \sin\psi &\rightarrow -\delta EW \sin\psi \\ NS\cdot EW &\rightarrow -NS\cdot EW \end{aligned} \qquad (140)$$

where $\delta$EW is negative if EW changes sign. The effect is therefore to change the sign of H(1,1), H(1,3) and H(2,2), and to change the sign of the three remaining terms only if EW changes sign. In other words

$$\begin{aligned} H(1,1)\,(\lambda)_{clockwise} &= -H(1,1)\,(-\lambda)_{clockwise} \\ H(1,3)\,(\lambda)_{clockwise} &= -H(1,3)\,(-\lambda)_{clockwise} \\ H(2,2)\,(\lambda)_{clockwise} &= -H(2,2)\,(-\lambda)_{clockwise} \end{aligned} \qquad (141)$$

and

$$\begin{aligned} H(2,1)\,(\lambda)_{NS=EW=1} &= -H(2,1)\,(-\lambda)_{NS=1,EW=-1} \\ &= H(2,1)\,(-\lambda)_{NS=-1,EW=1} \\ H(2,1)\,(\lambda)_{NS=EW=-1} &= H(2,1)\,(-\lambda)_{NS=1,EW=-1} \\ &= -H(2,1)\,(-\lambda)_{NS=-1,EW=1} \end{aligned} \qquad (142)$$

$$
\begin{aligned}
H(1,2)\ (\lambda)_{NS=EW=1} &= -H(1,2)\ (-\lambda)_{NS=1,EW=-1} \\
&= H(1,2)\ (-\lambda)_{NS=-1,EW=1} \\
H(1,2)\ (\lambda)_{NS=EW=-1} &= H(1,2)\ (-\lambda)_{NS=1,EW=-1} \\
&= -H(1,2)\ (-\lambda)_{NS=-1,EW=1}
\end{aligned}
\qquad (143)
$$

$$
\begin{aligned}
H(2,3)\ (\lambda)_{NS=EW=1} &= -H(2,3)\ (-\lambda)_{NS=1,EW=-1} \\
&= H(2,3)\ (-\lambda)_{NS=-1,EW=1} \\
H(2,3)\ (\lambda)_{NS=EW=-1} &= H(2,3)\ (-\lambda)_{NS=1,EW=-1} \\
&= -H(2,3)\ (-\lambda)_{NS=-1,EW=1}
\end{aligned}
\qquad (144)
$$

This exact symmetry now replaces the approximate symmetry of equation (137), and leaves only five "basic" families (for latitudes from -90° to +90°) of functions of $\sigma$, rather than the 7 families (some of which were only approximately equal, for latitudes 0 to +90) listed in (138). These five families can be represented by:

$$
\begin{aligned}
&H(1,1)_{\text{clockwise}} \\
&H(2,1)_{\text{clockwise}} \\
&H(1,2)_{\text{clockwise}} \\
&H(2,2)_{\text{clockwise}} \\
&H(1,3)_{\text{clockwise}}
\end{aligned}
\qquad (145)
$$

which are fully illustrated in Figures 38 to 43.

Figure 38. Latitude Dependence of H(1,1) (NS=EW=1)

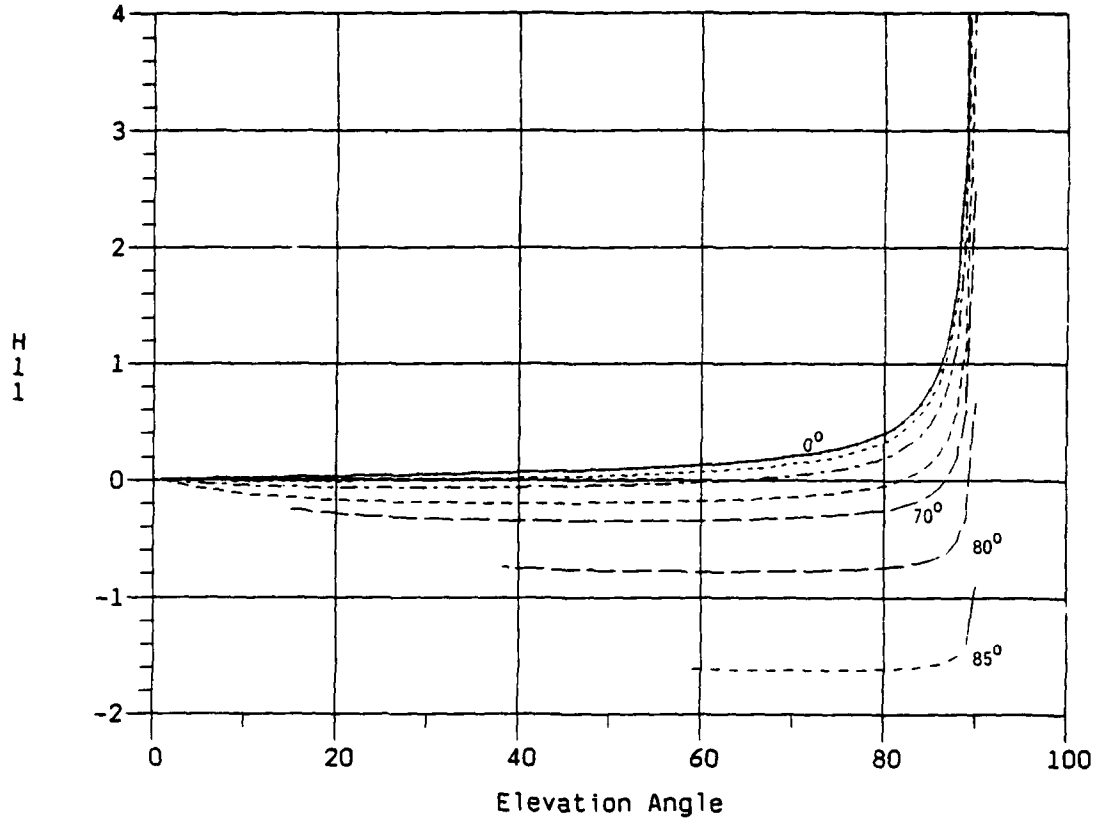


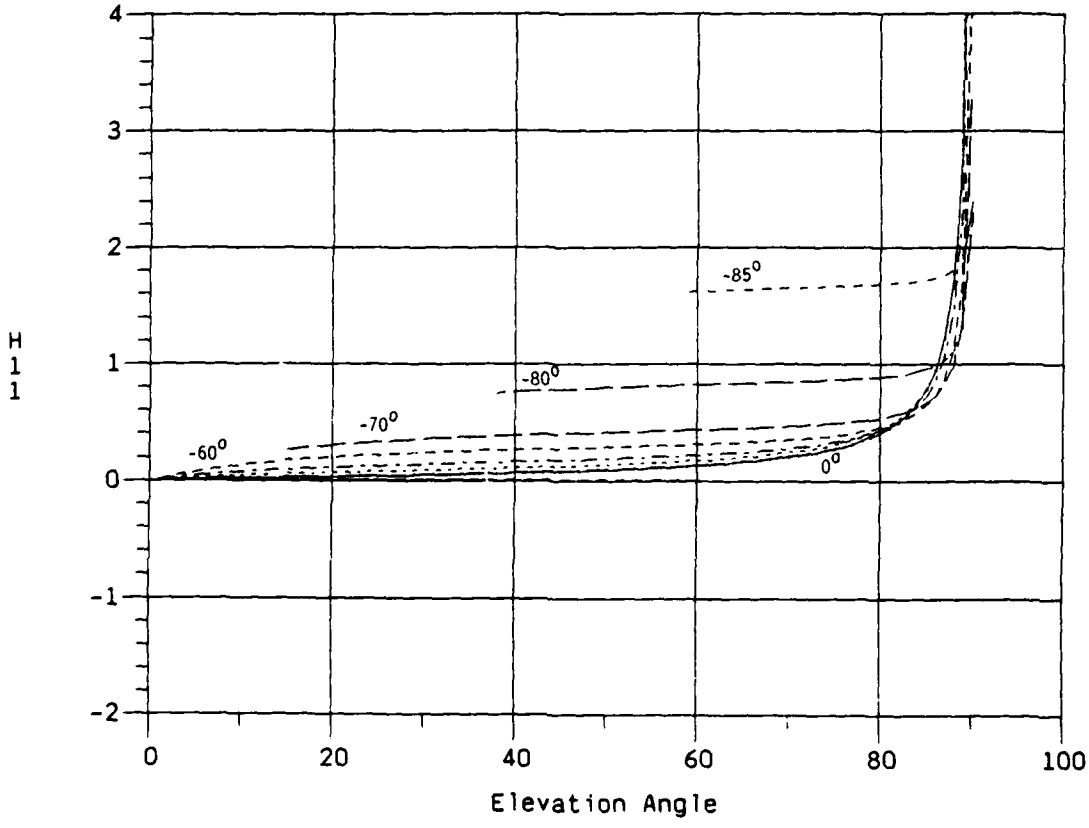

Figure 39. Latitude Dependence of H(2,1) (NS=EW=1)

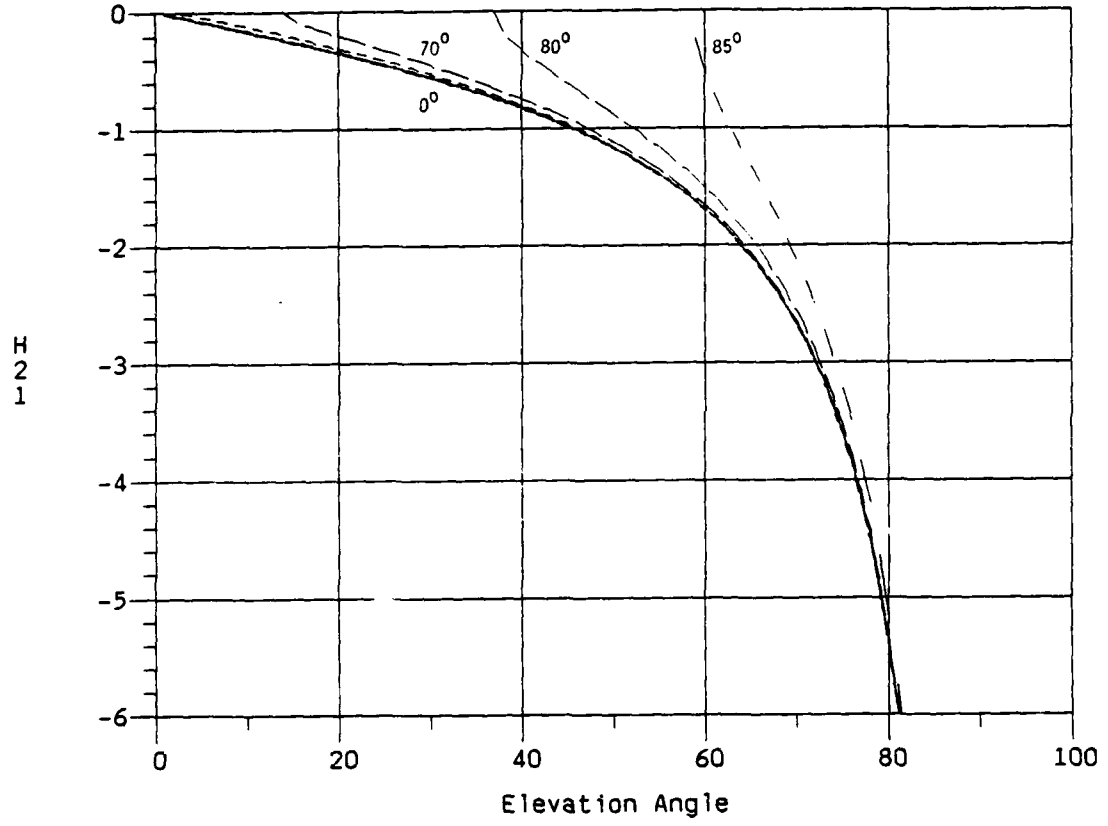


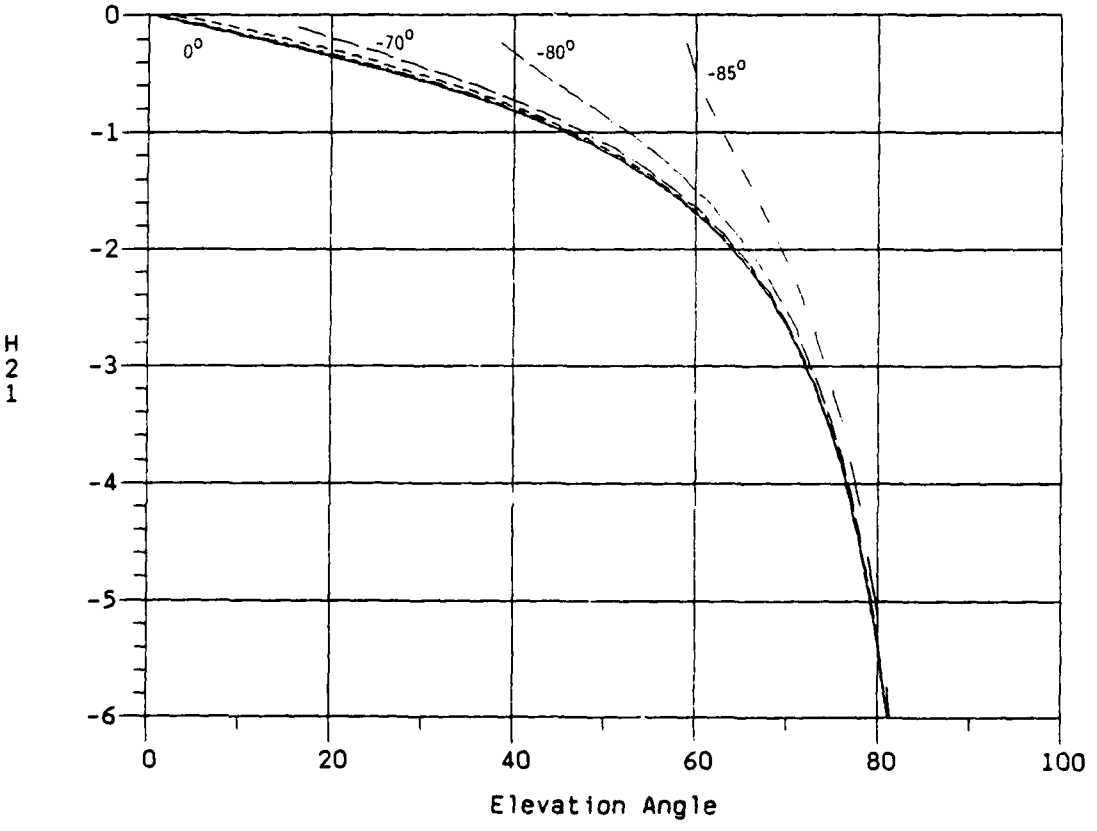

Figure 40. Latitude Dependence of H(1,2) (NS=EW=1)

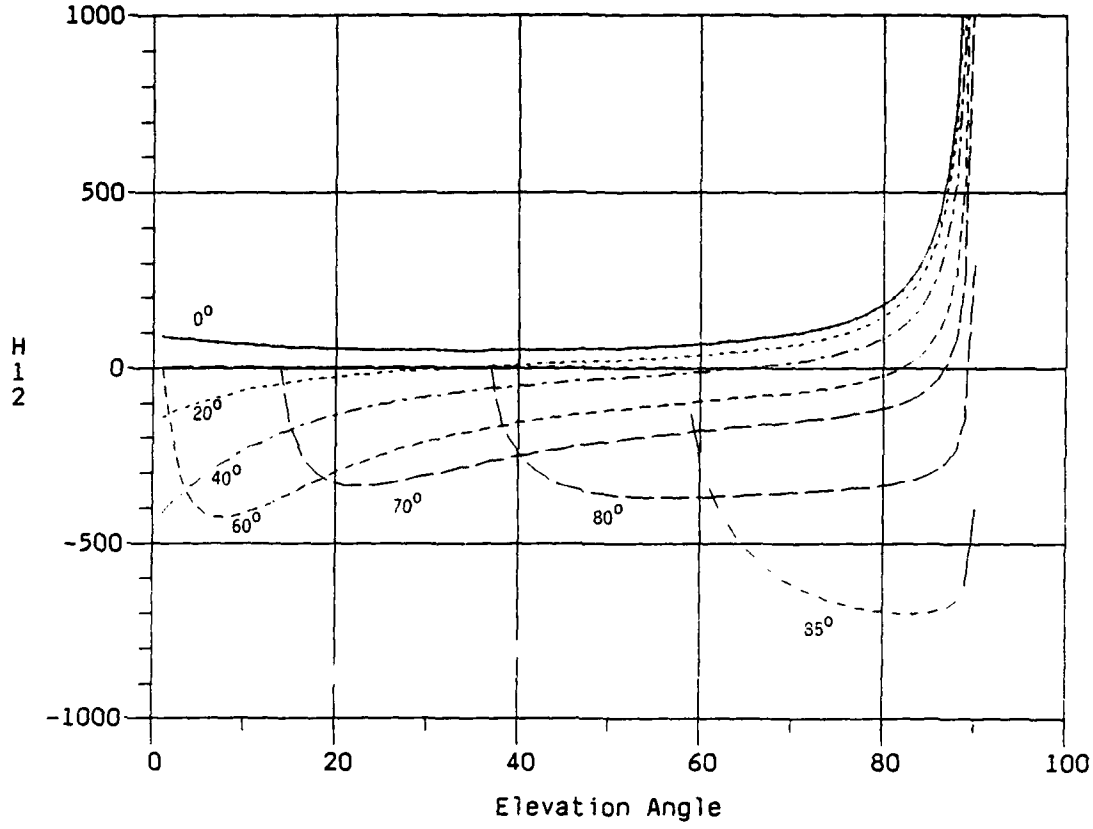


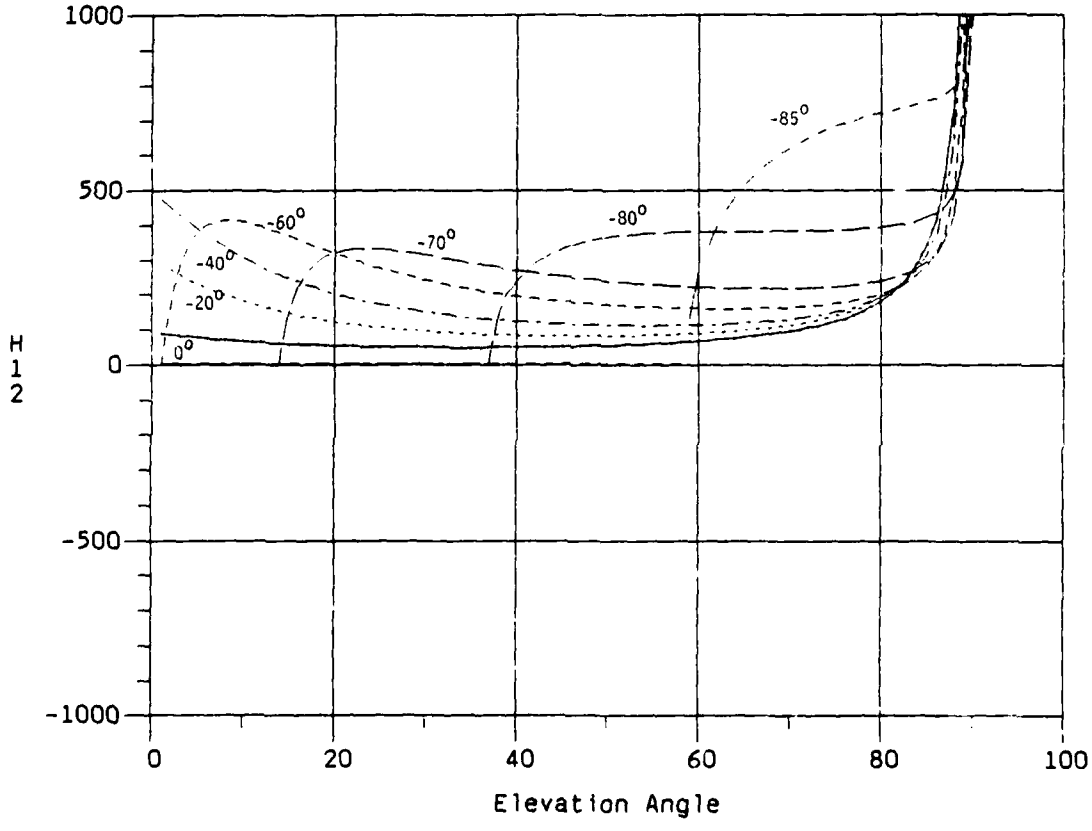

Figure 41. Latitude Dependence of H(2,2) (NS=EW=1)

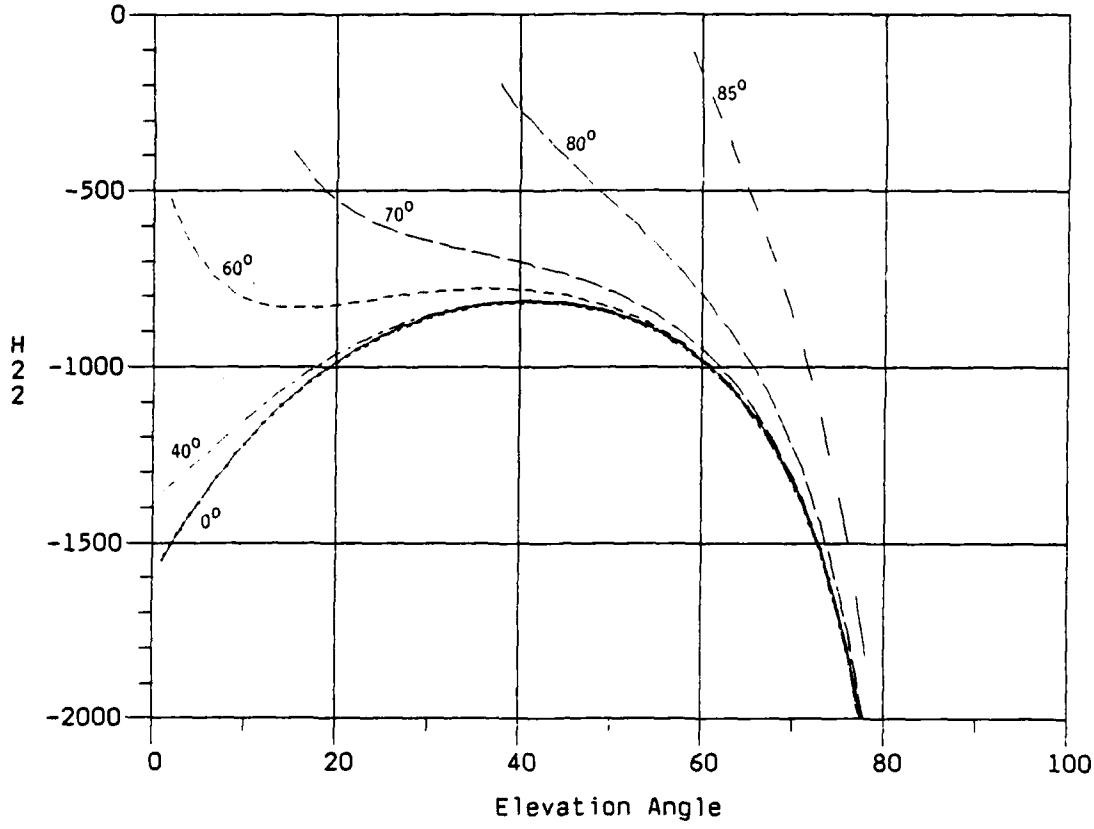


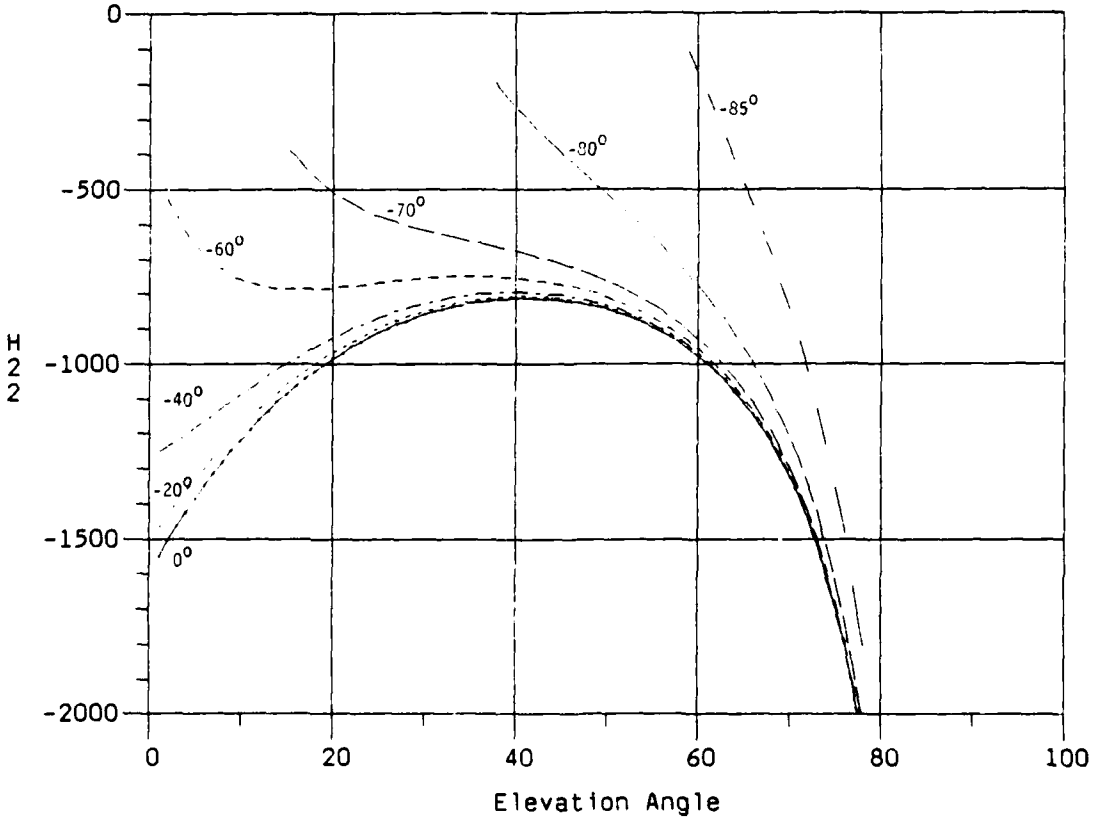

Figure 42. Latitude Dependence of H(1,3) (NS=EW=1)

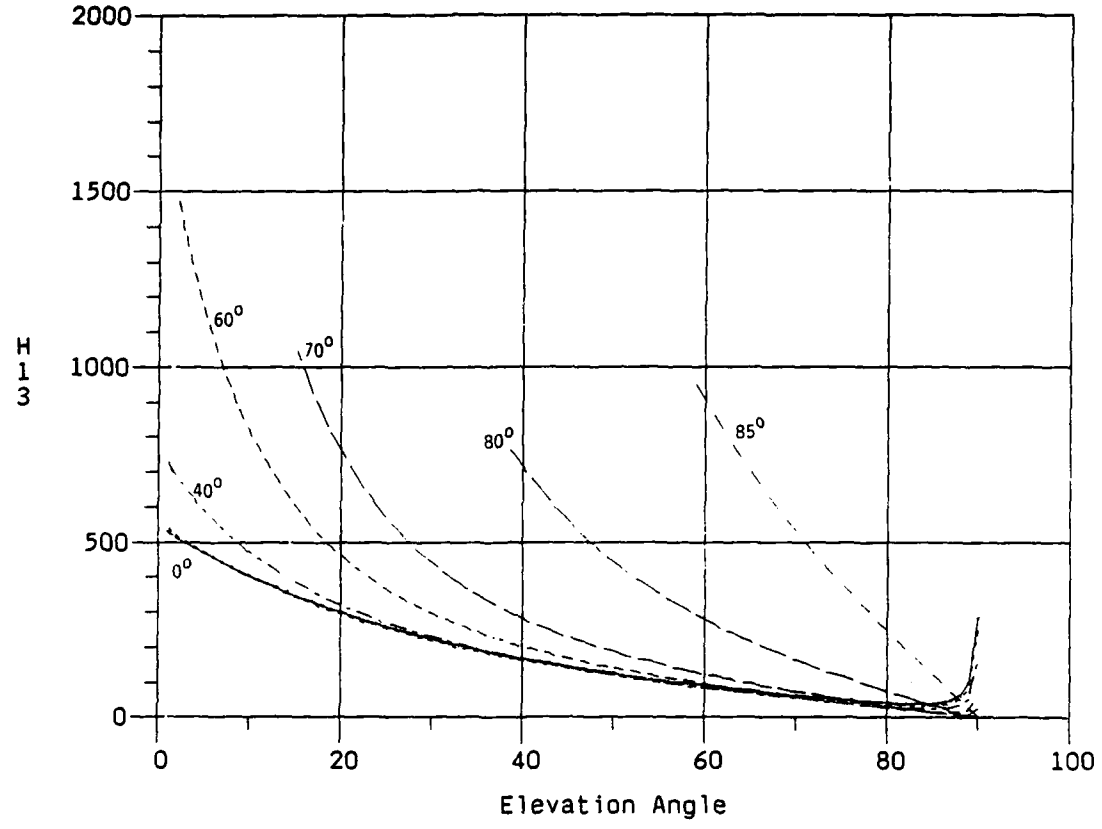


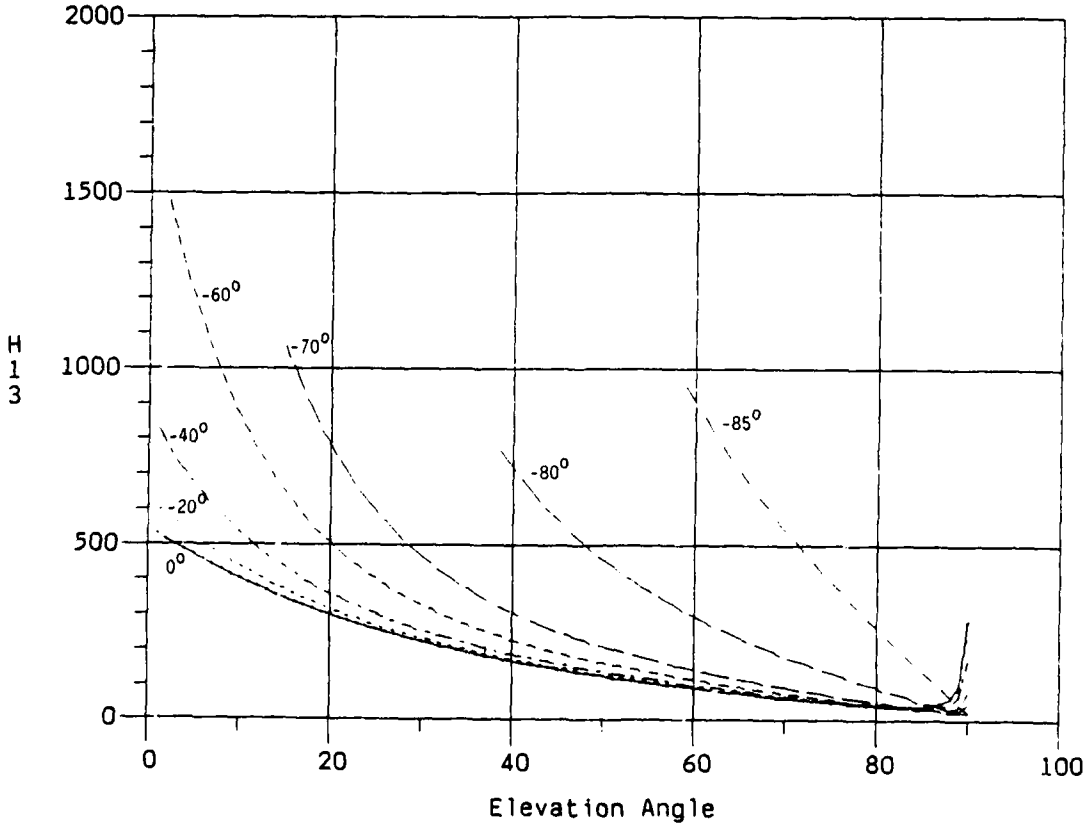

Figure 43. Latitude Dependence of H(2,3) (NS=EW=1)

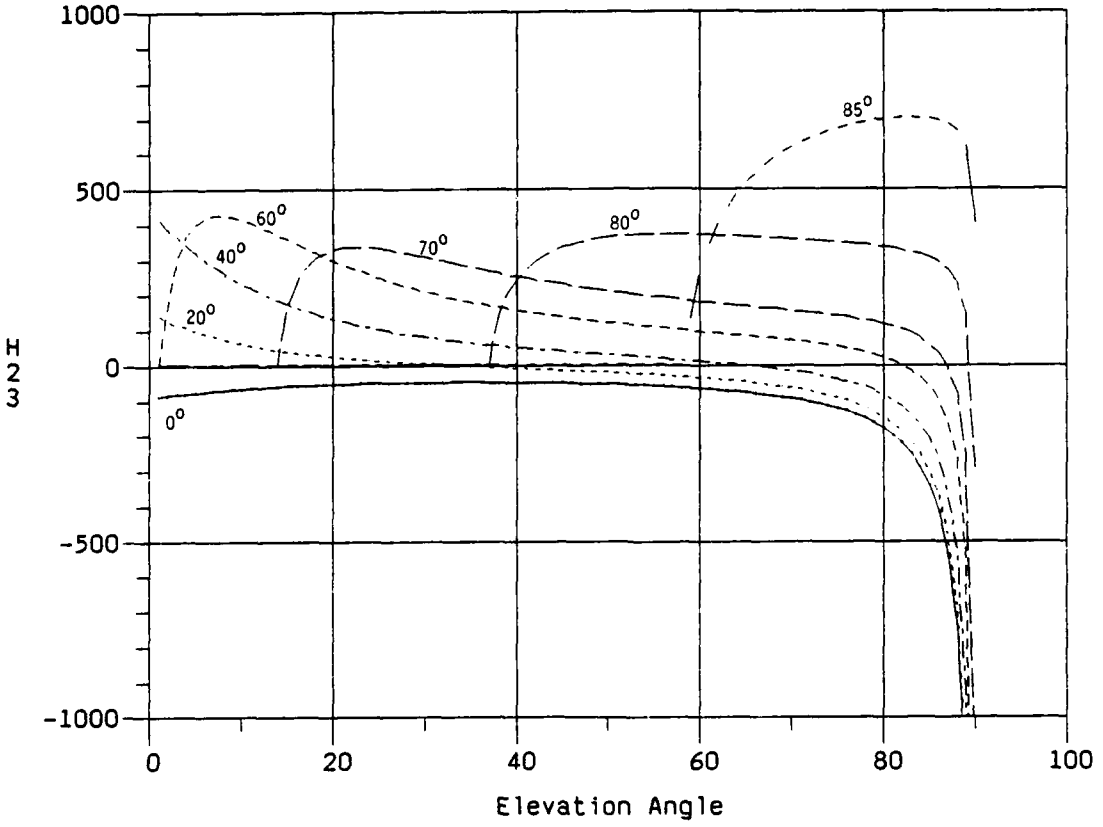


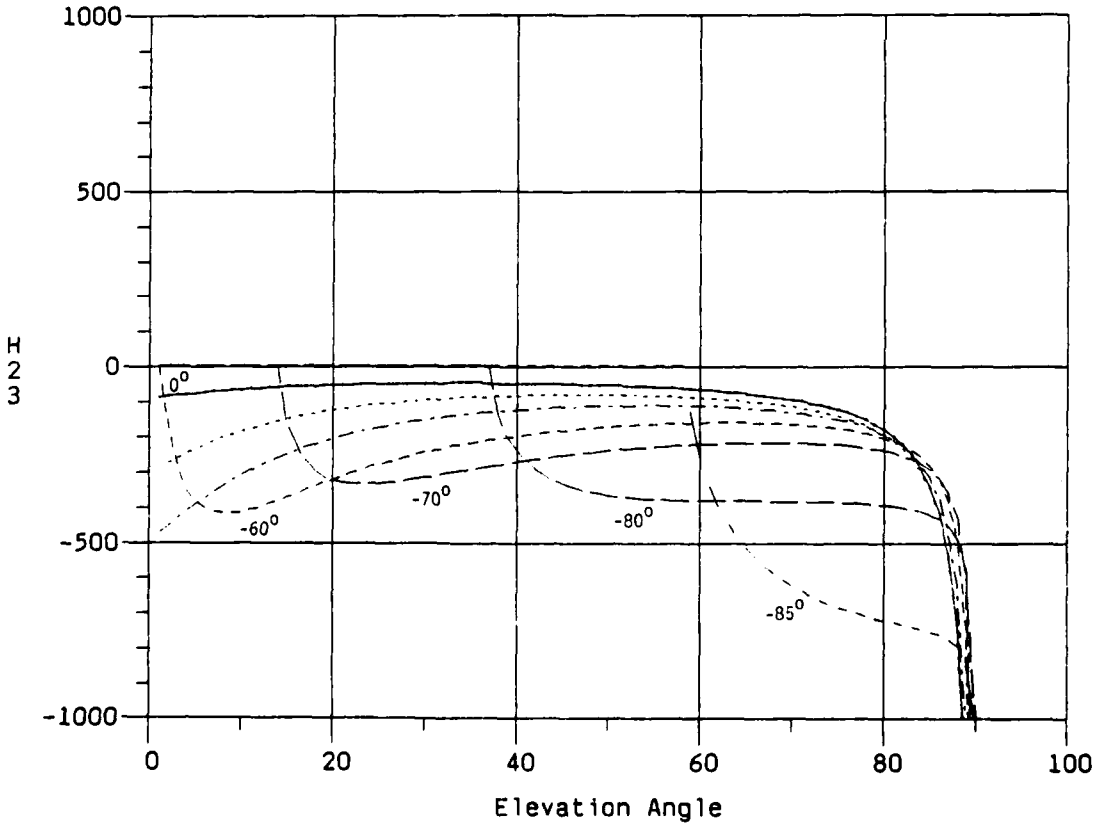

Figure 44. Latitude Dependence of PHI (NS=EW=1)

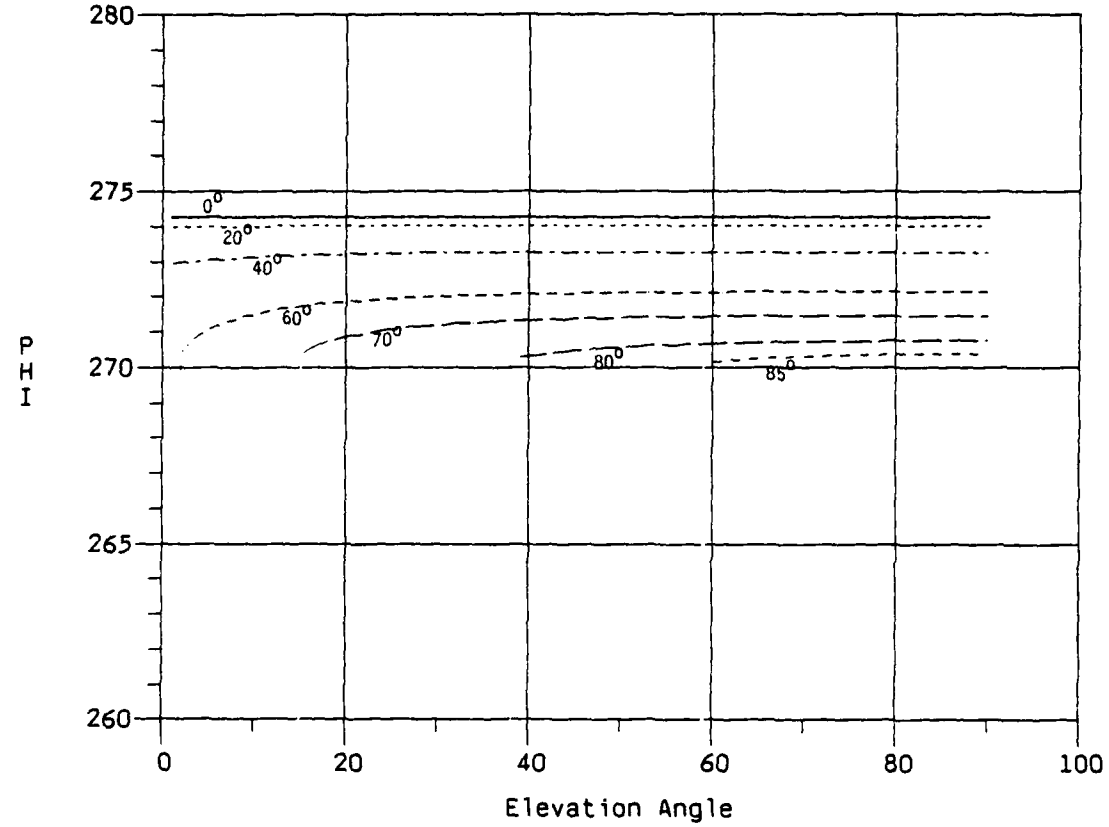


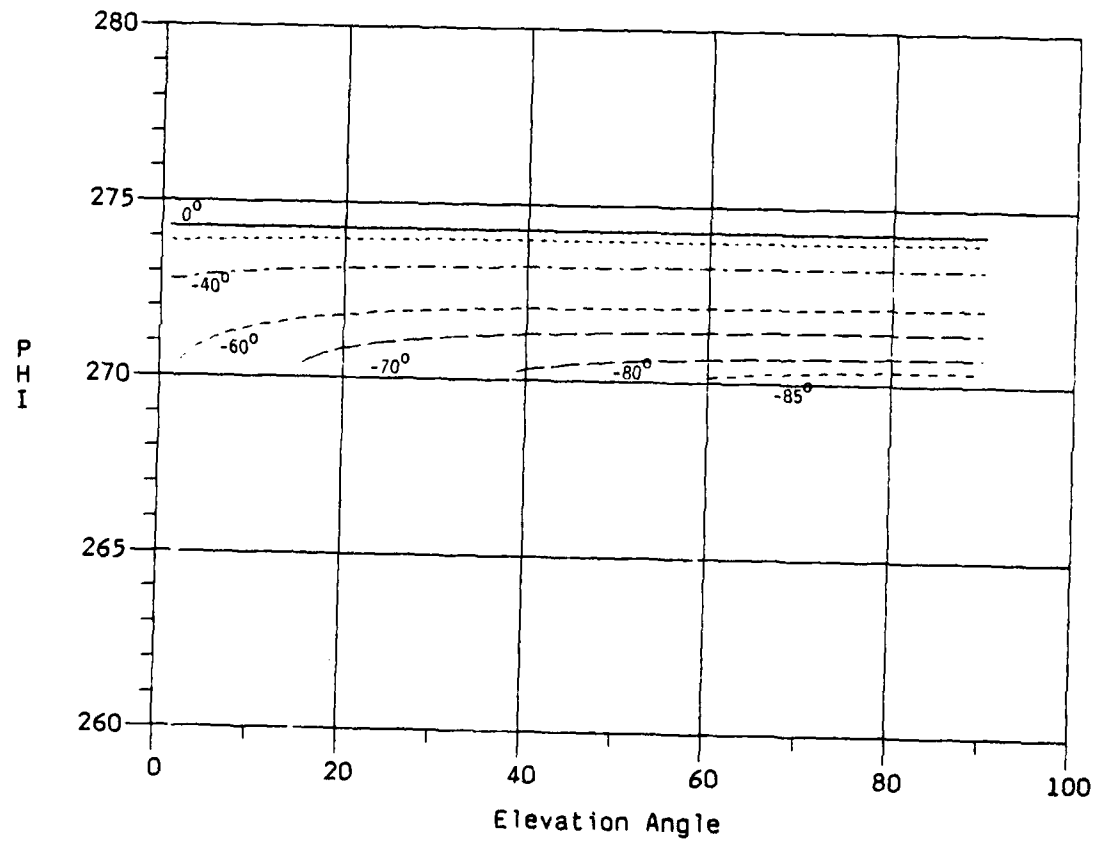

Figure 45. Latitude Dependence of PSI (NS=EW=1)

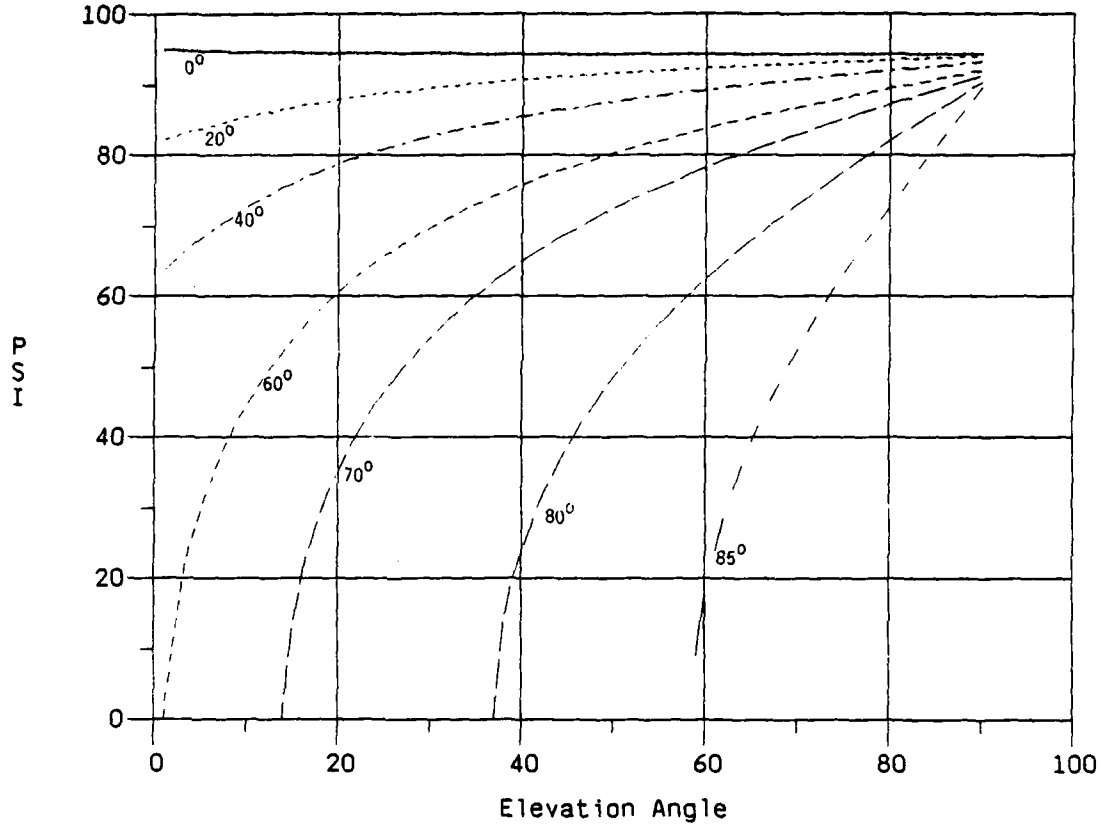


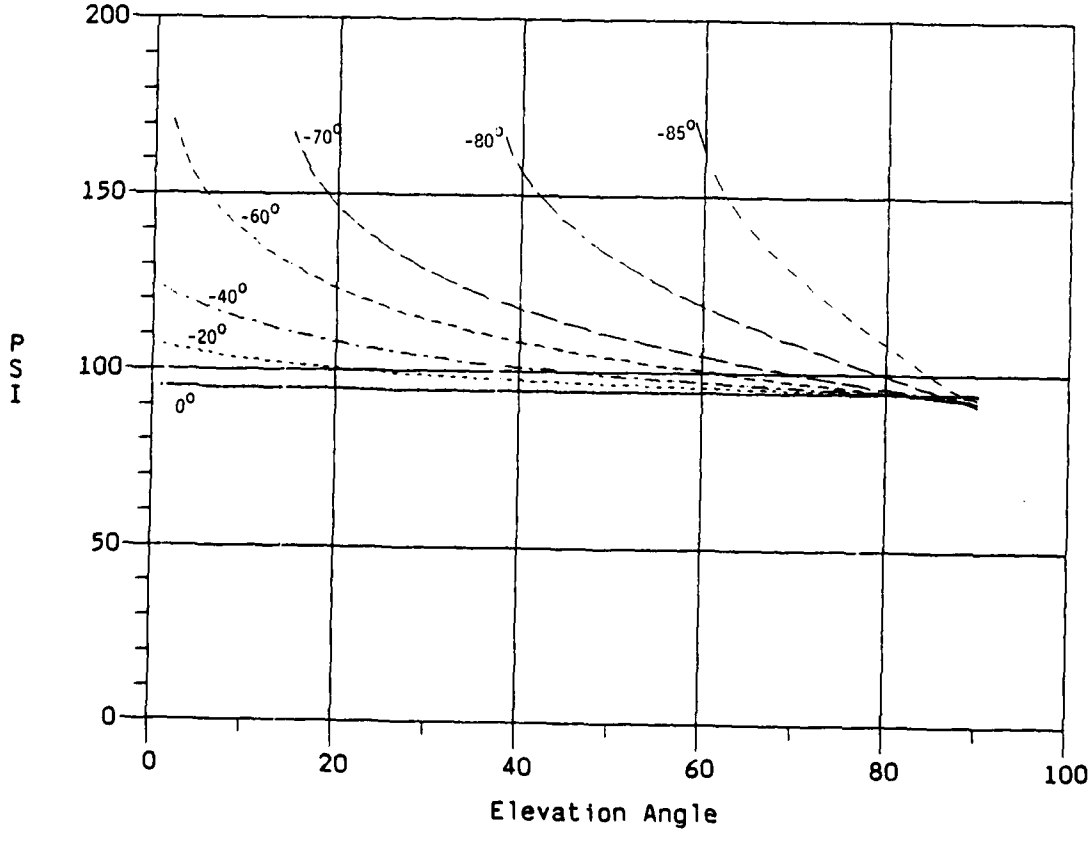

Figure 46. Latitude Dependence of H(1,1) (NS=1, EW=-1)

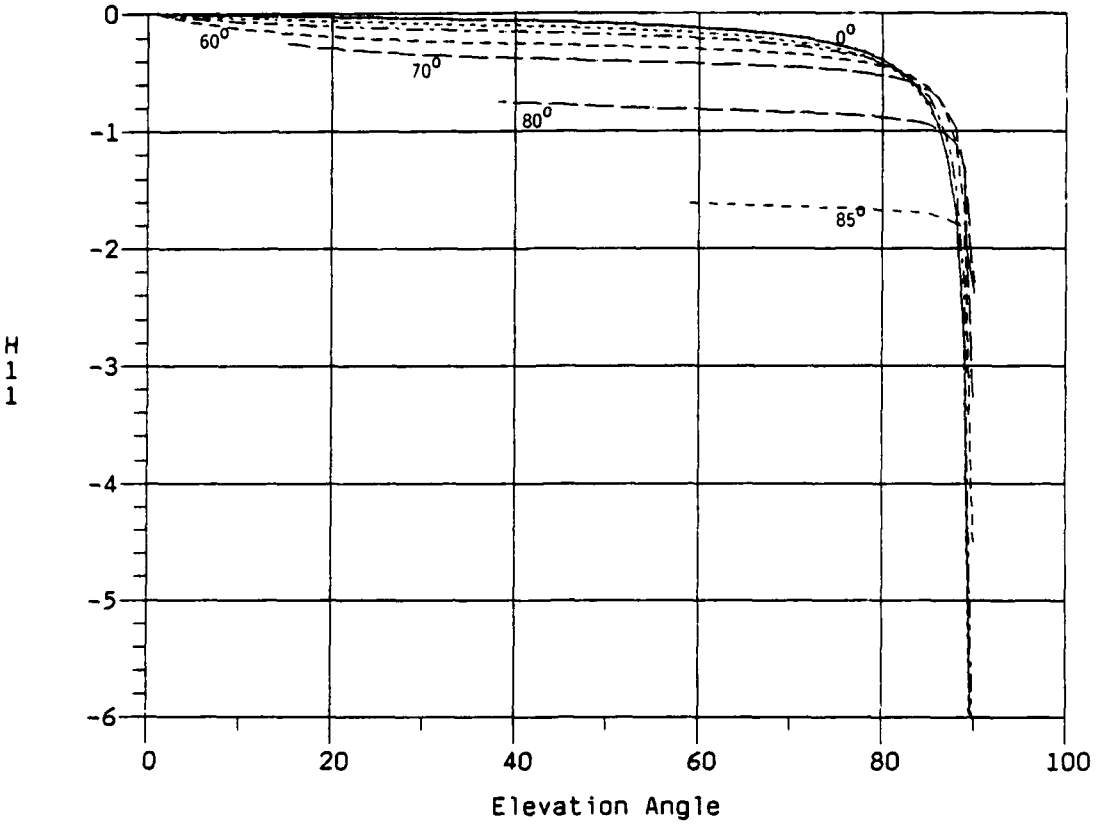


Figure 47. Latitude Dependence of H(2,1) (NS=1, EW=-1)

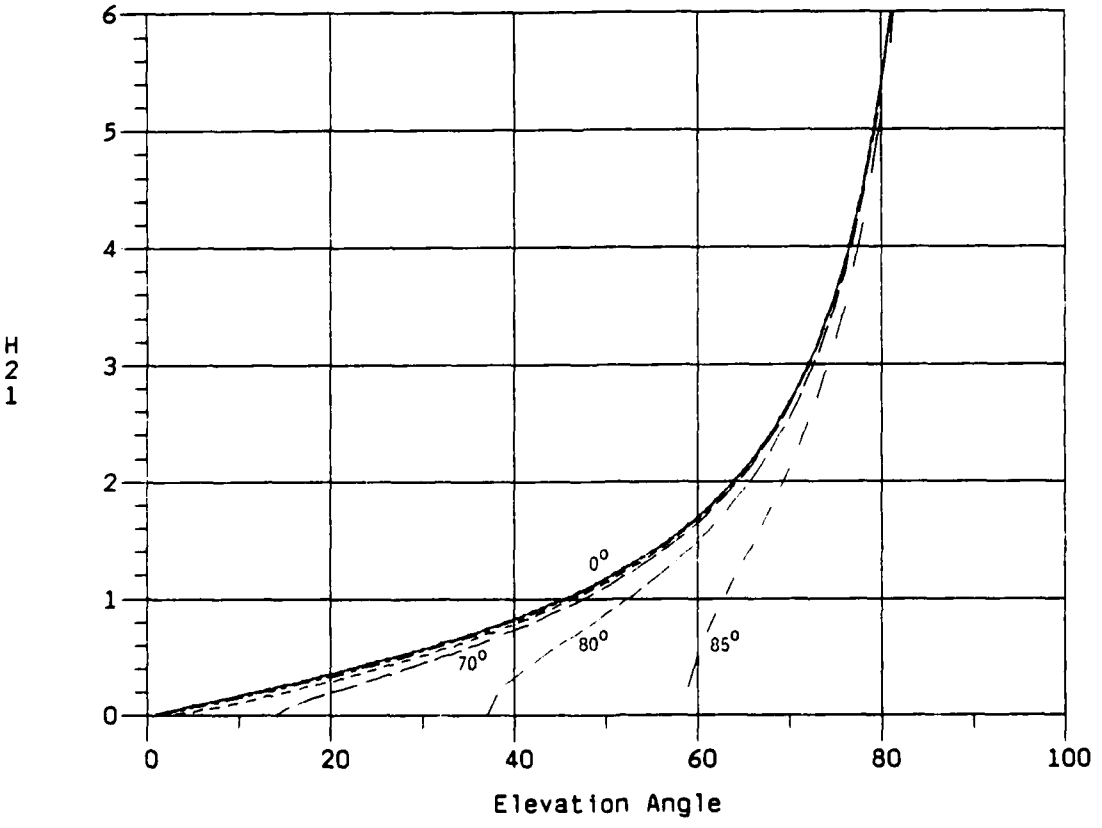

Figure 48. Latitude Dependence of H(1,2) (NS=1, EW=-1)

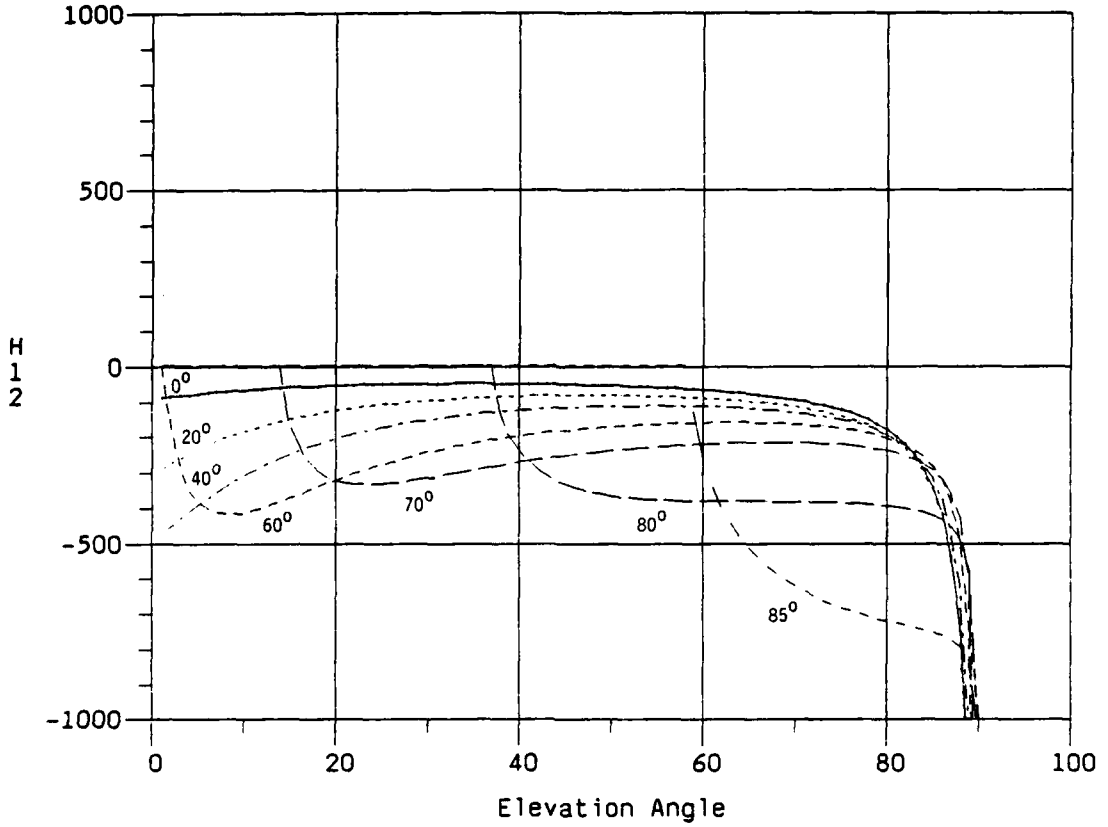


Figure 49. Latitude Dependence of H(2,2) (NS=1, EW=-1)

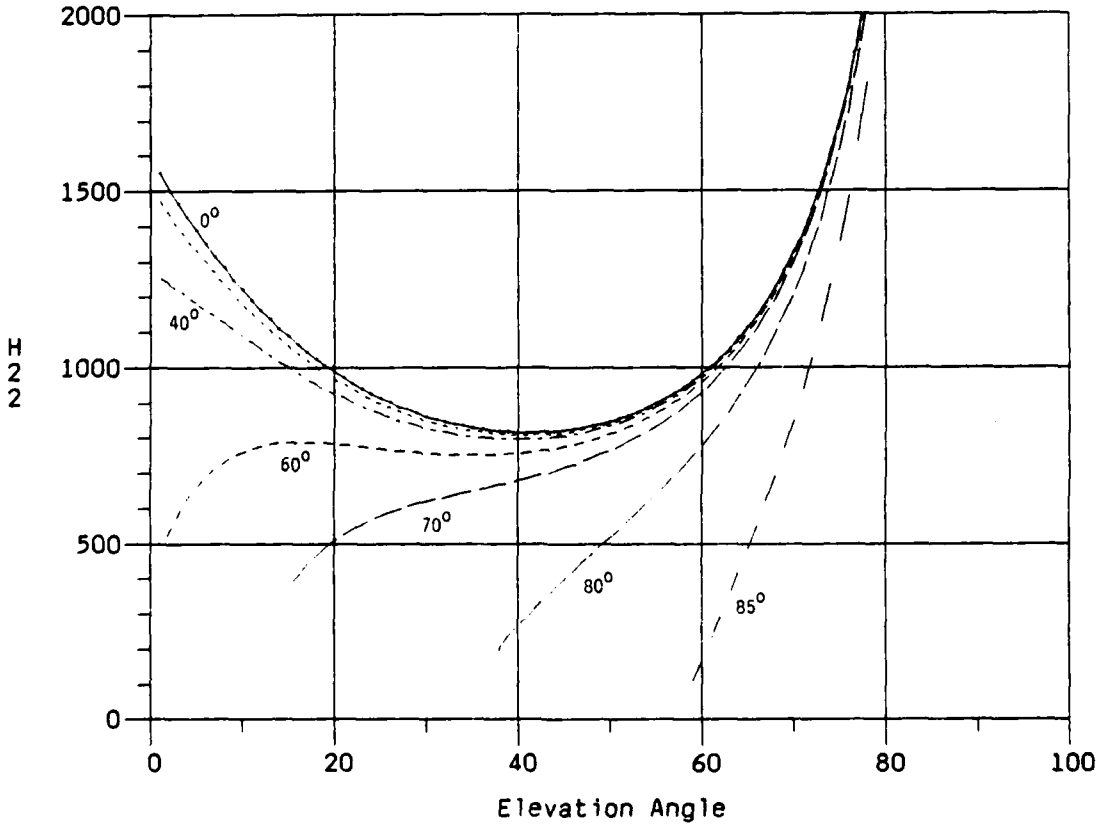

Figure 50. Latitude Dependence of H(1,3) (NS=1, EW=-1)

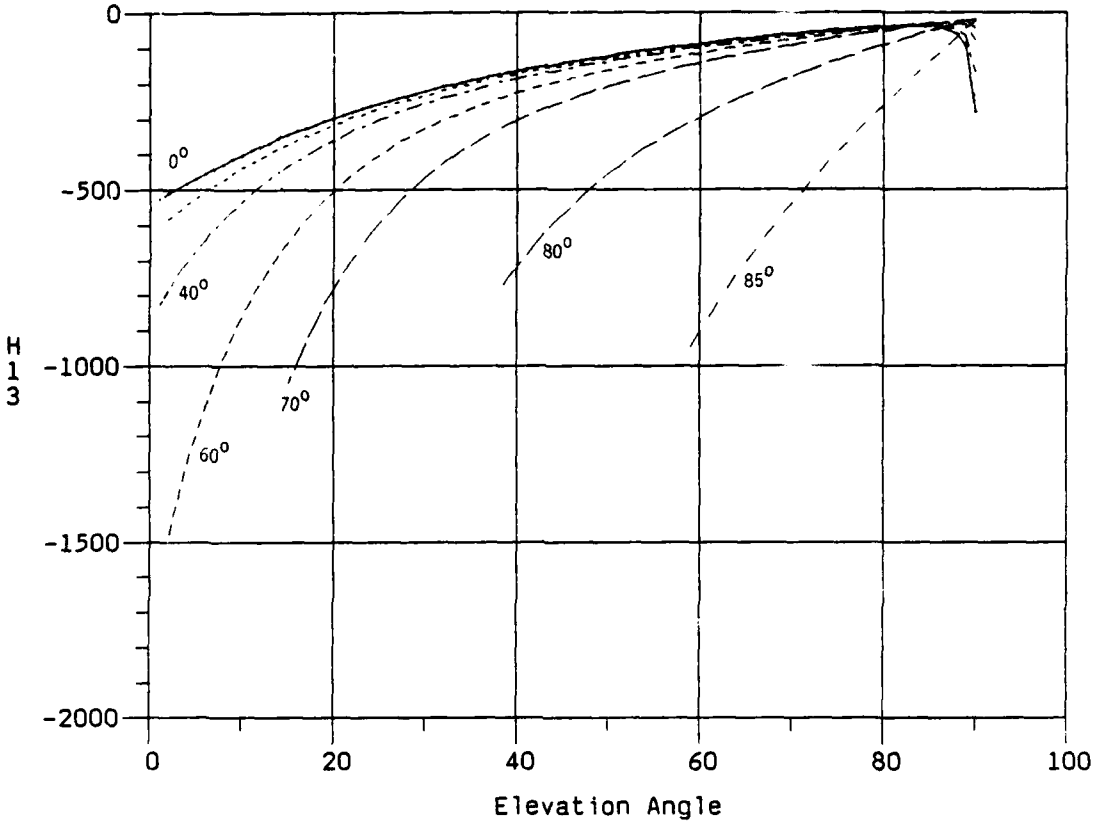


Figure 51. Latitude Dependence of H(2,3) (NS=1, EW=-1)

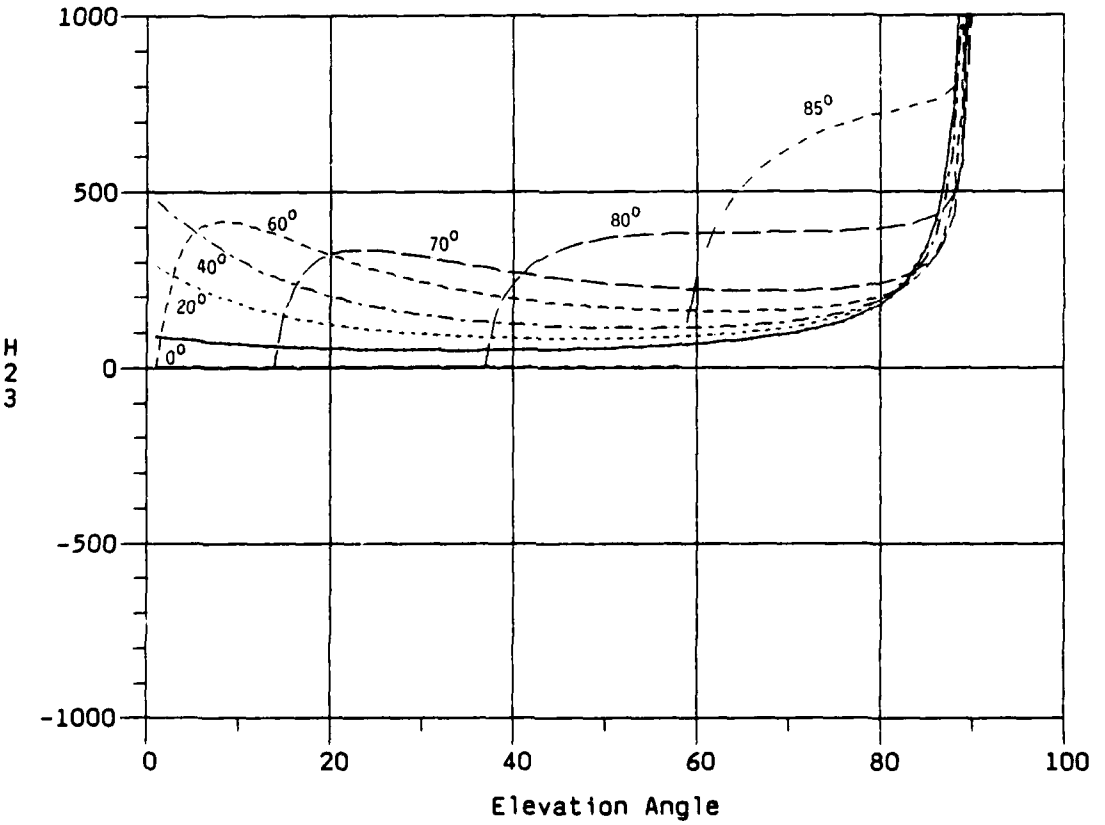

Figure 52. Latitude Dependence of PHI (NS=1, EW=-1)

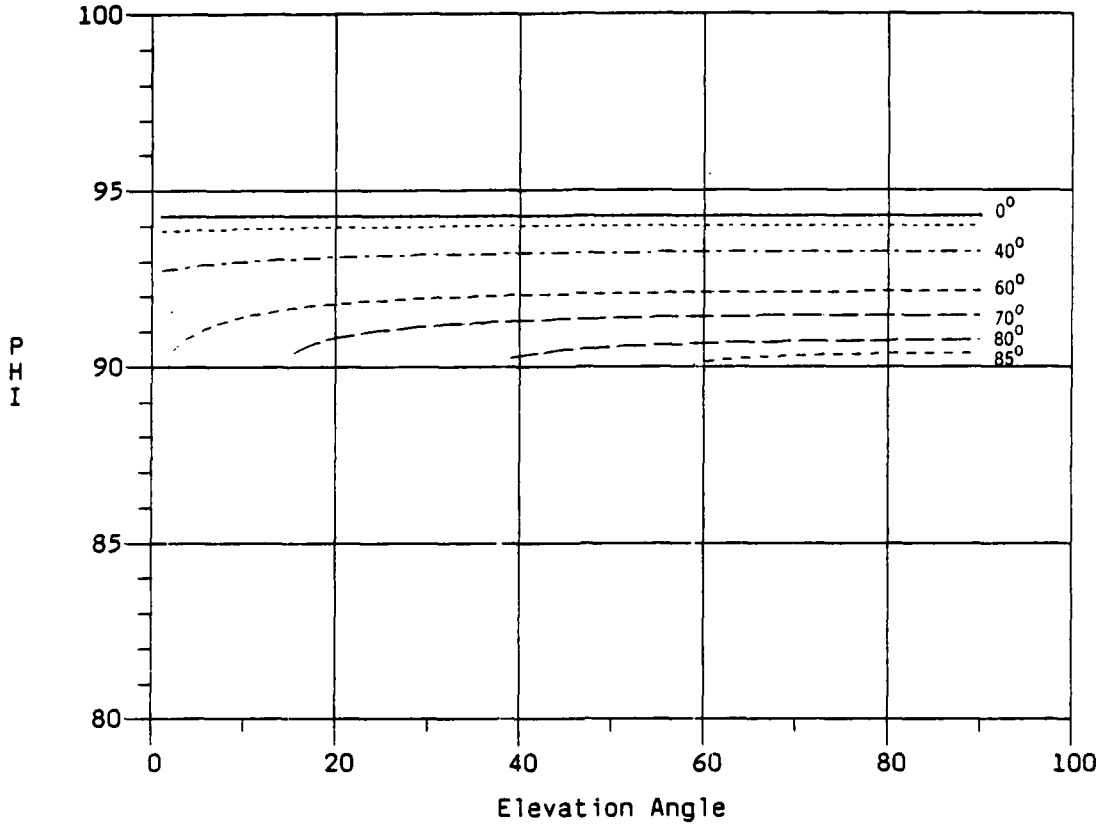


Figure 53. Latitude Dependence of PSI (NS=1, EW=-1)

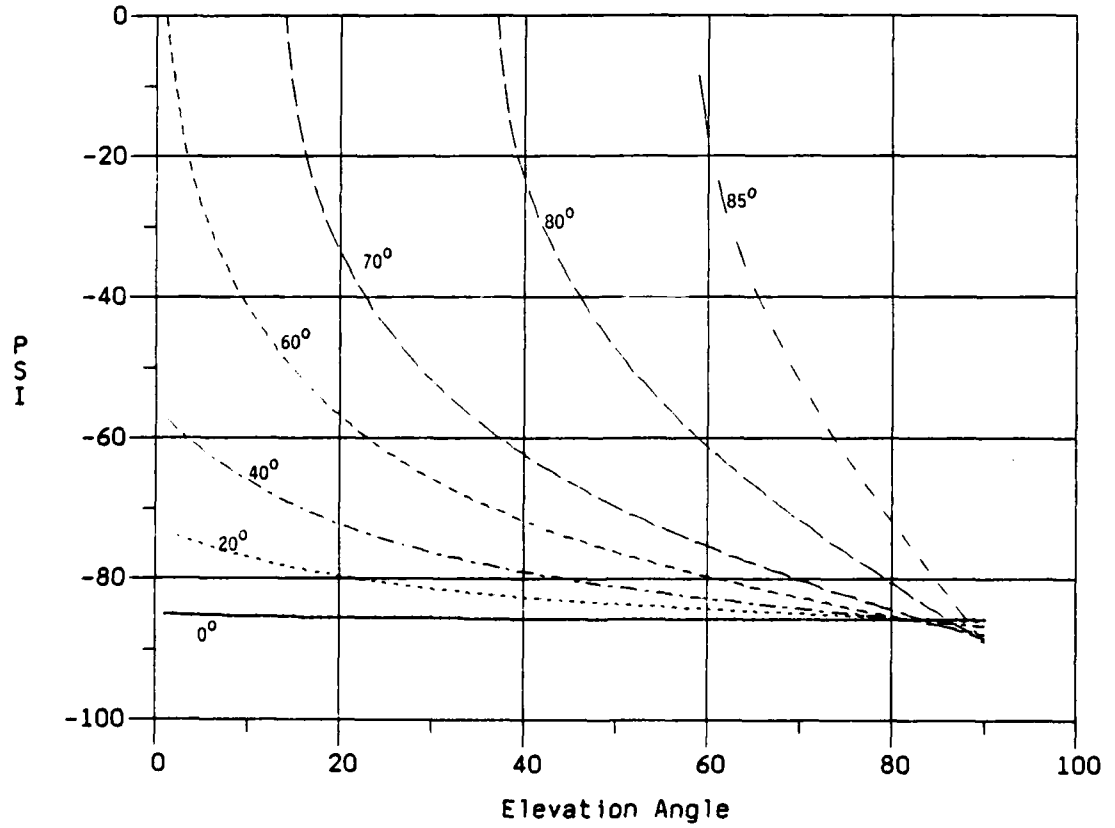

Figure 54. Latitude Dependence of H(1,1) (NS=-1, EW=1)

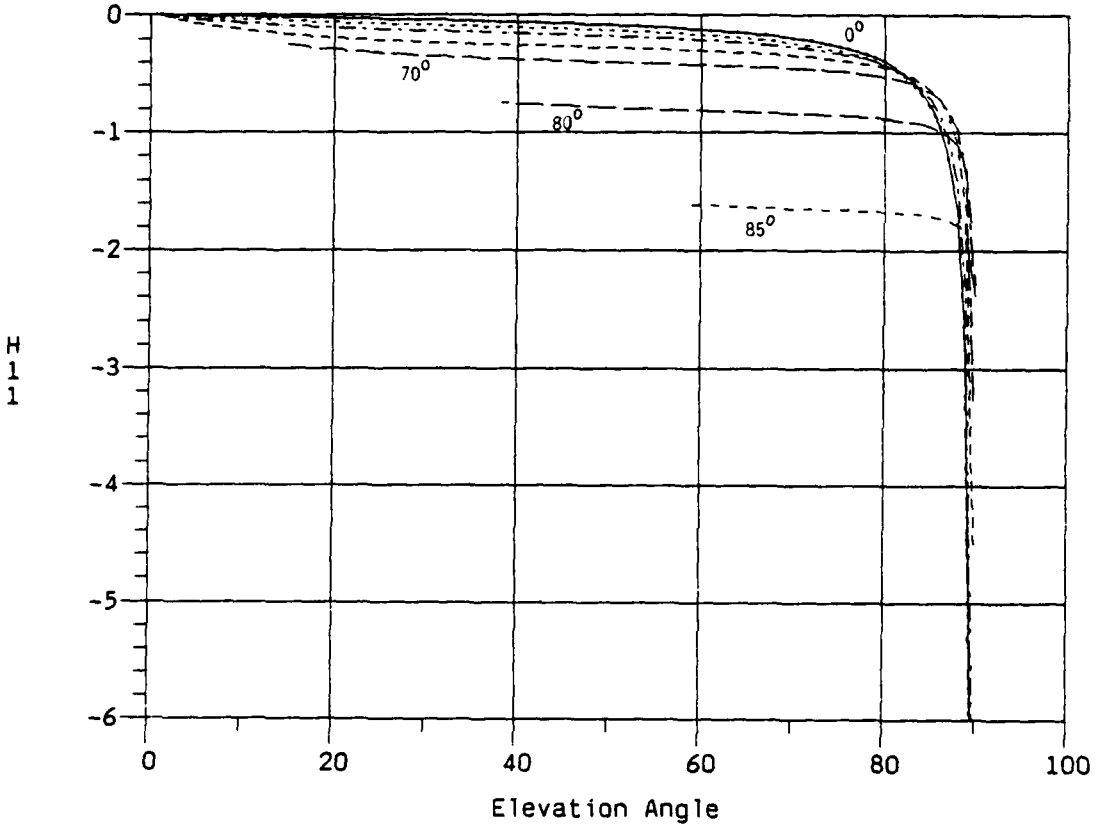


Figure 55. Latitude Dependence of H(2,1) (NS=-1, EW=1)

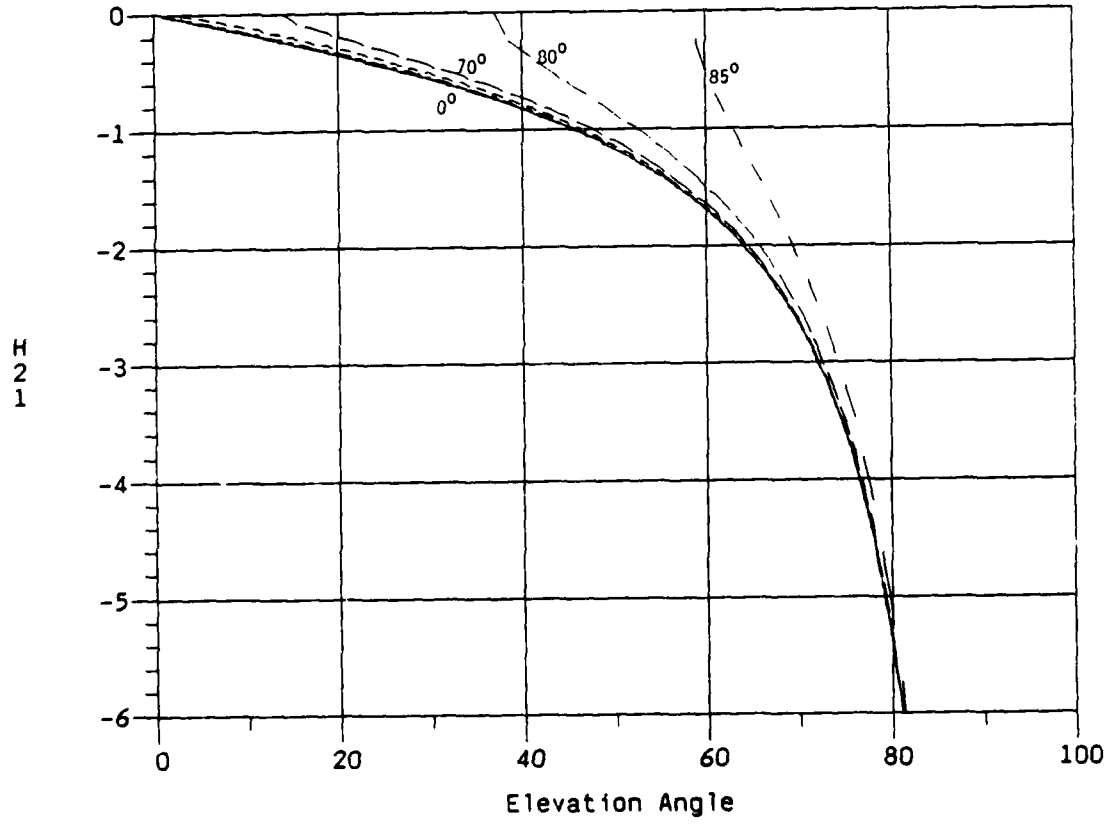

Figure 56. Latitude Dependence of H(1,2) (NS=-1, EW=1)

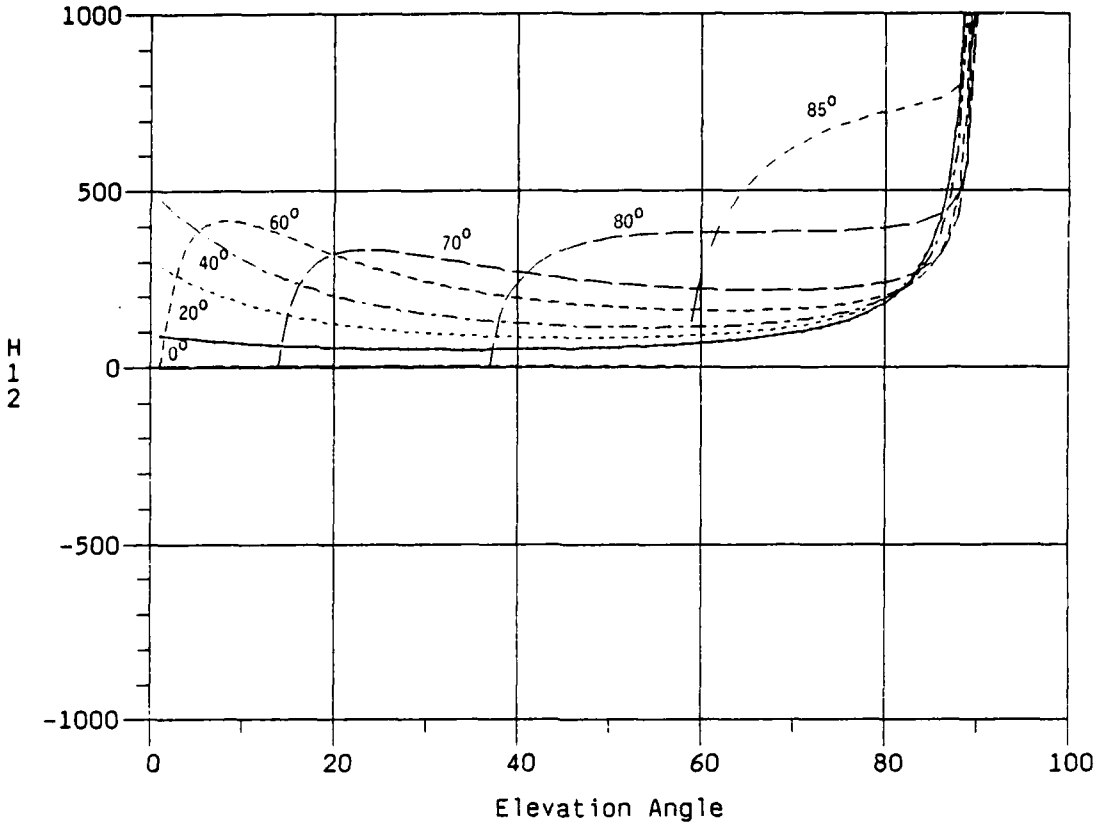


Figure 57. Latitude Dependence of H(2,2) (NS=-1, EW=1)

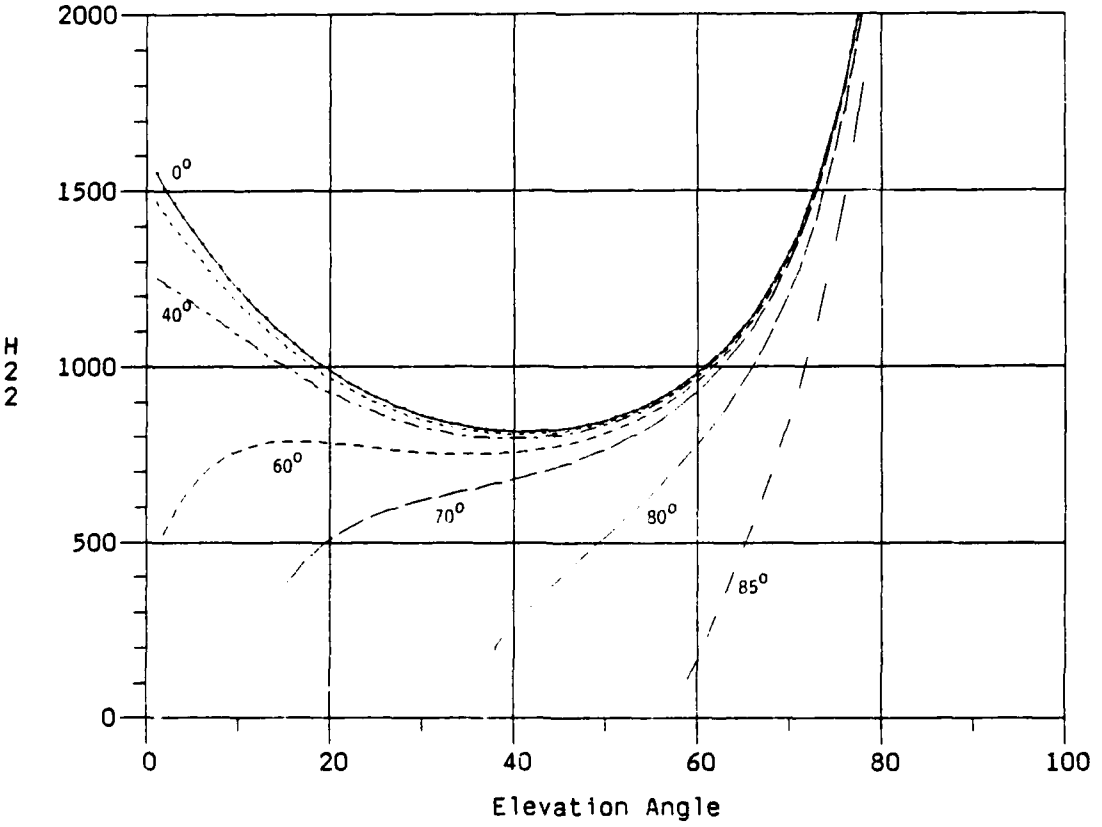

Figure 58. Latitude Dependence of H(1,3) (NS=-1, EW=1)

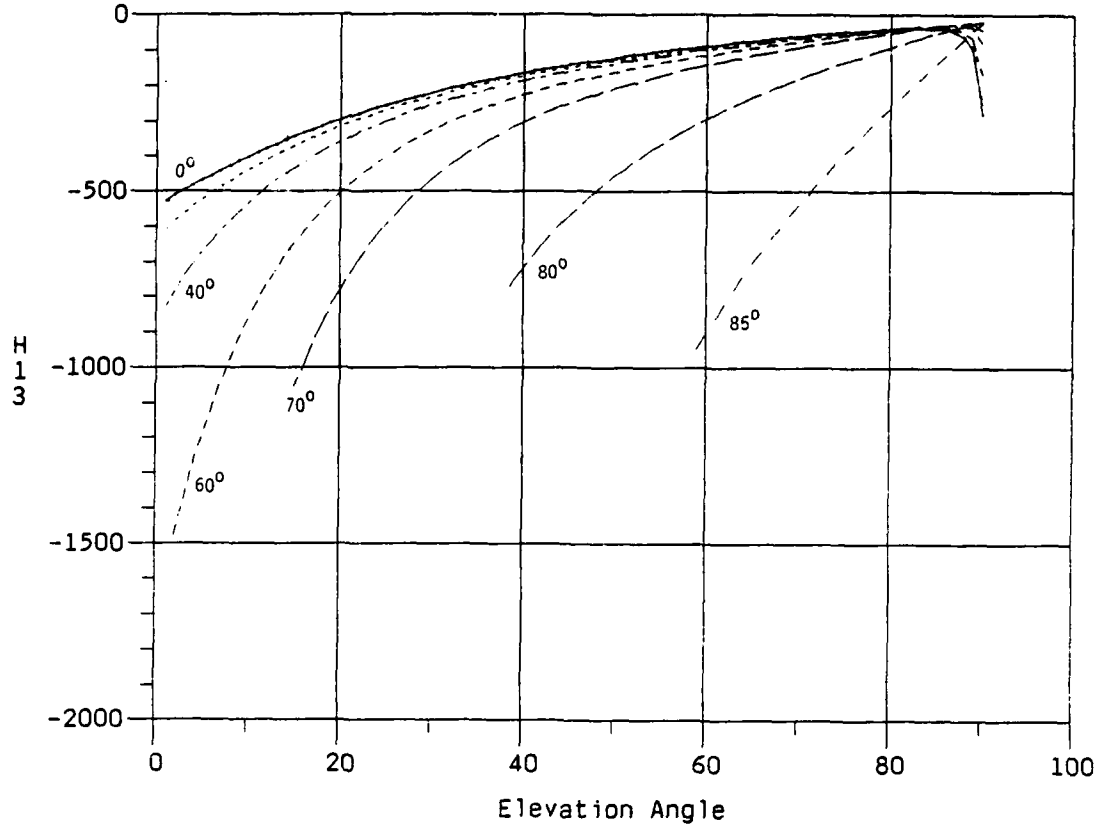


Figure 59. Latitude Dependence of H(2,3) (NS=-1, EW=1)

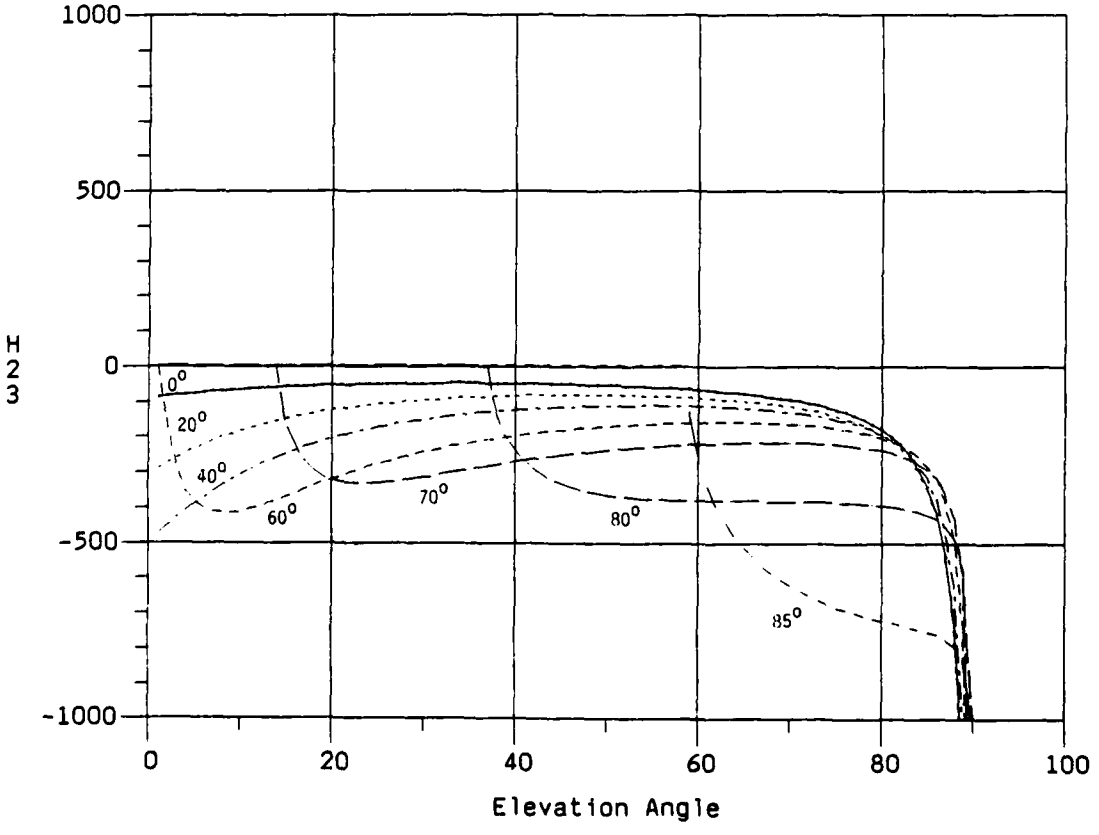

Figure 60. Latitude Dependence of PHI (NS=-1, EW=1)

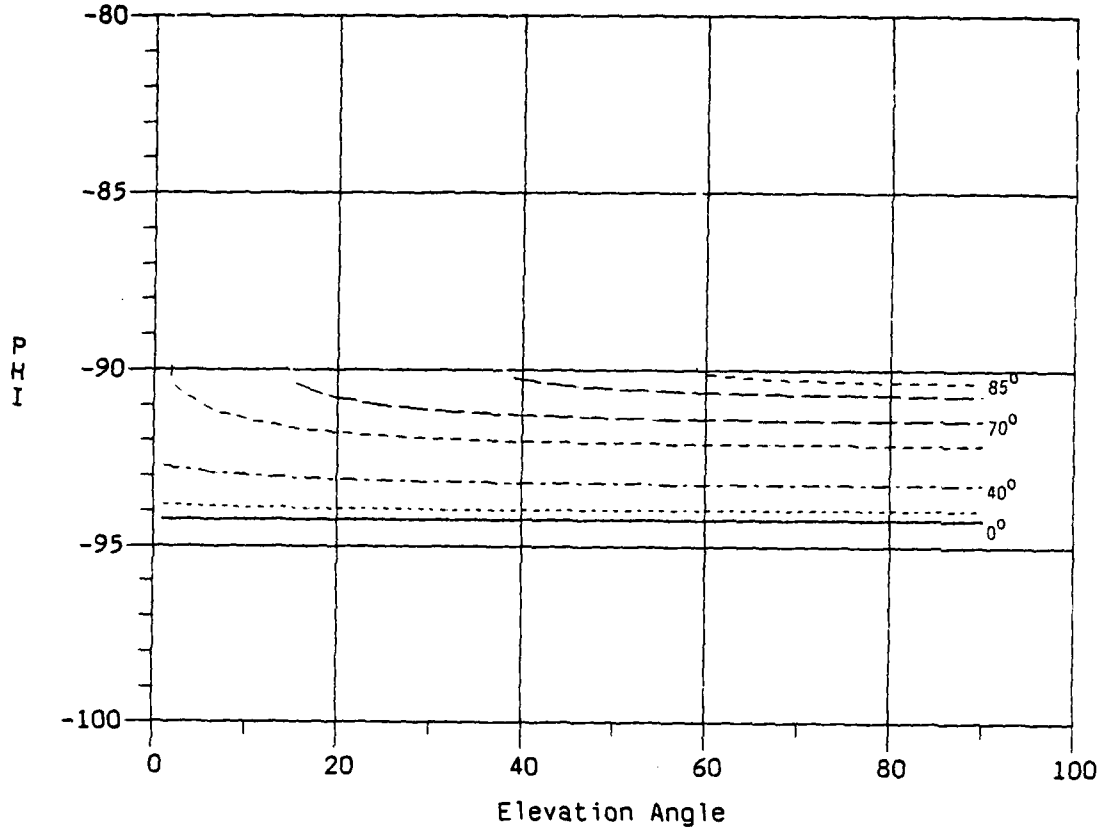


Figure 61. Latitude Dependence of PSI (NS=-1, EW=1)

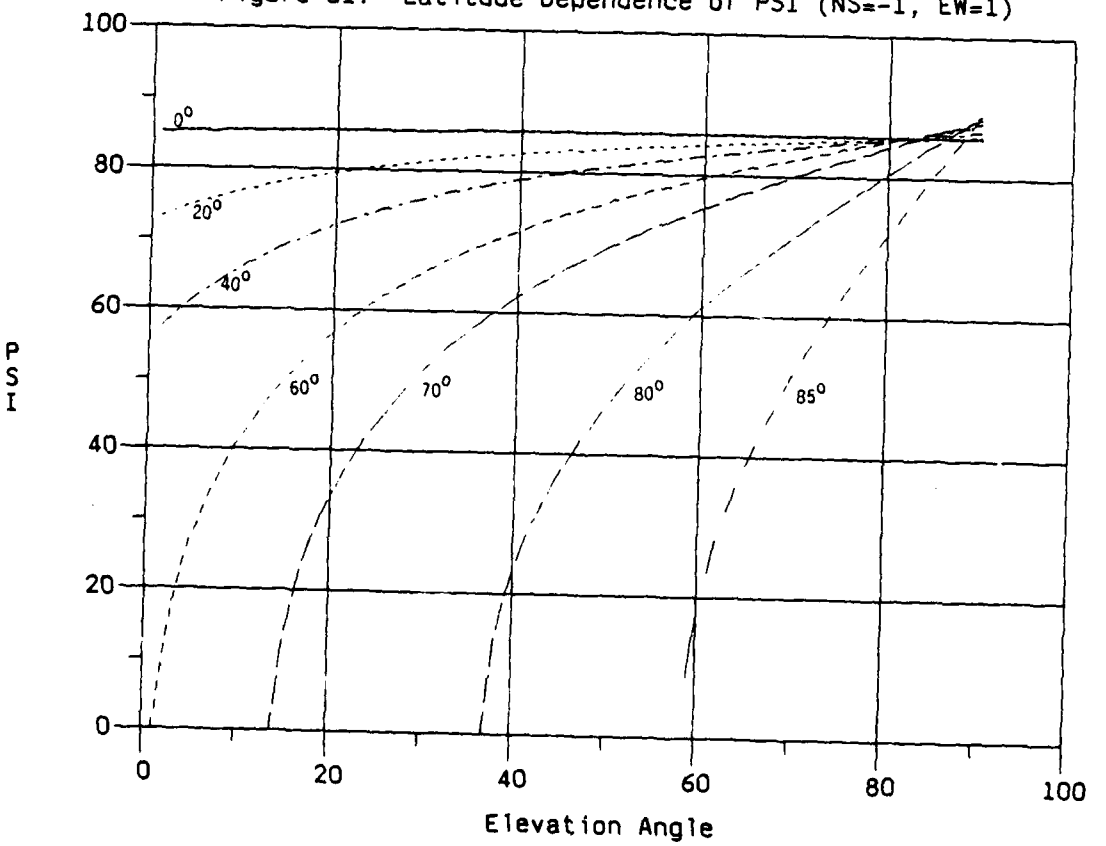

Figure 62. Latitude Dependence of H(1,1) (NS=EW=-1)

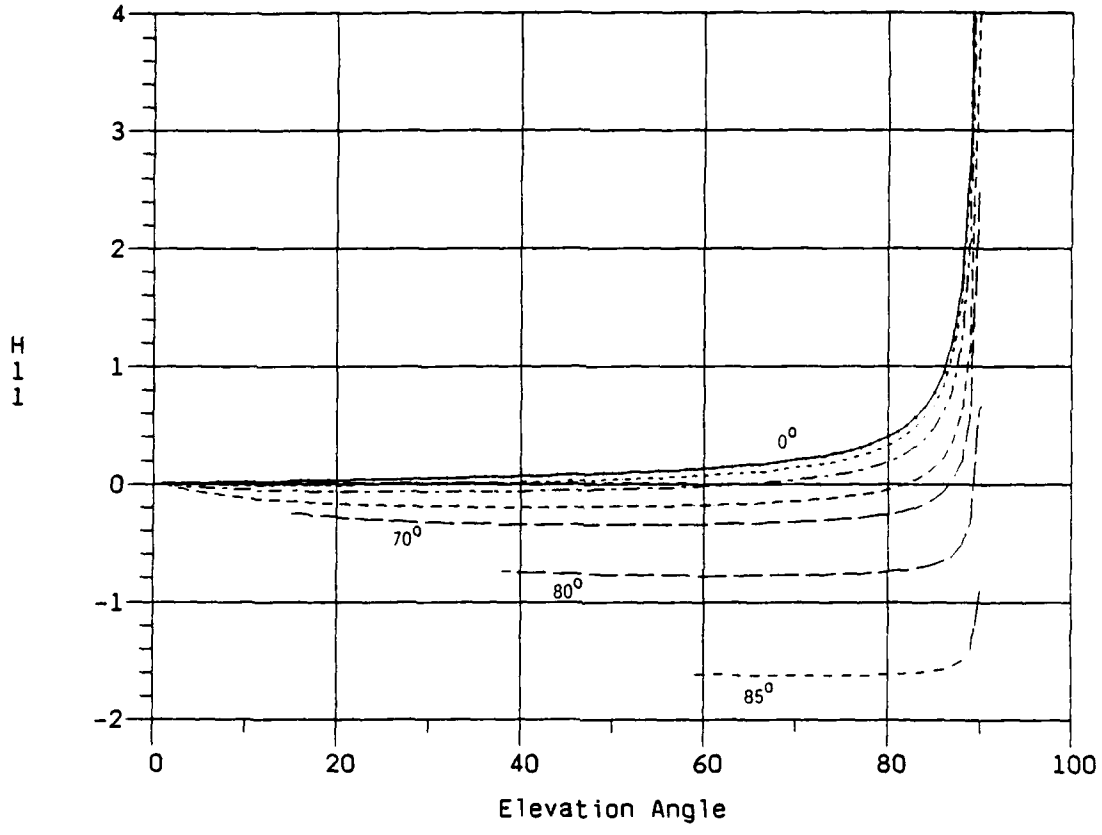


Figure 63. Latitude Dependence of H(2,1) (NS=EW=-1)

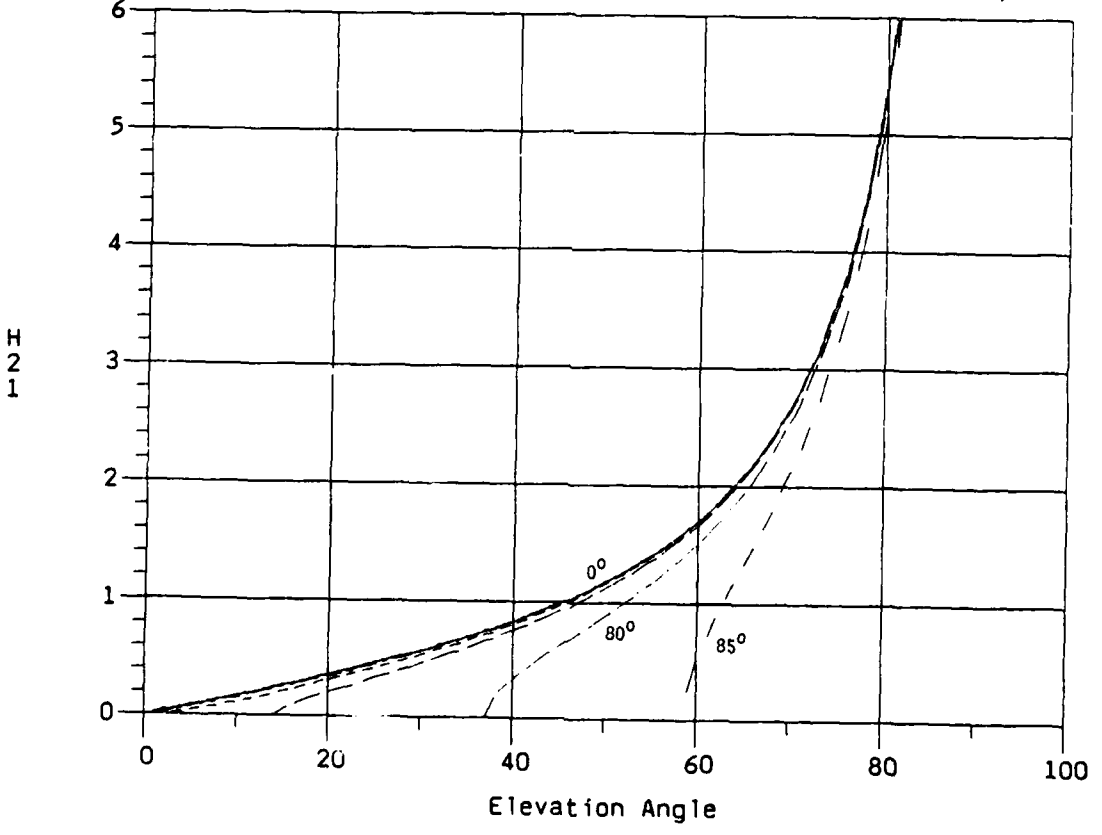

Figure 64. Latitude Dependence of H(1,2) (NS=EW=-1)

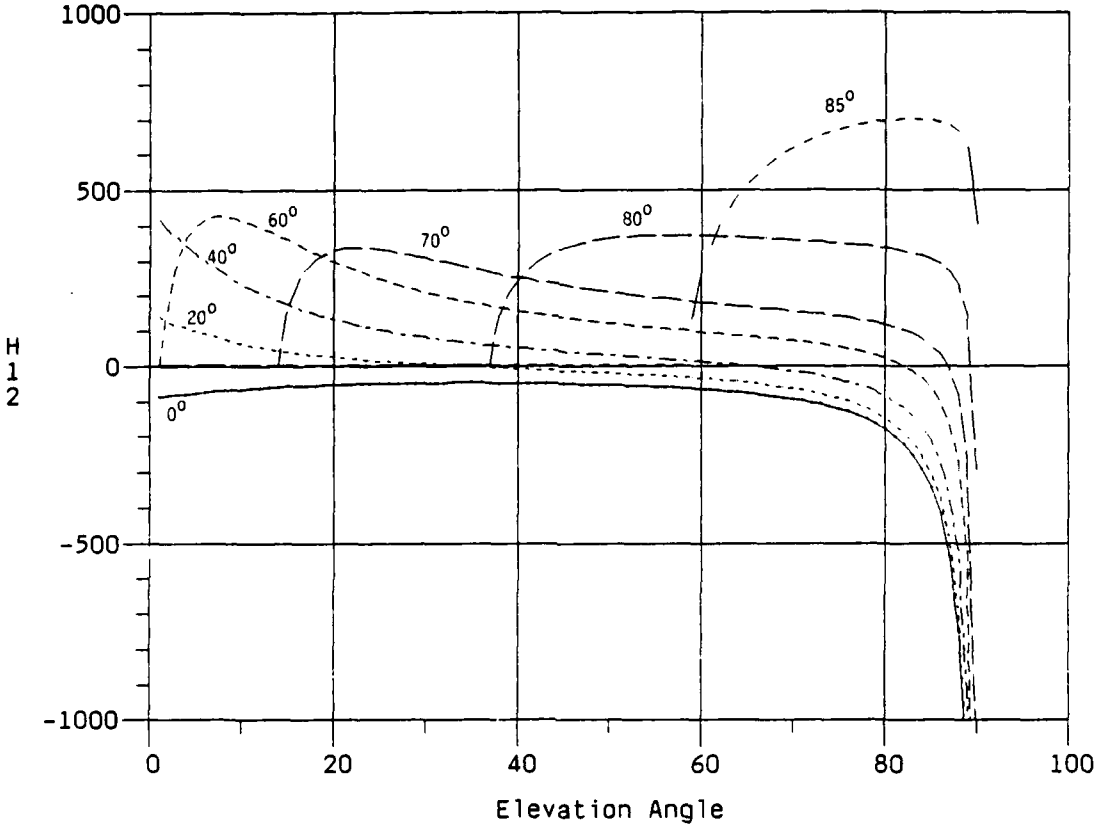


Figure 65. Latitude Dependence of H(2,2) (NS=EW=-1)

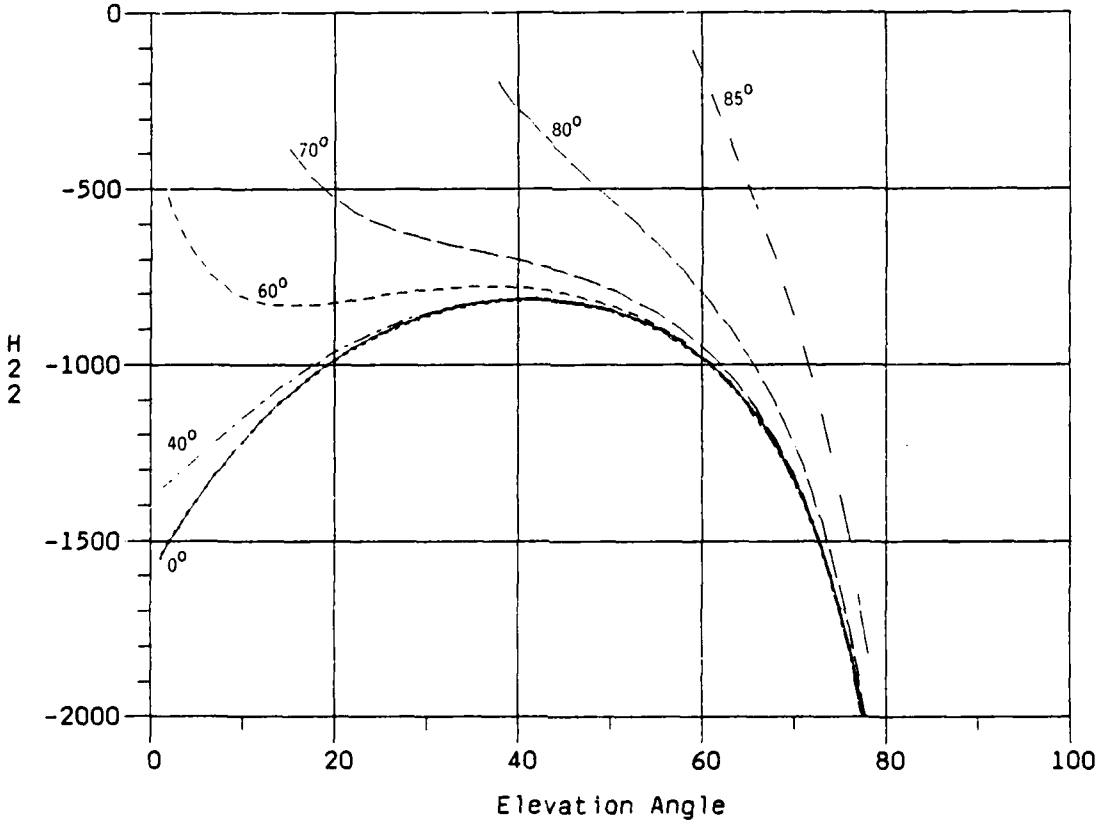

Figure 66. Latitude Dependence of H(1,3) (NS=EW=-1)

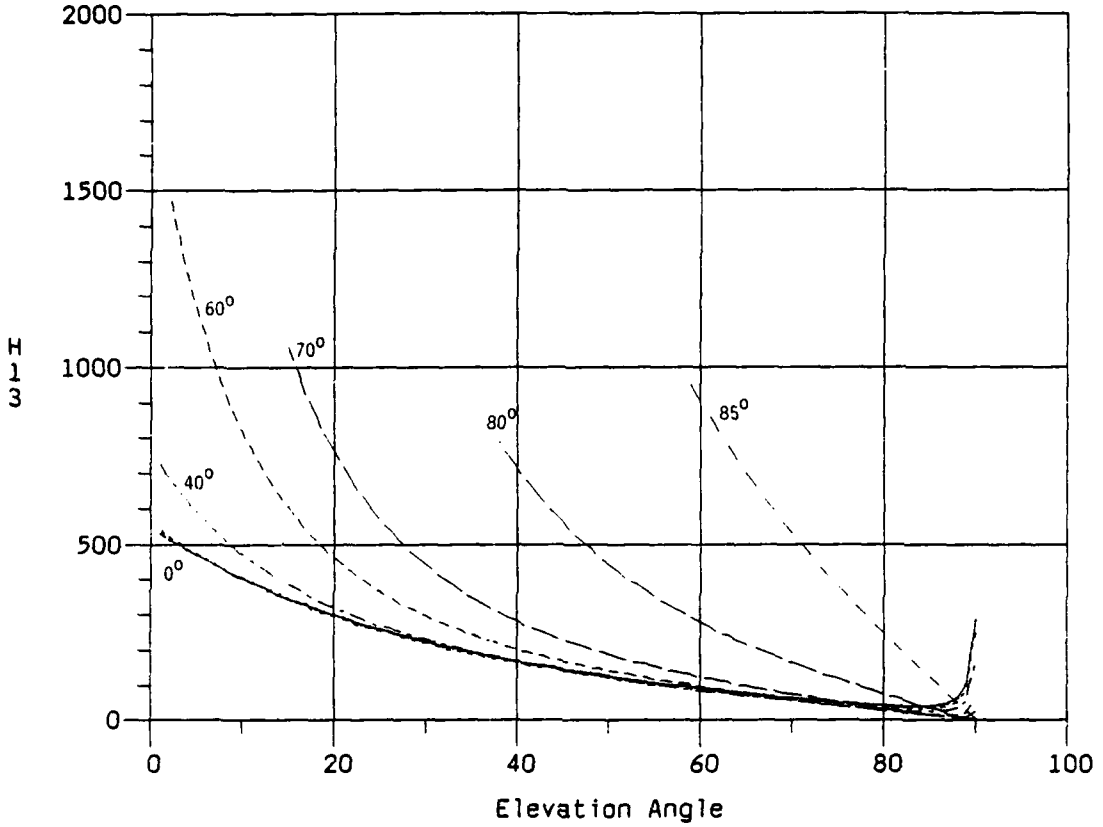


Figure 67. Latitude Dependence of H(2,3) (NS=EW=-1)

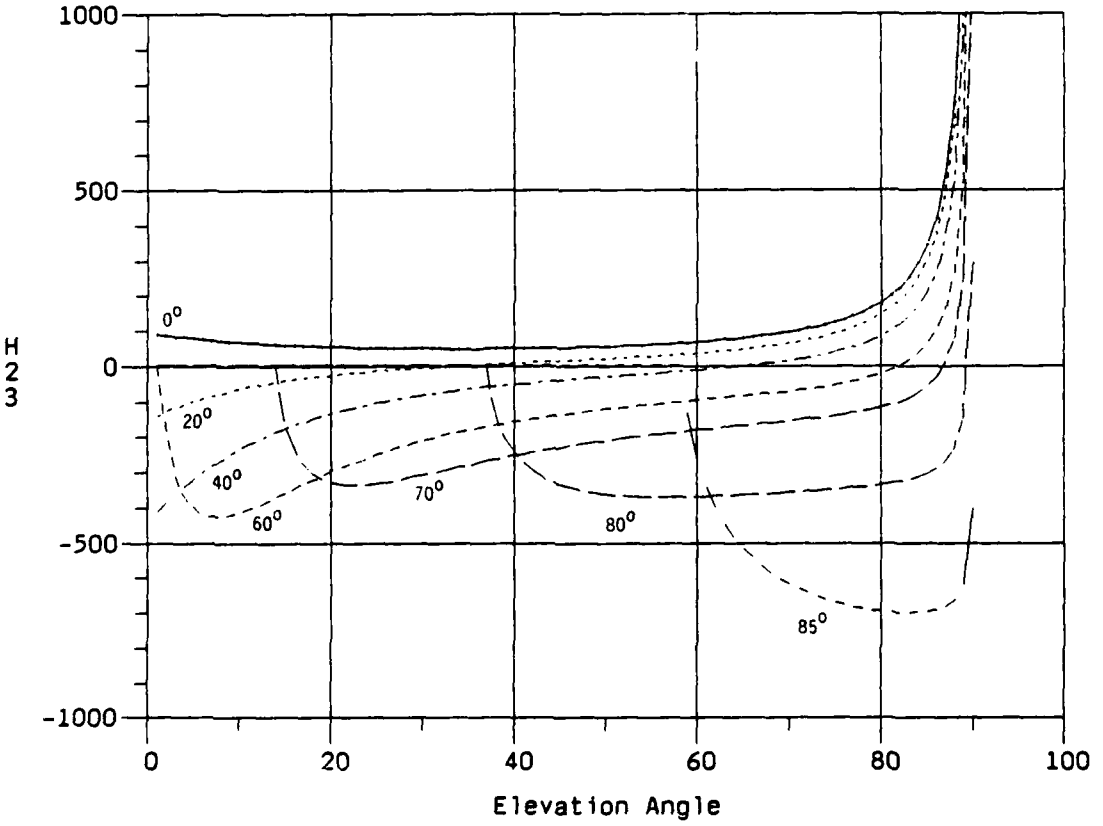

Figure 68. Latitude Dependence of PHI (NS=EW=-1)

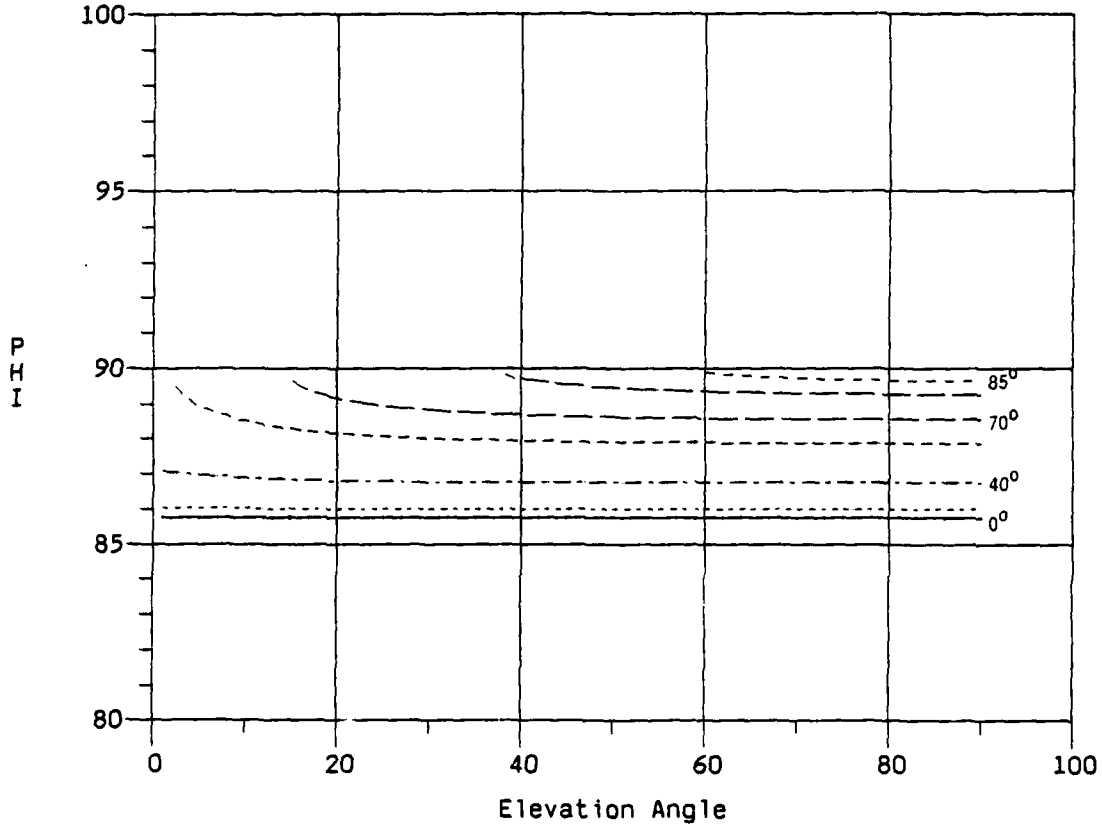


Figure 69. Latitude Dependence of PSI (NS=EW=-1)

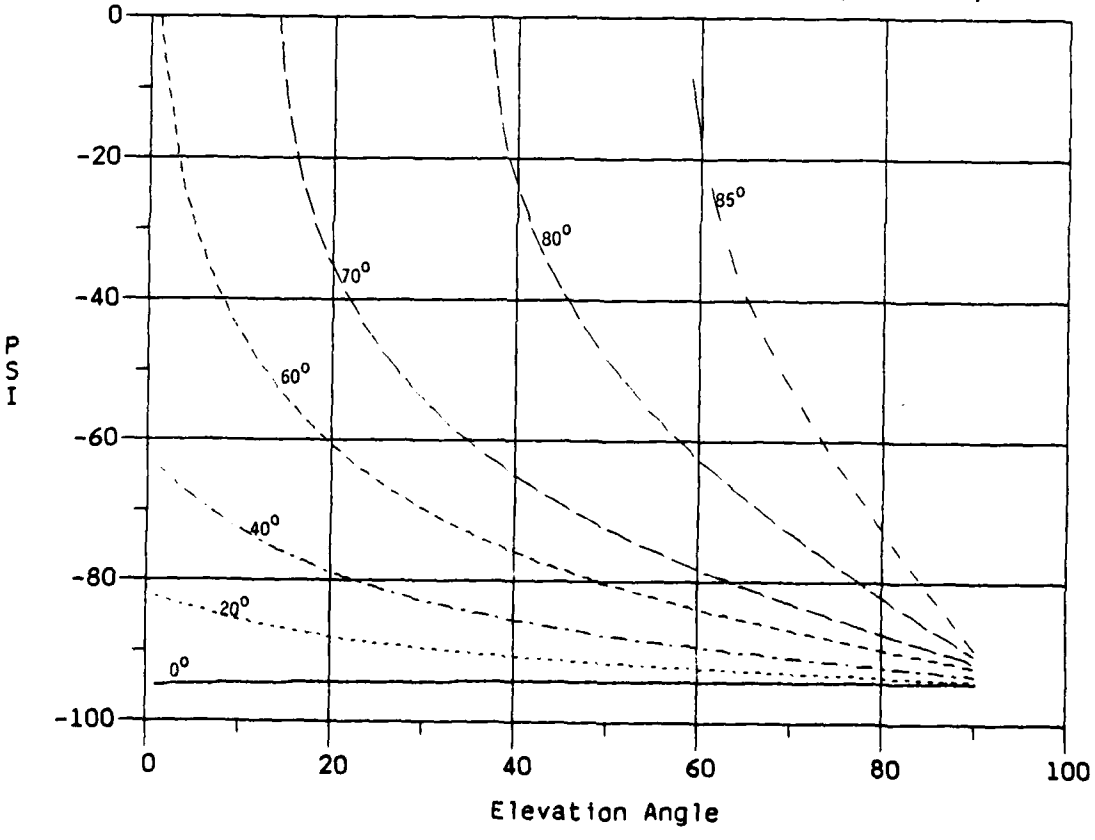

## 10.0 EXPERIMENTAL VERIFICATION

The sensitivity of the Transit position fix to the error of the input height, given by H(1,1) and H(2,1), is fairly straightforward and well understood, and hence does not require detailed verification.

The velocity sensitivities on the other hand are much more complicated and hence warrant careful experimental verification. Although reference [1] shows qualitatively how the magnitude of these errors vary with elevation angle $\sigma$ at low latitudes, nothing could be found in the open literature to indicate the sign of the errors, how they vary with satellite direction of travel (NS,EW), or how they vary with receiver latitude. Therefore experiments were conducted at DREO (latitude 45°) in 1983 and more extensively in 1985, to measure these errors. The 1985 results are presented here.

In this 1985 experiment two stationary receivers were used (an MX1107 and a JMR-4) with a -1.0 m/s velocity "measurement" fed into them, alternately in the north and east directions. This creates a velocity error (true - estimate) of +1.0 m/s in the north or east direction, to generate the appropriate velocity-error-induced position errors. These resulting position errors were recorded, and plotted as functions of $\sigma$, NS and EW. Although both receivers are dual channel (and hence able to remove most of the ionospheric induced error), there were of course other sources of position error beyond our control (as described in references [1] and [3]). These other errors appear mostly as additive noise on the error curves, although these other sources of error (especially the atmospheric induced sources) are not entirely uncorrelated with the elevation angle. To some extent these can mask the details of the smaller velocity induced terms (the clockwise H(1,2) and H(2,3) terms). Therefore we use this data here primarily to verify the general form of the curves (especially the sign). The dominant terms: H(1,3) and H(2,2) are naturally of most concern.

Figures 70 to 85 present the 1985 experimental results. Each figure shows three curves representing one component of the velocity error sensitivity H matrix: the modelled version (solid line), the JMR measured error (dashed line) and the MX1107 measured error (dot-dashed line). As expected, all errors clearly agree in sign and general form with the model. Even the smaller terms can be seen to agree on average with the model's prediction, however in this case the noise is almost at the same level as the deterministic error.

It should be mentioned that an adjustment had to be made

to the raw JMR H(1,2) and H(2,3) data, in an attempt to remove an unwanted error in the recorded position data which was not part of the actual position fix error. This is an error which is introduced by the JMR-4 receiver after the position fix is performed, but before the fix data is recorded for output. The MX1107 did not introduce this error during our experiment because it uses a slightly different procedure, as explained below.

The position fix output from the MX1107 is "at the fix mark", meaning that it is the measured position of the receiver at the point in time designated by the receiver as the "fix mark". The fix mark is generally near the centre of the satellite pass, near the point of closest approach. Of course this data is not available from the receiver until after the satellite pass has finished, and the calculations have been performed, which is generally about 5 to 9 minutes after the fix mark. The JMR-4, on the other hand, provides a position estimate that is deadreckoned from the fix mark to the time at which the data is output. Thus the JMR-4 position measurements have an additional error in the north or east direction, of about 300 to 540 metres, due to deadreckoning for 6 to 9 minutes with the 1.0 m/sec velocity error. This therefore changed the north position error due to a north velocity error, H(1,2), and the east position error due to an east velocity error, H(2,3), which are the small terms. In an attempt to remove this effect, 400 metres was added to these two terms (before plotting figures 70 to 85). When this error is taken into account, these terms are in good agreement with both the MX1107 data and the model.

Figure 70. Experimental Results: H(1,2) (NS=EW=1, lat=45)

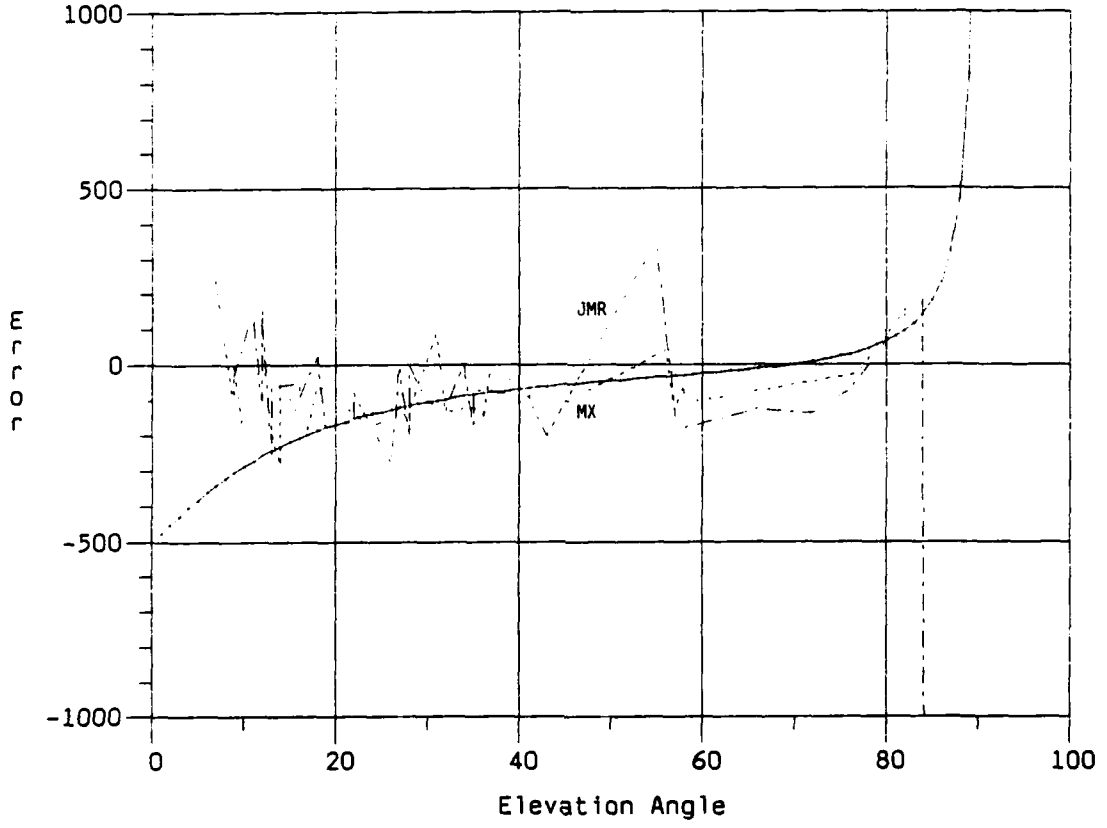


Figure 71. Experimental Results: H(2,2) (NS=EW=1, lat=45)

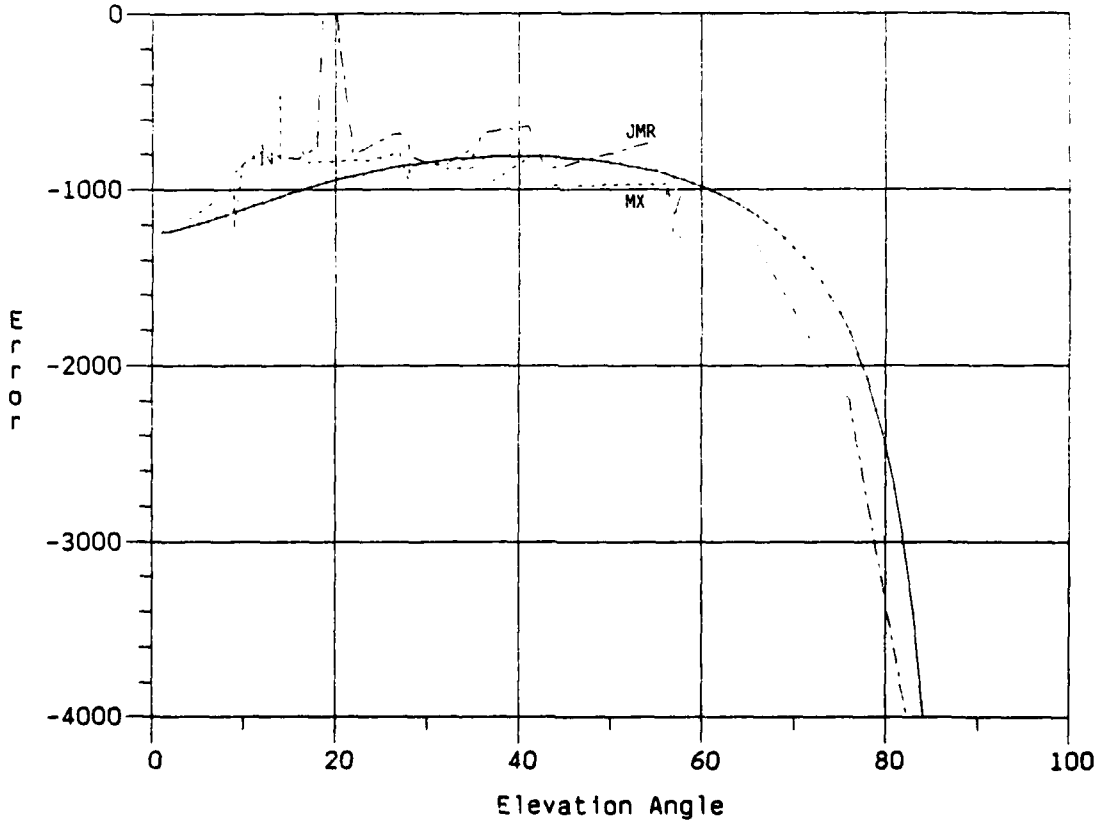

Figure 72. Experimental Results: H(1,3) (NS=EW=1,lat=45)

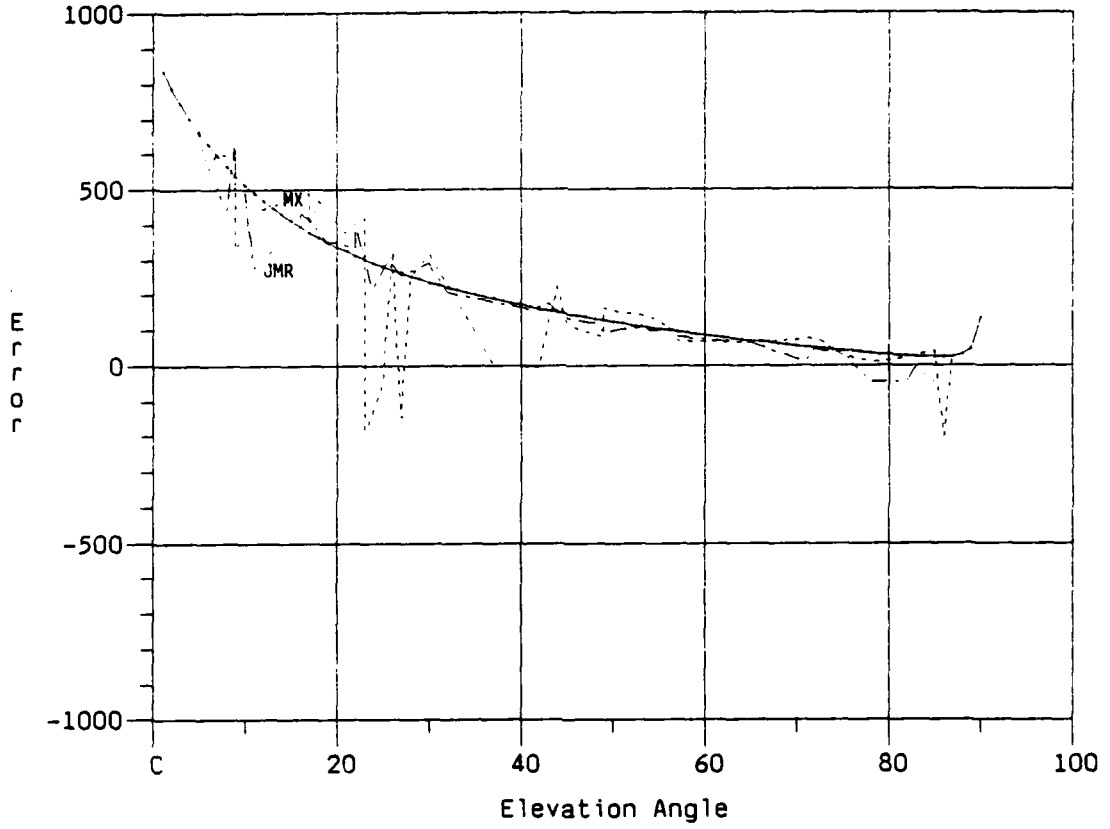


Figure 73. Experimental Results: H(2,3) (NS=EW=1,lat=45)

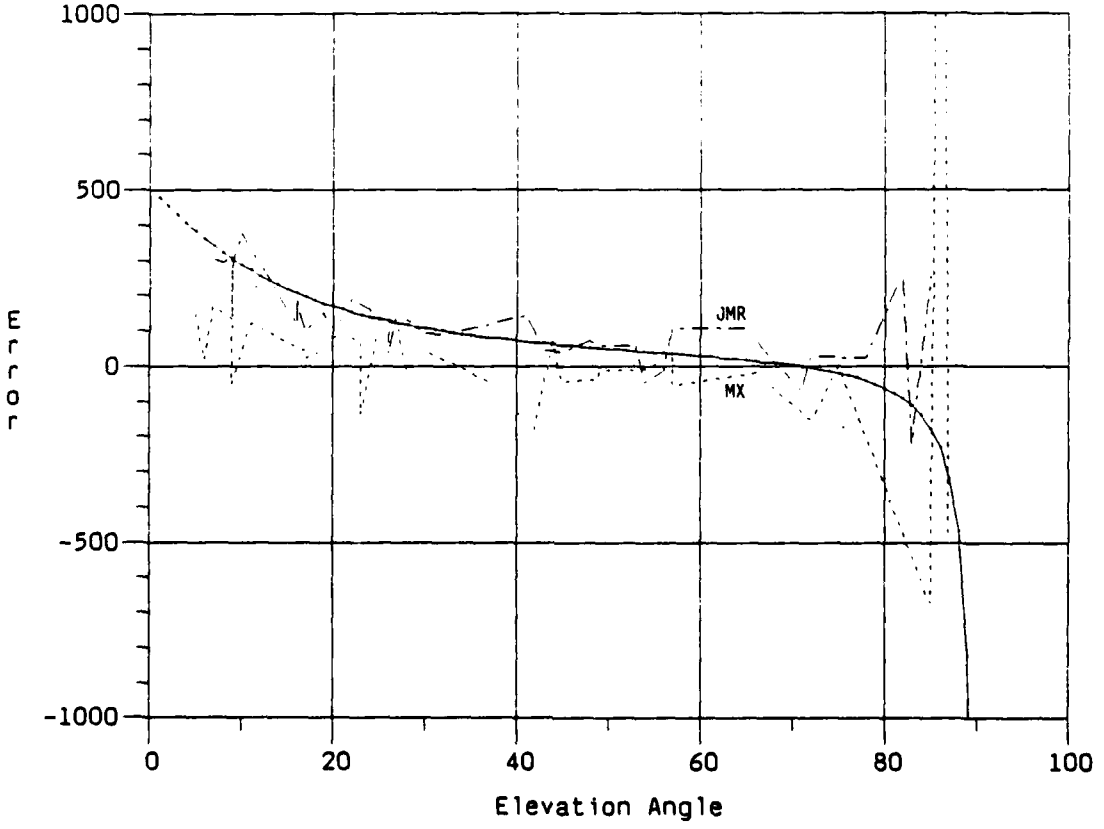

Figure 74. Experimental Results: H(1,2) (NS=1,EW=-1,lat=45)

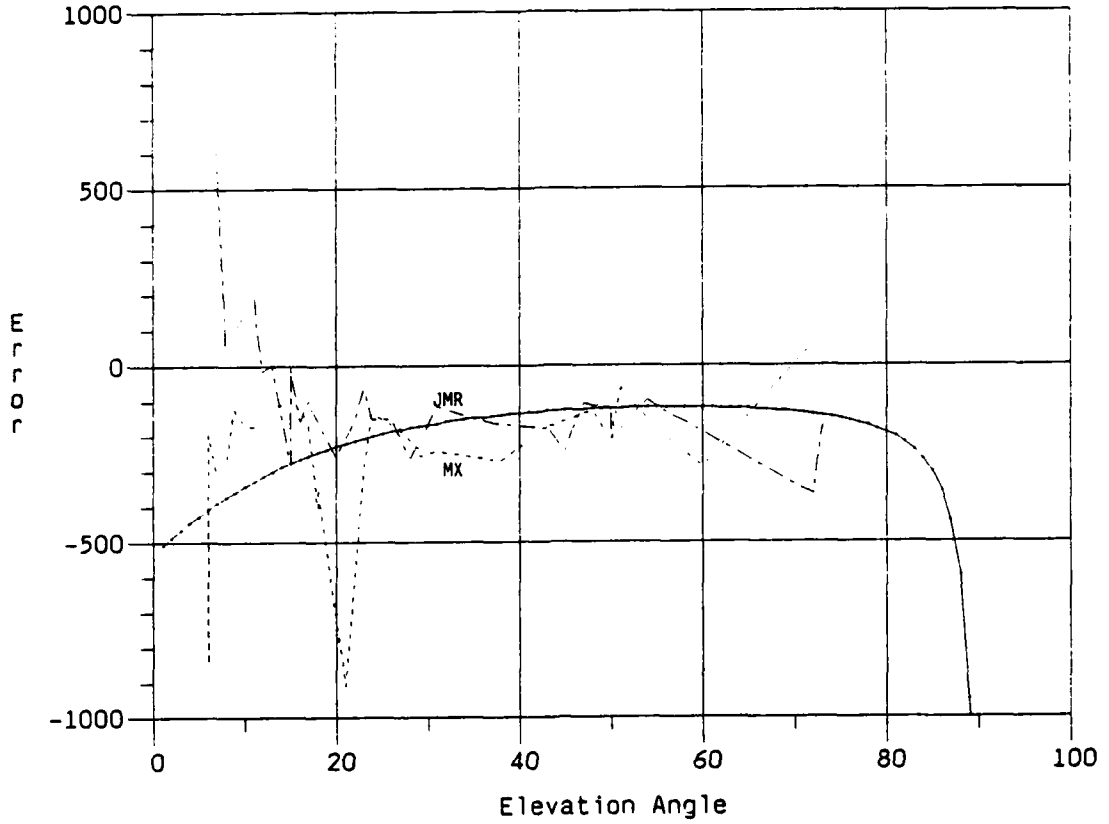


Figure 75. Experimental Results: H(2,2) (NS=1,EW=-1,lat=45)

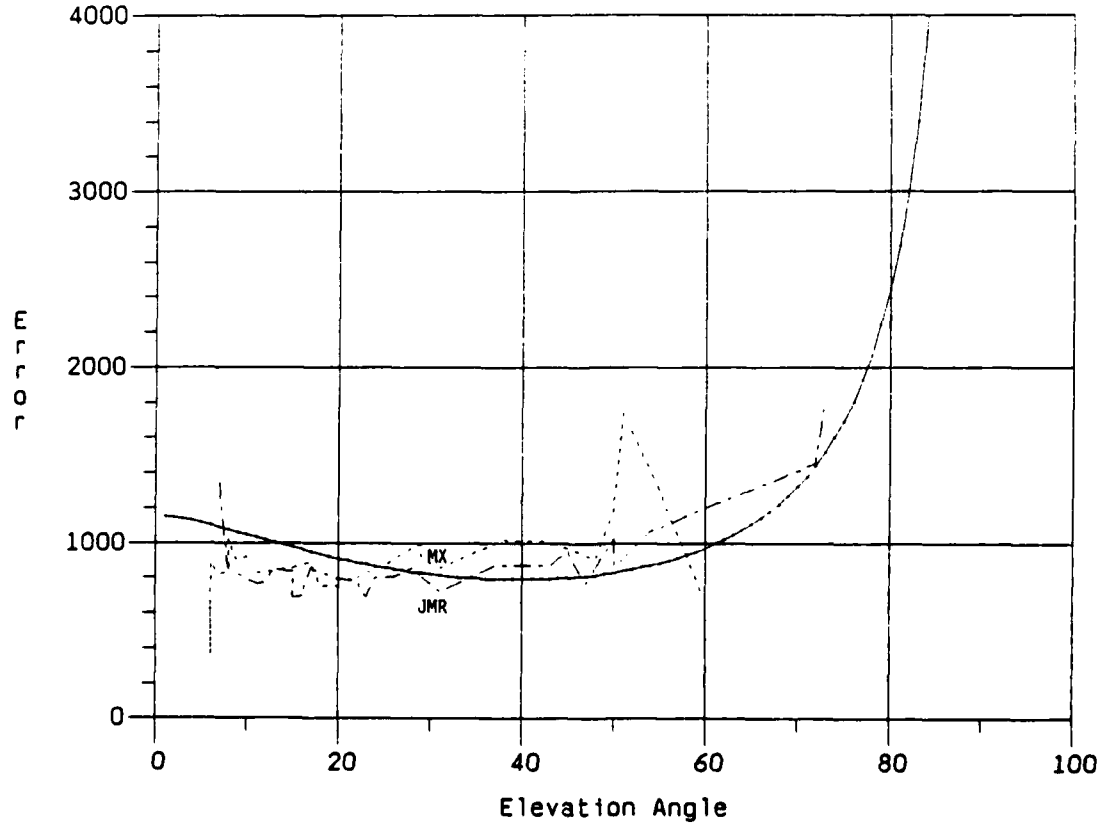

Figure 76. Experimental Results: H(1,3) (NS=1,EW=-1,lat=45)

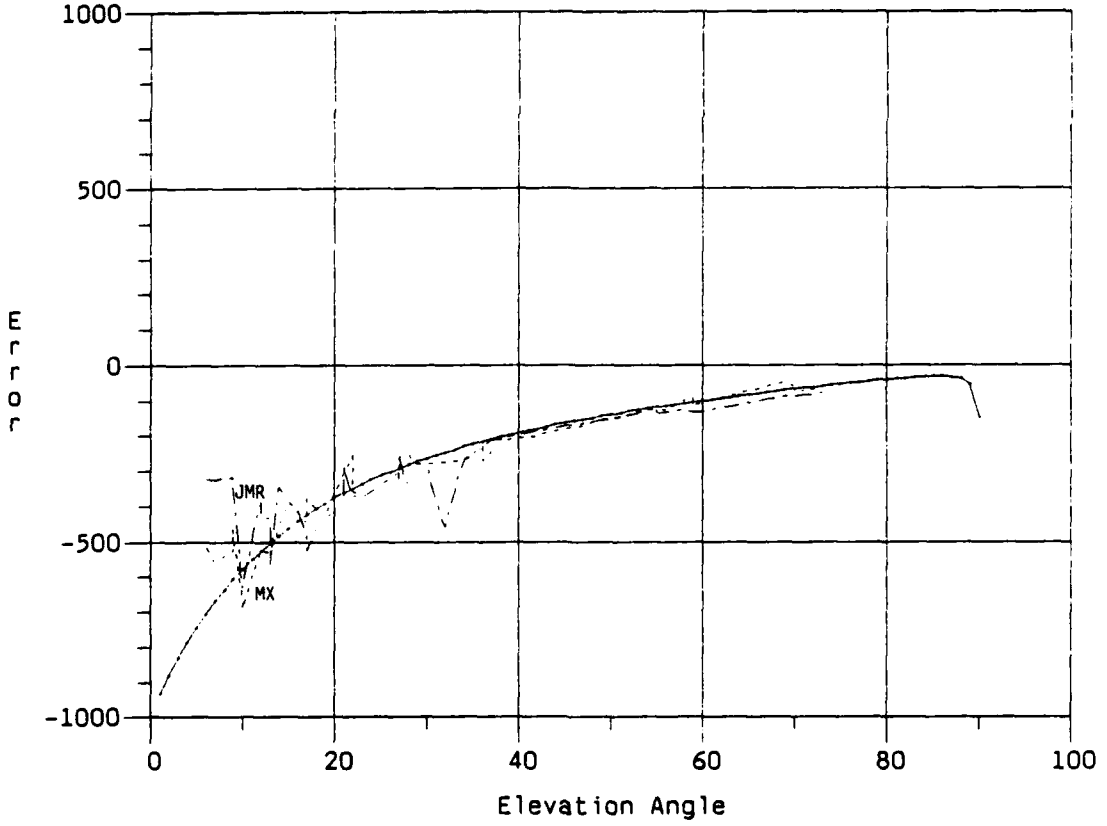


Figure 77. Experimental Results: H(2,3) (NS=1,EW=-1,lat=45)

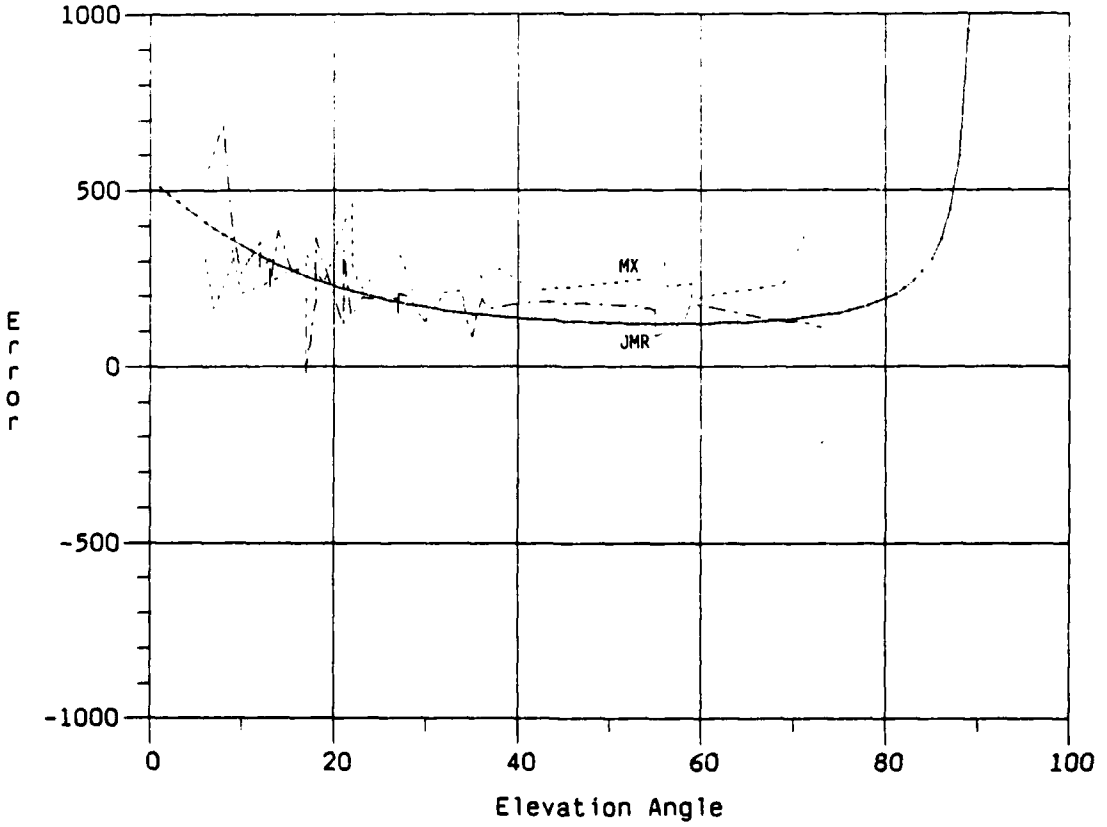

Figure 78. Experimental Results: H(1,2) (NS=-1,EW=1,lat=45)

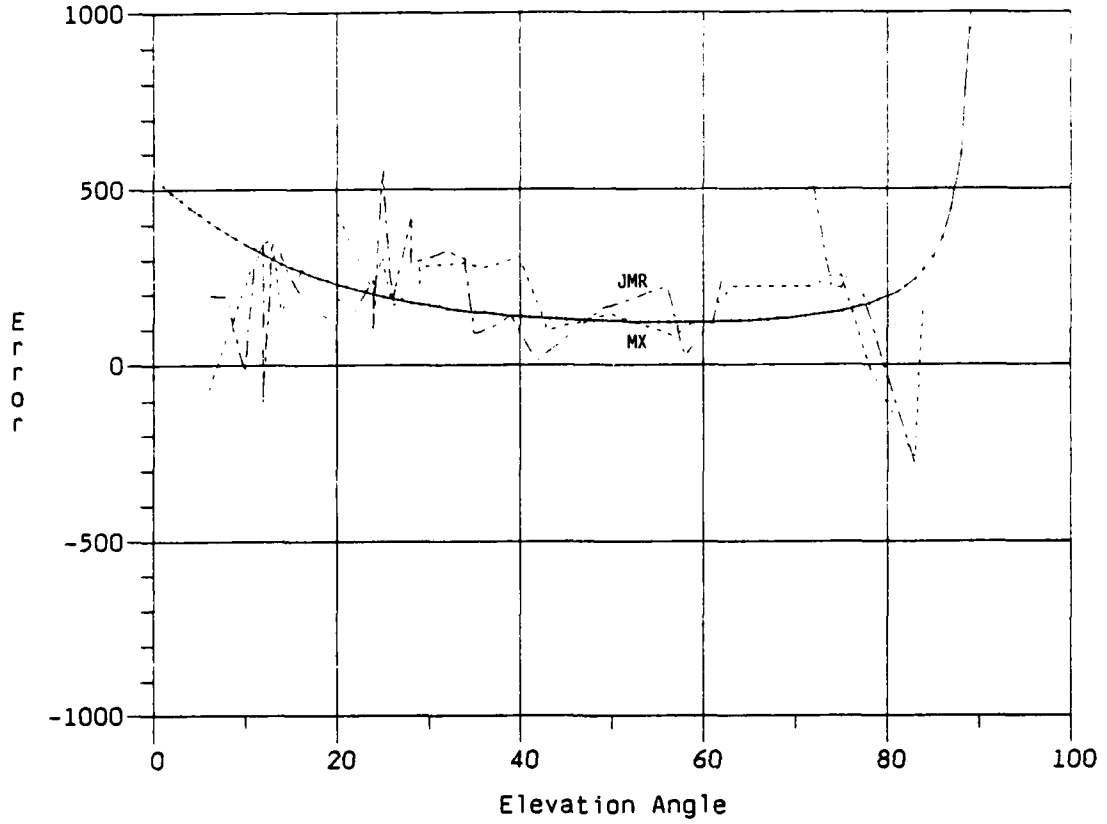


Figure 79. Experimental Results: H(2,2) (NS=-1,EW=1,lat=45)

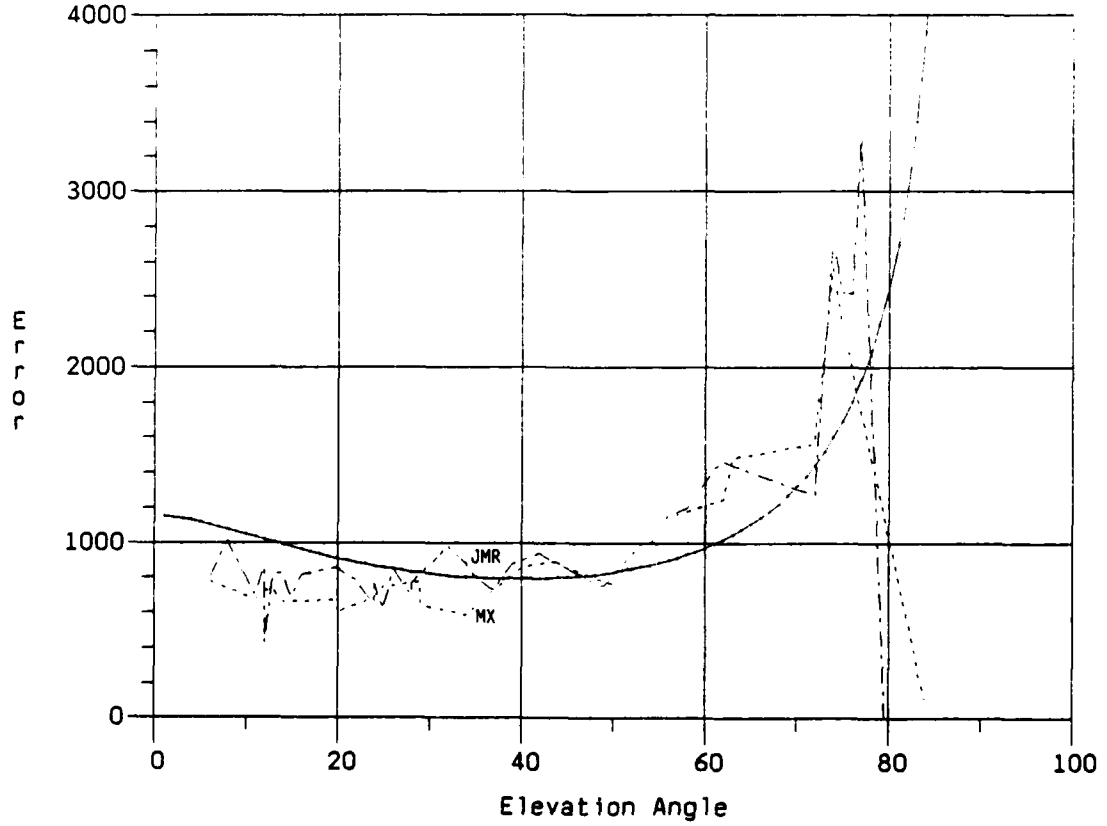

Figure 80. Experimental Results: H(1,3) (NS=-1,EW=1,lat=45)

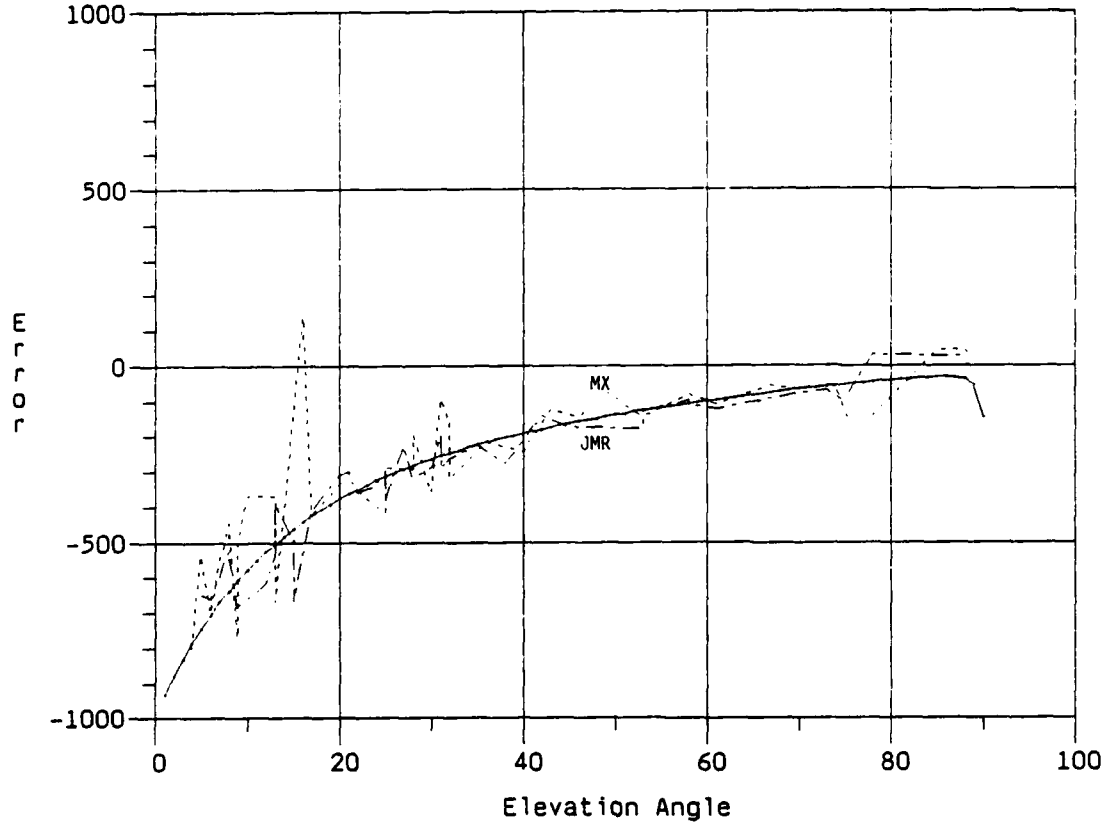


Figure 81. Experimental Results: H(2,3) (NS=-1,EW=1,lat=45)

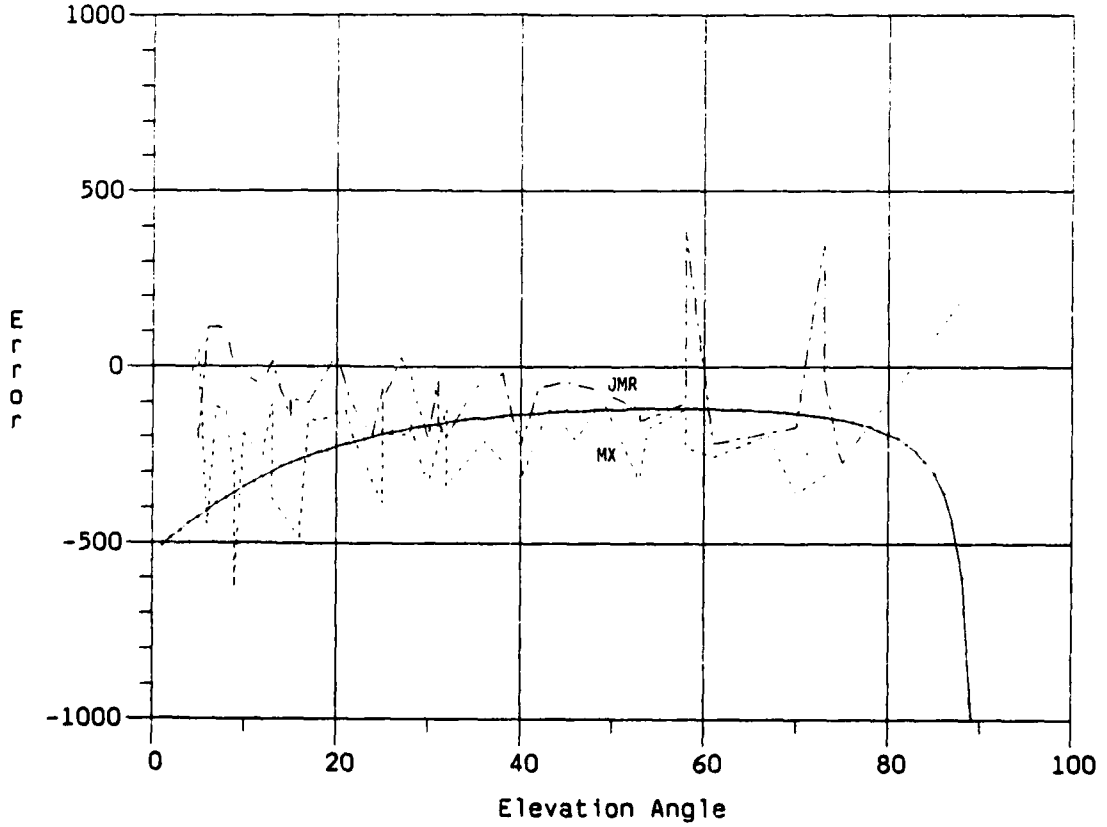

Figure 82. Experimental Results: H(1,2) (NS=EW=-1, lat=45)

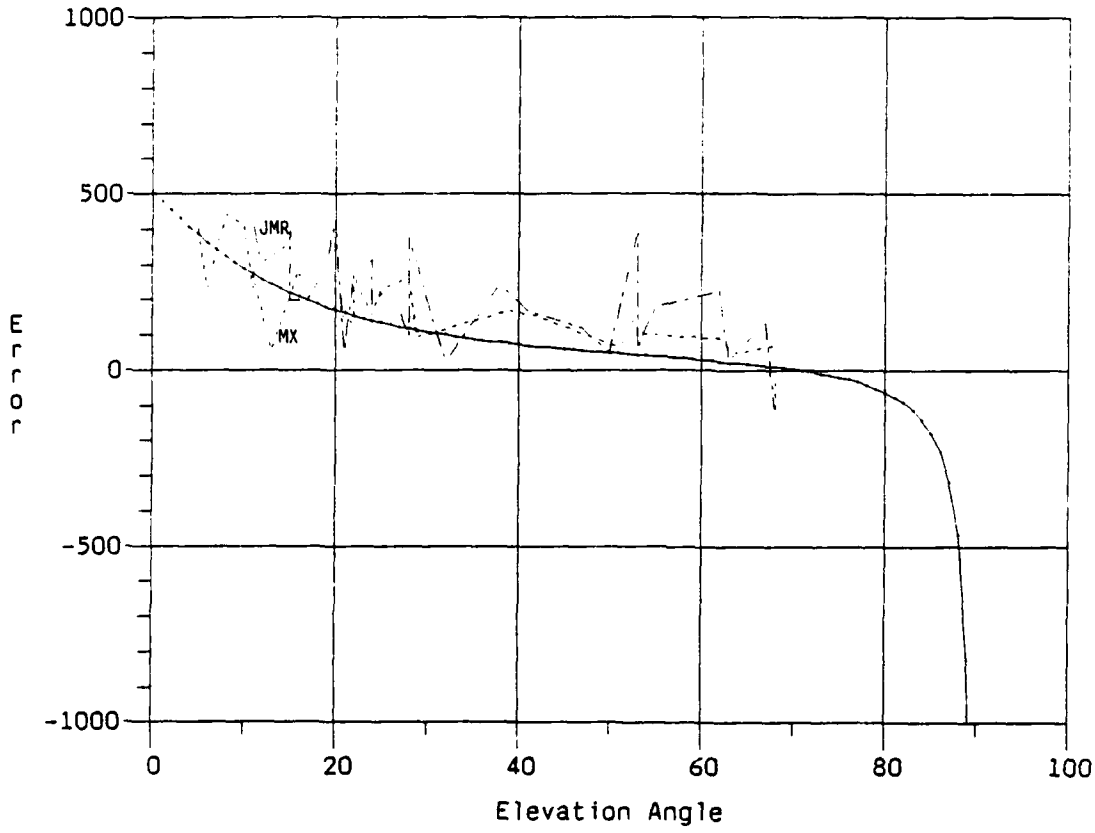


Figure 83. Experimental Results: H(2,2) (NS=EW=-1, lat=45)

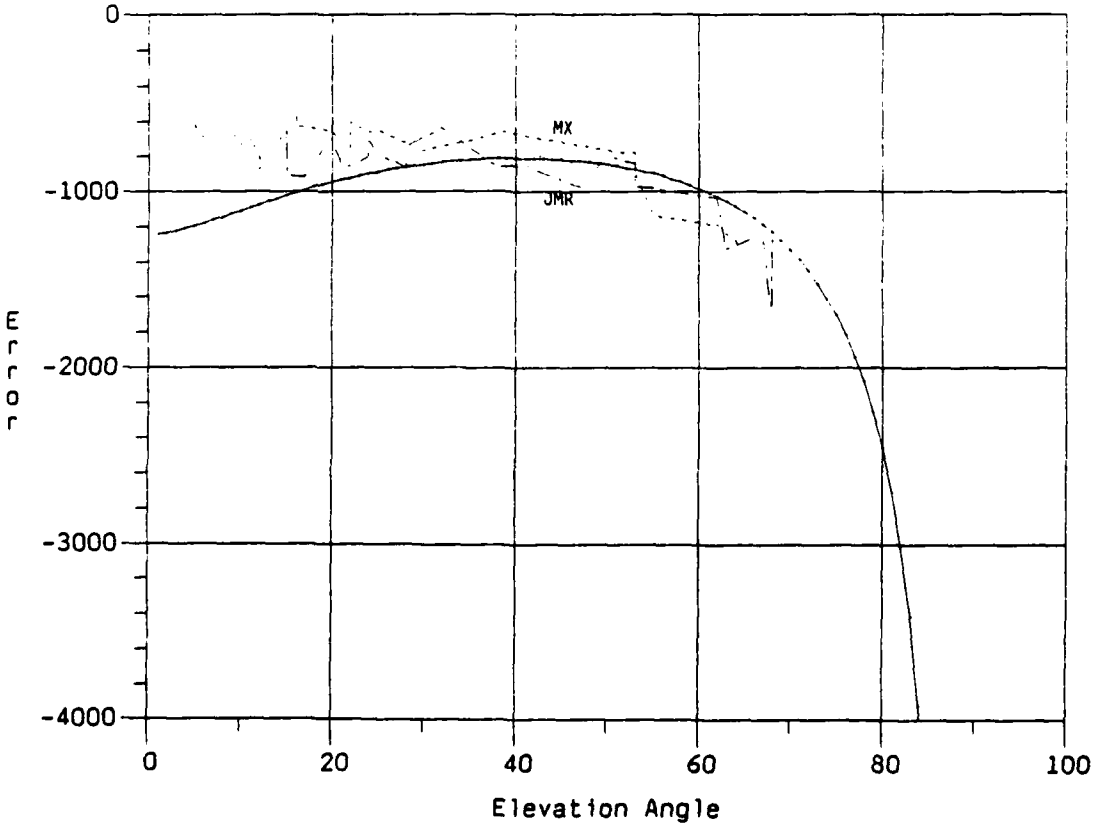

Figure 84. Experimental Results: H(1,3) (NS=EW=-1, lat=45)

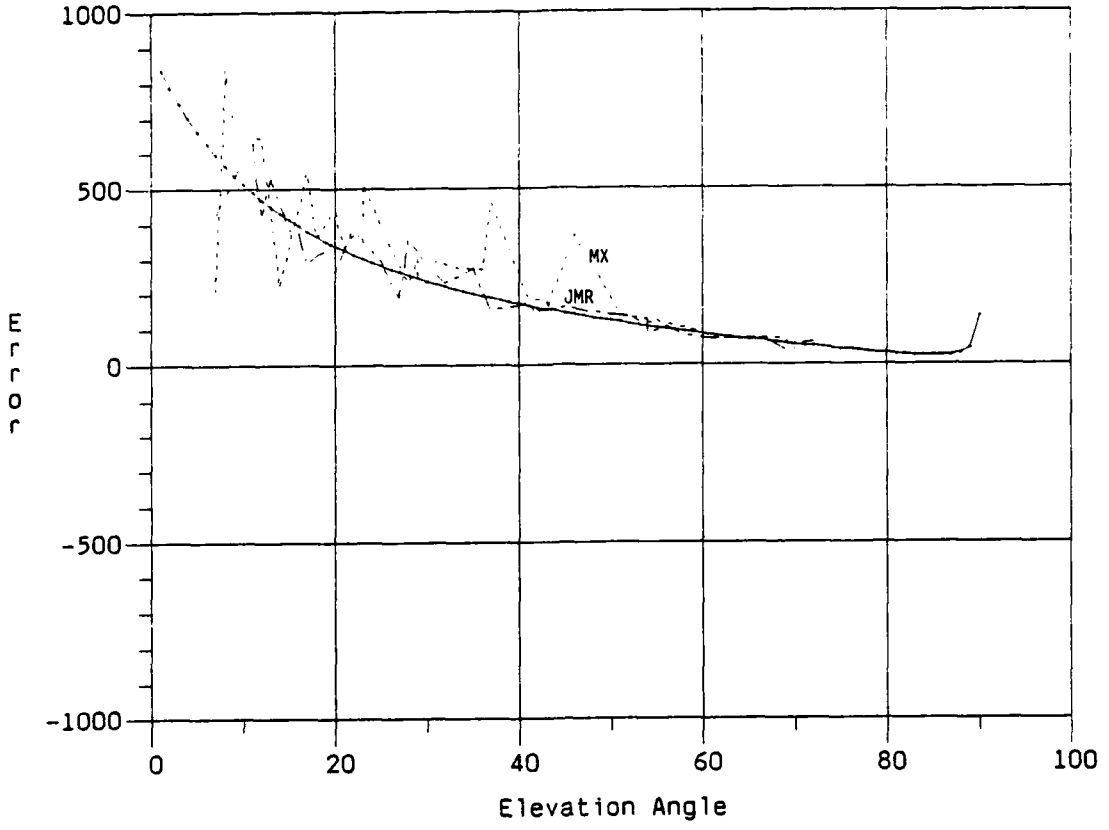


Figure 85. Experimental Results: H(2,3) (NS=EW=-1, lat=45)

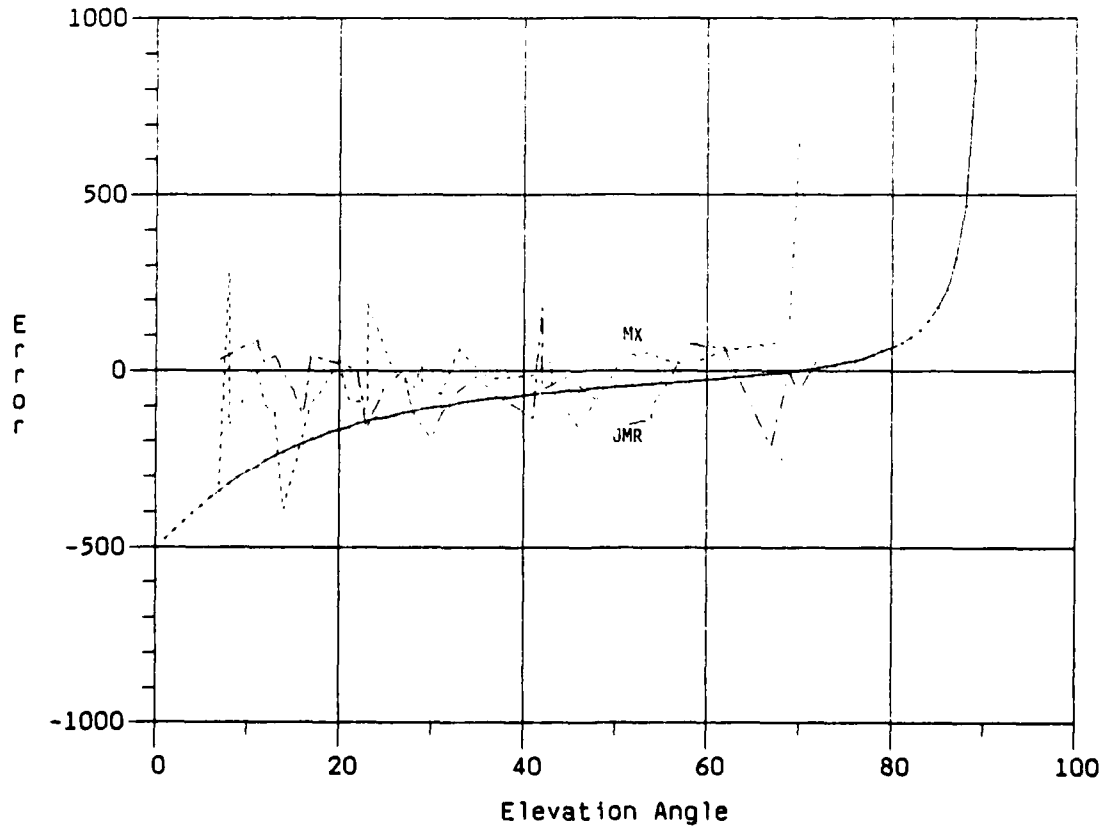

## 11.0 APPLICATIONS

This error model can be used to predict the accuracy of Transit fixes taken on a moving platform, as long as the accuracy of the velocity and height provided to the receiver is known.

Another application, and the one for which this error model was developed, is the design of Kalman filter based optimally integrated multi-sensor navigation systems which use Transit measurements. The H matrix described in this report is actually a submatrix of the Kalman filter "measurement matrix" for both the Marine Integrated Navigation System (MINS), described in reference [2], and the Primary Land Arctic Navigation System (PLANS), described in [3], both of which were developed at DREO.

Since the Transit orbital parameters (H,Vs) appear explicitly in the model, they can be easily varied to study the effect of different orbits. This offers two benefits: firstly it helps in selecting the optimal orbit from a system design point of view, and secondly it allows other similar satellite Doppler positioning systems to be modelled.

In the first case, when choosing the best orbit, one must account for velocity induced errors since these do account for a large portion of the total error budget. From the equations of Section 8.0, and in particular equation (129), we can see that the most direct effect of changing orbital parameters comes from the $\rho/V$ term. This will increase significantly as orbital height H increases, since this directly increases the slant range $\rho$, while at the same time decreasing the orbital velocity Vs (which of course is not independent of H) which decreases V. Therefore, as one would expect, lower faster orbits lead to less velocity error sensitivity. However, a lower orbit also leads to greater atmospheric drag, which causes other system problems, so to do the trade-off analysis one must have a quantitative model, such as provided here.

In the second case, this model can be applied directly to any similar Doppler positioning system, such as SARSAT (Search and Rescue Satellite) for example. SARSAT works on the same Doppler positioning principle as Transit does, and it also has circular orbits, which are almost polar (inclination of 98°). This extra 8° inclination can be accounted for by the appropriate coordinate transformation.

This error model could also have some more general use as a generic Doppler positioning error model, in that the same derivations could be followed, in the coordinate system appropriate to the problem.

## 12.0 CONCLUSIONS

A detailed and general velocity error and height error sensitivity model has been derived in full for dynamic Transit position fixing, explicitly showing the position error which would result from any error in the velocity and height (which must be provided as inputs to the Transit receiver during the position fix).

This model is presented in algorithmic form, and numerical results are graphically presented to illustrate the dependence on satellite maximum elevation angle, satellite direction of travel, and receiver latitude. Substantial experimental results are also presented, which verify the accuracy of the model for middle latitudes (for all satellite maximum elevation angles and all satellite directions of travel).

One somewhat surprising result of this general model is that at high latitudes the Transit error sensitivity matrix is significantly different than at low or medium latitudes. The terms which are small at low latitudes become much larger (and sometimes change sign!) at high latitudes, while the normally dominant terms become smaller. Thus the error model as previously described (qualitatively) in the literature was totally inadequate for use at high latitudes, a deficiency which had to be remedied for use in the DREO developed Primary Land Arctic Navigation System (PLANS).

## REFERENCES


[1] Thomas A. Stansell, "Transit, The Navy Navigation Satellite System," Navigation, Vol. 18, No. 1, Spring 1973.

[2] J.C. McMillan, "Multisensor Integration Techniques in the DREO Marine Integrated Navigation System (MINS)," DREO Report No. 986, 1988.

[3] J.C. McMillan, "Design of a Primary Land Arctic Navigation System," DREO Report No. 946, 1986.

[4] J.C. McMillan et al, "Integration of Transit, Omega, Loran-C and DR for Marine Navigation," presented at the 5th Canadian Symposium on Navigation, May 1983, Calgary Alberta.

## APPENDIX A. Angular Separation and Slant Range: $\Theta(\sigma)$, $\rho(\sigma)$

This appendix shows how the angular separation $\Theta$, between the receiver and the satellite subpoint, can be expressed as a function of the satellite elevation angle $\sigma$. In the process we will also obtain an expression for the slant range $\rho$. This slant range is used in the equation (61) for the measurement matrix, whereas $\Theta$ is needed to evaluate V and $\psi$ in (61).

Figure A1 illustrates the quantities of interest in the plane containing the receiver, the satellite, the subpoint and the earth's centre. Applying the law of cosines we obtain:

$$\rho^2 = R^2 + (R+H)^2 - 2R(R+H)\cos\Theta \qquad \text{(A1)}$$

and applying it again we have:

$$(R+H)^2 = \rho^2 + R^2 - 2\rho R\cos(\sigma+\pi/2)$$

$$= \rho^2 + R^2 + 2\rho R\sin\sigma \qquad \text{(A2)}$$

$$\therefore \quad \sin\sigma = \frac{1}{2\rho R}[\,(H+R)^2 - \rho^2 - R^2\,] \qquad \text{(A3)}$$

Using (A1) in (A3) we have:

$$\sin\sigma = \{\,(H+R)^2 - [\,R^2 + (R+H)^2 - 2R(R+H)\cos\Theta\,] - R^2\,\}/2\rho R$$

$$= [\,2R(R+H)\cos\Theta - 2R^2\,]/2\rho R$$

$$= [\,(R+H)\cos\Theta - R\,]/\rho \qquad \text{(A4)}$$

This gives an expression for the slant range $\rho$ as a function of the elevation angle $\sigma$ and separation angle $\Theta$:

**Figure A1. Separation Angle in Vertical Plane of Receiver & Satellite.**

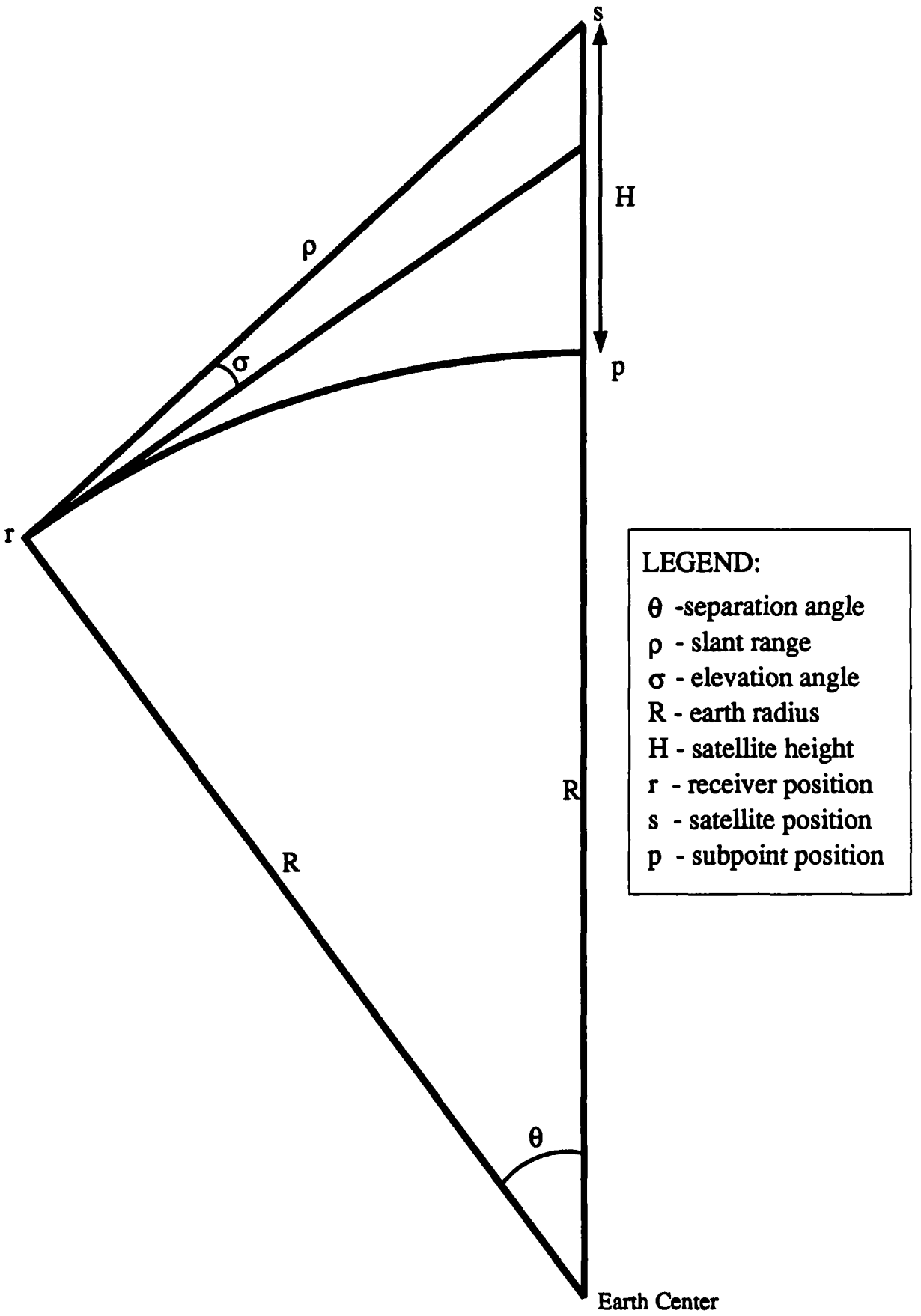

$$\rho = [\ (R+H)\cos\theta - R\ ]/\sin\sigma \qquad \text{(A5)}$$

This can now be squared and substituted in (A1) to obtain a quadratic equation for $\cos\theta$. Squaring (A5) gives:

$$\rho^2 = [\ (R+H)^2\cos^2\theta + R^2 - 2R(R+H)\cos\theta\ ]/\sin^2\sigma \qquad \text{(A6)}$$

Substituting this in (A1) produces:

$$(R+H)^2\cos^2\theta + R^2 - 2R(R+H)\cos\theta = \sin^2\sigma[\ R^2 + (R+H)^2 - 2R(R+H)\cos\theta\ ] \qquad \text{(A7)}$$

or

$$(R+H)^2\cos^2\theta - 2R(R+H)\cos^2\sigma\cos\theta + [R^2\cos^2\sigma - (R+H)^2\sin^2\sigma] = 0 \qquad \text{(A8)}$$

This is quadratic in $(R+H)\cos\theta$, and therefore has solution:

$$(R+H)\cos\theta = \frac{2R\cos^2\sigma \pm \sqrt{(2R\cos^2\sigma)^2 - 4[R^2\cos^2\sigma - (R+H)^2\sin^2\sigma]}}{2}$$

$$= R\cos^2\sigma \pm \sqrt{R^2\cos^2\sigma(\cos^2\sigma - 1) + (R+H)^2\sin^2\sigma}$$

$$= R\cos^2\sigma \pm \sin\sigma\sqrt{(R+H)^2 - R^2\cos^2\sigma} \qquad \text{(A9)}$$

Since the satellite must be between the horizon and the zenith, we know that $0 < \sigma < \pi/2$ and hence $\sin\sigma > 0$. This positive

elevation angle also implies (as can see from figure A1) that

$$(R+H)\cos\Theta > R \tag{A10}$$

and so the positive sign must be chosen in (A9). Therefore:

$$\cos\Theta = \frac{R}{R+H}\cos^2\sigma + \sin\sigma\sqrt{1 - \left(\frac{R}{R+H}\right)^2\cos^2\sigma} \tag{A11}$$

and

$$\boxed{\Theta = \cos^{-1}\left(\frac{R}{R+H}\cos^2\sigma + \sin\sigma\sqrt{1 - \left(\frac{R}{R+H}\right)^2\cos^2\sigma}\right)} \tag{A12}$$

The validity of equation (A12) can be easily checked for various limiting cases. For example if the satellite orbital height H goes to zero then the separation angle from the receiver to the satellite subpoint $\Theta$ (at the point of closest approach) should approach zero, which it does according to (A12). Also if the elevation angle $\sigma$ goes to $\pi/2$ then the separation angle $\Theta$ should go to zero, to which (A12) does comply.

Equation (A12) incidentally places a strict upper bound on the separation angle $\Theta$, at zero elevation angle $\sigma$:

$$\Theta(\sigma) \leq \Theta(0) = \cos^{-1}\left(\frac{R}{R+H}\right) \simeq 31^\circ \tag{A13}$$

More importantly, we can use (A12) to check the consistancy of the inputs $\sigma$ and $\lambda$. Since all Transit satellites are in polar orbits, all orbits contain the points directly above the poles (at orbital height). Therefore the point of closest approach (PCA) cannot be further than these north or south polar points. (If the receiver is located exactly at a pole, then the PCA will be the polar point.) Therefore $\Theta$ cannot be greater than the angle of separation from the nearest pole, which is $\pi/2 - |\lambda|$. Thus we have

$$\Theta \leq \frac{\pi}{2} - |\lambda| \tag{A14}$$

so that

$$\cos\theta \geq \cos\left(\frac{\pi}{2} - |\lambda|\right) = \sin|\lambda|$$

or

$$\boxed{\cos\theta \geq \sin|\lambda|} \qquad \text{(A15)}$$

This is a physical constraint that, through (A12) effectively places a lower limit on the elevation angle $\sigma$ at high latitudes. Another interpretation of this limit is that when the receiver is close enough to the pole so that the satellite orbital position over the pole is visible above the horizon, then the maximum elevation angle $\sigma$ must be at least as great as the elevation to this polar orbital point. In view of (A13) we can see that this polar orbital point can be seen anywhere within 31° of the pole, so that (A15) limits the value of $\sigma$ for all latitudes above 59° (and below -59°).

Now (A11) can be used in (A5) to obtain an expression for the slant range $\rho$ directly as a function of the elevation angle $\sigma$:

$$\rho = [\, R\cos^2\sigma + \sin\sigma\sqrt{(R+H)^2 - R^2\cos^2\sigma} - R]/\sin\sigma \qquad \text{(A16)}$$

$$= R(\cos^2\sigma - 1)/\sin\sigma + \sqrt{R^2(1-\cos^2\sigma) + 2RH + H^2} \qquad \text{(A17)}$$

$\therefore$

$$\boxed{\rho = \sqrt{R^2\sin^2\sigma + 2RH + H^2} - R\sin\sigma} \qquad \text{(A18)}$$

This is easily verified for $\sigma = \pi/2$, in which case the satellite is directly overhead at range $\rho=H$, in agreement with (A18). It can also be verified for $\sigma=0$, in which case the

satellite is on the horizon. In this case the range $\rho$ forms one edge of a right angle triangle with hypotenuse (R+H) and opposite side R. This makes

$$\rho = \sqrt{(R+H)^2 - R^2}$$

$$= \sqrt{2RH + H^2} \qquad \text{(A19)}$$

which is also in agreement with (A18). This coincidentally places bounds on the slant range to the satellite at clossest approach:

$$1{,}075{,}000 \leq \rho \leq 3{,}853{,}716 \qquad \text{(A20)}$$

**APPENDIX B. Heading of & Bearing from the Subpoint:**
**$\beta(NS,\lambda_p)$, $\phi(NS,EW,\lambda_p)$**

This appendix shows how the latitude of the satellite subpoint $\lambda_p$, and the heading of the subpoint path $\beta$ can be expressed as functions of the known quantities $\lambda$, NS and EW (the receiver latitude, the satellite north-to-south direction of travel and the satellite east-or-west direction from the receiver) and the separation angle $\theta$. This angle $\theta$ can be expressed in terms of the known satellite elevation angle $\sigma$ (as shown in Appendix A).

The heading of the subpoint path $\beta$ can be easily found by finding the north and east components of the subpoint velocity in the locally horizontal earth fixed frame. We know that the satellite is in a polar orbit of radius (R+H) with orbital speed $V_s$. Therefore the subpoint moves directly "north" (or south if NS=1) in an earth centred inertial (non-rotating) frame in an "orbit" of radius R with speed $RV_s/(R+H)$. In the locally horizontal earth fixed frame the northerly component of the subpoint velocity is therefore $-NS\ RVs/(R+H)$ and easterly component of the subpoint velocity is due entirely to earth rate, which is $-R\omega\cos\lambda_p$. Therefore as seen from Figure B1, the subpoint heading satisfies:

$$\tan\beta = \frac{R\omega\cos\lambda_p}{NS\cdot R\cdot V_s/(R+H)} \qquad (B1)$$

Careful consideration of satellite direction of travel can be used to resolve the ambiguity of the inverse tangent function, leading to the following solution. This consideration indicates that the subpath is slightly to the west of north if the satellite is moving north (NS=-1) and slightly to the west of south if the satellite is moving south (NS=1), and hence:

$$\beta = NS\ \tan^{-1}\left(\frac{(R+H)\omega}{V_s}\cos\lambda_p\right) + \frac{\pi}{2}(1+NS) \qquad (B2)$$

This can now be used to express the bearing $\phi$ from the subpoint to the receiver at the point of closest approach, since this bearing line (great circle from subpoint to receiver) is

**Figure B1. Bearing β of Satellite Subpath.**

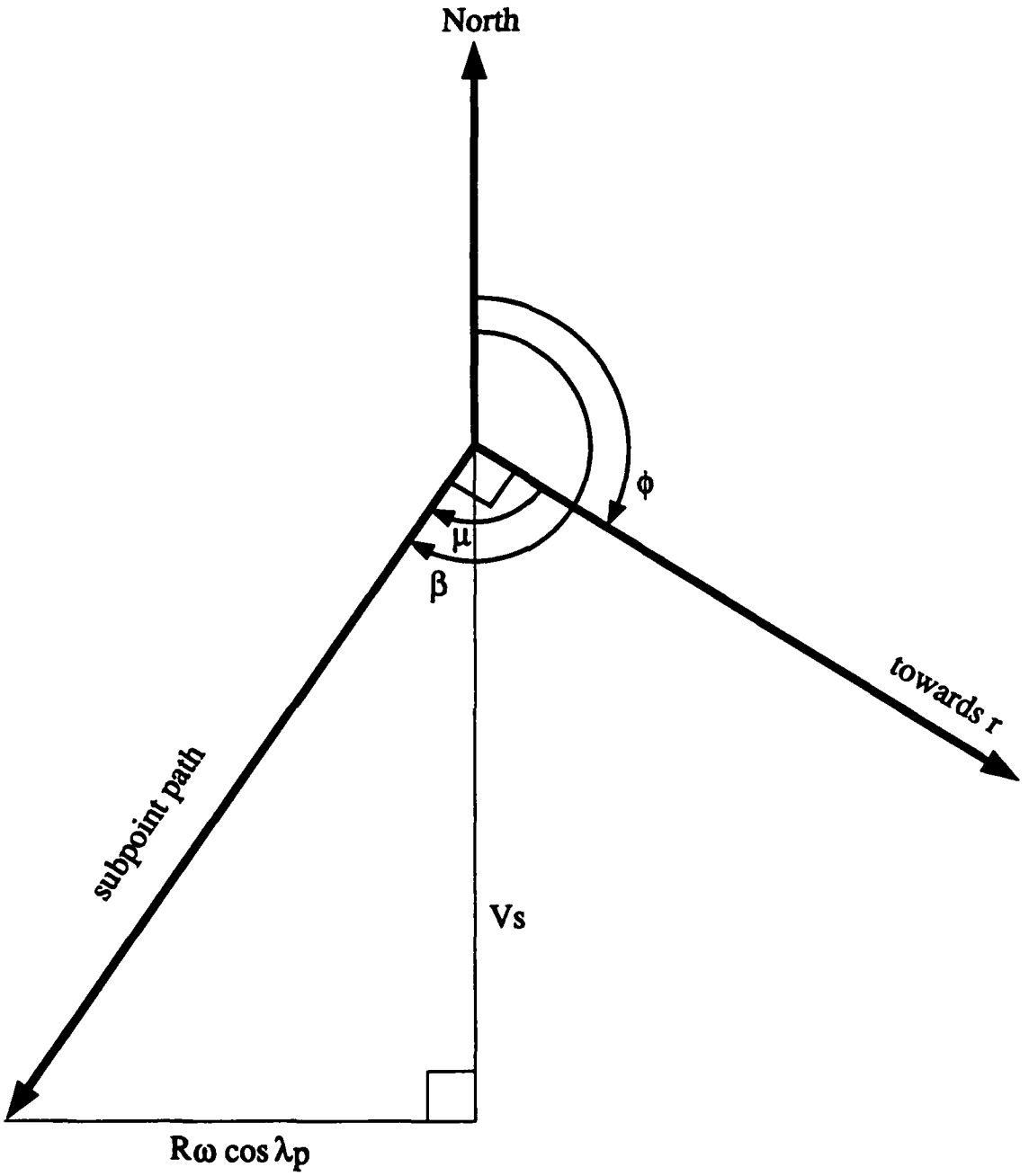

orthogonal to the subpoint path (a fact easily proven by definition of closest approach) as shown in Figure B1. Thus:

$$\phi = \beta + \mu \tag{B3}$$

where direction of travel consideration (in Figure B1 we have NS=-1 and EW=1) gives:

$$\mu = NS \cdot EW \; \pi/2 \tag{B4}$$

therefore:

$$\boxed{\phi = NS \tan^{-1}\left(\frac{(R+H)\omega}{V_s}\cos\lambda_p\right) + \frac{\pi}{2}(1 + NS + NS \cdot EW)} \tag{B5}$$

It will turn out that we actually need $\sin\phi$, which is simpler:

$$\sin\phi = \sin\left(NS \tan^{-1}\left(\frac{(R+H)\omega}{V_s}\cos\lambda_p\right) + \frac{\pi}{2}(1 + NS + NS \cdot EW)\right) \tag{B6}$$

$$= \cos\left(NS \tan^{-1}\left(\frac{(R+H)\omega}{V_s}\cos\lambda_p\right) + NS\left(\frac{\pi}{2} + EW\frac{\pi}{2}\right)\right) \tag{B7}$$

$$= \cos\left(\tan^{-1}\left(\frac{(R+H)\omega}{V_s}\cos\lambda_p\right) + \frac{\pi}{2} + EW\frac{\pi}{2}\right) \tag{B8}$$

$$= -\sin\left(\tan^{-1}\left(\frac{(R+H)\omega}{V_s}\cos\lambda_p\right) + EW\frac{\pi}{2}\right) \tag{B9}$$

$$= -EW\cos\left(\tan^{-1}\left(\frac{(R+H)\omega}{V_s}\cos\lambda_p\right)\right) \tag{B10}$$

This can be further simplified by using a trigonometric identity. By setting

$$D \equiv \frac{(R+H)\omega\cos\lambda_p}{V_s} \tag{B11}$$

we have

$$\cos(\tan^{-1}D) = \frac{1}{\sqrt{1+D^2}} \tag{B12}$$

so that

$$\boxed{\sin\phi = \frac{-EW}{\sqrt{1+D^2}}} \tag{B13}$$

**APPENDIX C. Latitude of the Subpoint: $\lambda_p(\Theta, \lambda, NS, EW)$**

This appendix shows how the latitude of the satellite subpoint $\lambda_p$ can be expressed as a function of the known quantities $\lambda$, NS and EW. To do this we consider the spherical triangle shown in Figure C1, with vertices at the receiver, the satellite subpoint (at the point of closest approach) and the north pole. We can consider $\lambda$ and $\Theta$ to be known, and we seek to find $\lambda_p$. (In Appendix D we shall also find an expression for $\psi$.) From the law of cosines for spherical triangles, where the "sides" as shown in Figure C1 are treated as angles subtended at the earth's centre, we have:

$$\cos(\pi/2-\lambda) = \cos\Theta\cos(\pi/2-\lambda_p) + \sin\Theta\sin(\pi/2-\lambda_p)\cos(2\pi-\phi) \quad (C1)$$

$$\therefore \quad \sin\lambda = \cos\Theta\sin\lambda_p + \sin\Theta\cos\lambda_p\cos\phi \quad (C2)$$

Now from equation (B5) we can expand $\cos\phi$, and using simple trigonometric identities, simplify it:

$$\cos\phi = \cos\left( NS\ \tan^{-1}\left(\frac{(R+H)\omega}{V_s}\cos\lambda_p\right) + \frac{\pi}{2} + NS\frac{\pi}{2}(1+EW) \right) \quad (C3)$$

$$\cos\phi = -\sin\left( NS\ \tan^{-1}\left(\frac{(R+H)\omega}{V_s}\cos\lambda_p\right) + NS\left(\frac{\pi}{2} + EW\frac{\pi}{2}\right) \right) \quad (C4)$$

$$= -NS\sin\left( \tan^{-1}\left(\frac{(R+H)\omega}{V_s}\cos\lambda_p\right) + \frac{\pi}{2} + EW\frac{\pi}{2} \right) \quad (C5)$$

$$= -NS\cos\left( \tan^{-1}\left(\frac{(R+H)\omega}{V_s}\cos\lambda_p\right) + EW\frac{\pi}{2} \right) \quad (C6)$$

**Figure C1. Bearing Angles on the Receiver-Subpoint-Pole Spherical Triangle.**

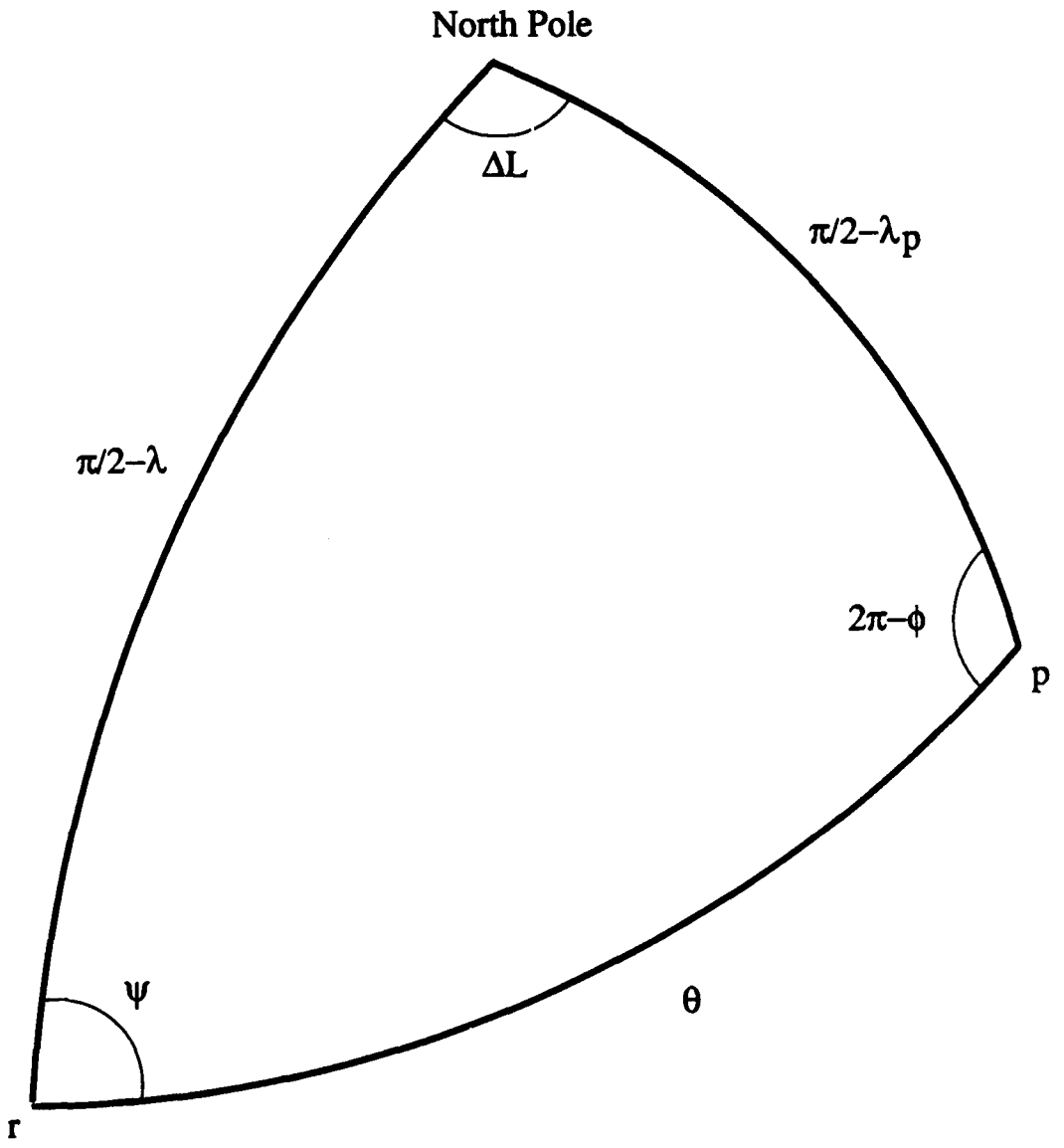

$$= NS \cdot EW \sin\left( \tan^{-1}\left(\frac{(R+H)\omega}{V_s}\cos\lambda_p\right)\right) \qquad (C7)$$

Now the argument of $\tan^{-1}$ in (C7) is a small angle (the angle between the satellite subpoint path and the meridian). Its maximum value is at the equator, (where the horizontal earth rate is maximum), where it is approximately 4 degrees. Therefore to a good approximation we can write:

$$\cos\phi \simeq NS \cdot EW\left(\frac{(R+H)\omega}{V_s}\cos\lambda_p\right) \qquad (C8)$$

This can now be used in (C2) to create a quadratic equation in $\sin\lambda_p$:

$$\sin\lambda = \cos\theta\sin\lambda_p + NS \cdot EW\frac{(R+H)\omega}{V_s}\sin\theta\cos^2\lambda_p \qquad (C9)$$

$$= \cos\theta\sin\lambda_p + NS \cdot EW \cdot K\sin\theta(1-\sin^2\lambda_p) \qquad (C10)$$

where

$$K \equiv (R+H)\omega/V_s \simeq 0.074416 \qquad (C11)$$

Thus (C10) can be written:

$$(NS \cdot EW \cdot K\sin\theta)\sin^2\lambda_p - \cos\theta\sin\lambda_p + (\sin\lambda - NS \cdot EW \cdot K\sin\theta) = 0 \qquad (C12)$$

which is quadratic in $\sin\lambda_p$, and hence has solutions:

$$\sin\lambda_p = \frac{\cos\theta \pm \sqrt{\cos^2\theta - 4NS \cdot EW \cdot K\sin\theta(\sin\lambda - NS \cdot EW \cdot K\sin\theta)}}{2NS \cdot EW \cdot K\sin\theta}$$

(C13)

Choosing the positive or negative sign is not difficult. As was seen from equation (A13), the separation angle $\theta$ cannot be greater than 32 degrees, so that $\cos\theta > 0.84$ and $\sin\theta < 0.53$. We also saw in (C11) above that K is small (<0.075). This implies that

$$\frac{\cos\theta}{2K\sin\theta} > 11 \qquad \text{(C14)}$$

Therefore the negative sign in equation (C13) yields the only possible solution. Also as the separation angle $\theta$ becomes small, we must have $\lambda_p$ approaching $\lambda$, as is the case with the negative sign. Thus the satellite subpoint latitude $\lambda_p$ is (note that $NS^2 = EW^2 = 1$ and that by definition $\lambda_p \subset [-\pi/2, \pi/2]$):

$$\lambda_p = \sin^{-1}\left(\frac{\cos\theta - \sqrt{\cos^2\theta - 4K\sin\theta(NS\cdot EW\sin\lambda - K\sin\theta)}}{2NS\cdot EW\cdot K\sin\theta}\right) \qquad \text{(C15)}$$

where K is given by (C11).

Now we can find a simple approximation to equation (C15) by ignoring higher order terms in K:

$$\sin\lambda_p \approx \frac{\cos\theta - \sqrt{\cos^2\theta - 4K\cdot NS\cdot EW\sin\theta\sin\lambda)}}{2NS\cdot EW\cdot K\sin\theta} \qquad \text{(C16)}$$

Using the Taylor series:

$$(x+\varepsilon)^{1/2} = x^{1/2} + \varepsilon\cdot\tfrac{1}{2}x^{-1/2} + \frac{\varepsilon^2}{2}\cdot[-\tfrac{1}{4}x^{-3/2}] + \ldots \qquad \text{(C17)}$$

we have:

$$\sqrt{\cos^2\theta - 4K\cdot NS\cdot EW\sin\theta\sin\lambda} \approx \cos\theta - \frac{4K\cdot NS\cdot EW\sin\theta\sin\lambda}{2\cos\theta} \qquad \text{(C18)}$$

$$\approx -2K\cdot NS\cdot EW\tan\theta\sin\lambda \qquad \text{(C19)}$$

Thus (C16) becomes:

$$\sin\lambda_p \simeq \frac{2K \cdot NS \cdot EW \tan\theta \sin\lambda}{2NS \cdot EW \cdot K \sin\theta} \qquad (C20)$$

$$= \frac{\sin\lambda}{\cos\theta} \qquad (C21)$$

This approximation is included here for its intuitive value, and to provide a simple test of reasonableness which can be applied to the solution of (C15).

## APPENDIX D. Bearing to Subpoint: $\psi(\theta, \lambda_p, \lambda)$

Now the spherical triangle in Figure C1 can be used to find the other angles. This Figure shows the situation in which the satellite is east of the receiver (EW=1). For the other case (EW=-1) the Figure is simply reflected about the receiver meridian. In this case $-\phi$ becomes $\phi$ and the bearing angle $\psi$ from north is negative. Therefore the law of sines for spherical triangles can be applied to solve for the bearing $\psi$ to the receiver at the subpoint.:

$$\frac{\sin(\pi/2 - \lambda)}{EW \cdot \sin(-\phi)} = \frac{\sin(\pi/2 - \lambda_p)}{EW \cdot \sin\psi} \qquad (D1)$$

$$\therefore \quad \frac{\cos\lambda}{-\sin\phi} = \frac{\cos\lambda_p}{\sin\psi} \qquad (D2)$$

so

$$\boxed{\sin\psi = \frac{-\sin\phi\cos\lambda_p}{\cos\lambda}} \qquad (D3)$$

Applying the law of cosines for sides gives:

$$\cos(\pi/2-\lambda_p) = \cos\theta\cos(\pi/2-\lambda) + \sin\theta\sin(\pi/2-\lambda)\cos\psi \qquad (D4)$$

or

$$\sin\lambda_p = \cos\theta\sin\lambda + \sin\theta\cos\lambda\cos\psi \qquad (D5)$$

so that

$$\boxed{\cos\psi = \frac{\sin\lambda_p - \cos\theta\sin\lambda}{\sin\theta\cos\lambda}} \qquad (D6)$$

## DOCUMENT CONTROL DATA

(Security classification of title, body of abstract and indexing annotation must be entered when the overall document is classified)

1. ORIGINATOR (the name and address of the organization preparing the document. Organizations for whom the document was prepared, e.g. Establishment sponsoring a contractor's report, or tasking agency, are entered in section 8.)

Defence Research Establishment Ottawa
Department of National Defence
Ottawa, Ontario K1A 0Z4

2. SECURITY CLASSIFICATION (overall security classification of the document. including special warning terms if applicable)

UNCLASSIFIED

3. TITLE (the complete document title as indicated on the title page. Its classification should be indicated by the appropriate abbreviation (S,C,R or U) in parentheses after the title.)

An Error Sensitivity Model For Doppler Positioning Using Transit Satellites (U)

4. AUTHORS (Last name, first name, middle initial)

McMillan, J. Christopher

5. DATE OF PUBLICATION (month and year of publication of document)

August 1989

6a. NO. OF PAGES (total containing information. Include Annexes, Appendices, etc.)

138

6b. NO. OF REFS (total cited in document)

4

7. DESCRIPTIVE NOTES (the category of the document, e.g. technical report, technical note or memorandum. If appropriate, enter the type of report, e.g. interim, progress, summary, annual or final. Give the inclusive dates when a specific reporting period is covered.)

DREO Report

8. SPONSORING ACTIVITY (the name of the department project office or laboratory sponsoring the research and development. Include the address.)

Defence Research Establishment Ottawa
Department of National Defence
Ottawa, Ontario K1A 0Z4

9a. PROJECT OR GRANT NO. (if appropriate, the applicable research and development project or grant number under which the document was written. Please specify whether project or grant)

DLAEEM 108 041LJ

9b. CONTRACT NO. (if appropriate, the applicable number under which the document was written)

10a. ORIGINATOR'S DOCUMENT NUMBER (the official document number by which the document is identified by the originating activity. This number must be unique to this document.)

DREO REPORT 1015

10b. OTHER DOCUMENT NOS. (Any other numbers which may be assigned this document either by the originator or by the sponsor)

11. DOCUMENT AVAILABILITY (any limitations on further dissemination of the document, other than those imposed by security classification)

(X) Unlimited distribution
( ) Distribution limited to defence departments and defence contractors; further distribution only as approved
( ) Distribution limited to defence departments and Canadian defence contractors; further distribution only as approved
( ) Distribution limited to government departments and agencies; further distribution only as approved
( ) Distribution limited to defence departments; further distribution only as approved
( ) Other (please specify):

12. DOCUMENT ANNOUNCEMENT (any limitation to the bibliographic announcement of this document. This will normally correspond to the Document Availabilty (11). However, where further distribution (beyond the audience specified in 11) is possible, a wider announcement audience may be selected.)

UNLIMITED

UNCLASSIFIED

SECURITY CLASSIFICATION OF FORM

13. ABSTRACT ( a brief and factual summary of the document. It may also appear elsewhere in the body of the document itself. It is highly desirable that the abstract of classified documents be unclassified. Each paragraph of the abstract shall begin with an indication of the security classification of the information in the paragraph (unless the document itself is unclassified) represented as (S), (C), (R), or (U). It is not necessary to include here abstracts in both offical languages unless the text is bilingual).

(U) The Transit satellite positioning system is a commonly used navigation aid and was included in the DREO developed Marine Integrated Navigation System (MINS-B II) and Primary Land Arctic Navigation System (PLANS). MINS and PLANS are both Kalman filter based multi-sensor optimally integrated navigation systems and as such require detailed stochastic and deterministic error models for all of their sensors (to form the Kalman filter measurement error sensitivity matrices). This paper provides a detailed geometric derivation of the deterministic error model relating the position error of a Transit satellite Doppler position fix (or similarly a SARSAT fix) to the error in the velocity and height that is fed into the Transit receiver (or assumed for the SARSAT transponder). This error model is presented in the form of explicit functions of variables which are normally provided by a Transit receiver with each position fix, namely the satellite maximum elevation angle, the satellite direction of travel and the receiver latitude. For generality the satellite orbital parameters are left in the expressions. Sample plots of these sensitivity functions are presented, along with experimental results for verification. The high latitude results are particularly interesting, as they differ substantially from those at low latitudes, and from the qualitative descriptions in the literature.

14. KEYWORDS, DESCRIPTORS or IDENTIFIERS (technically meaningful terms or short phrases that characterize a document and could be helpful in cataloguing the document. They should be selected so that no security classification is required. Identifiers, such as equipment model designation, trade name, military project code name, geographic location may also be included. If possible keywords should be selected from a published thesaurus. e.g. Thesaurus of Engineering and Scientific Terms (TEST) and that thesaurus-identified. If it is not possible to select indexing terms which are Unclassified, the classification of each should be indicated as with the title.)

Transit Satellite
Error Modelling
Kalman Filter
Doppler Positioning
MINS
PLANS
SARSAT

UNCLASSIFIED

SECURITY CLASSIFICATION OF FORM